United Arab Emirates University

Scholarworks@UAEU

6-2021

EXPERIMENTAL INVESTIGATION AND PREDICTION OF LONG-TERM EFFECT OF SUSTAINED LOAD AND HARSH ENVIRONMENT ON FIBER-REINFORCED POLYMER COMPOSITES

Amir Hussain Idrisi

United Arab Emirates University

College of Engineering

EXPERIMENTAL INVESTIGATION AND PREDICTION OF LONG-TERM EFFECT OF SUSTAINED LOAD AND HARSH ENVIRONMENT ON FIBER-REINFORCED POLYMER COMPOSITES

Amir Hussain Idrisi

This dissertation is submitted in partial fulfilment of the requirements for the degree of Doctor of Philosophy

Under the Supervision of Prof. Abdel-Hamid I. Mourad

June 2021

Declaration of Original Work

I, Amir Hussain Idrisi, the undersigned, a graduate student at the United Arab Emirates University (UAEU), and the author of this dissertation entitled "*Experimental Investigation and Prediction of Long-Term Effect of Sustained Load and Harsh Environment on Fiber-Reinforced Polymer Composites*", hereby, solemnly declare that this dissertation is my own original research work that has been done and prepared by me under the supervision of Prof. Abdel-Hamid I. Mourad in the College of Engineering at UAEU. This work has not previously been presented or published, or formed the basis for the award of any academic degree, diploma or a similar title at this or any other university. Any materials borrowed from other sources (whether published or unpublished) and relied upon or included in my dissertation have been properly cited and acknowledged in accordance with appropriate academic conventions. I further declare that there is no potential conflict of interest with respect to the research, data collection, authorship, presentation and/or publication of this thesis.

Student's Signature: _____   Date: 18/06/2021

Advisory Committee

1) Advisor: Prof. Abdel-Hamid I. Mourad

Title: Professor

Department of Mechanical Engineering

College of Engineering

2) Member: Prof. Yaser Mohamed Greish

Title: Professor

Department of Chemistry

College of Science

3) Member: Dr. A.S. Mohammad Sayem Mozumder

Title: Associate Professor

Department of Chemical & Petroleum

College of Engineering

4) Co-advisor: Prof. Abdel-Magid Beckry

Title: Professor

Department of Composite Materials Engineering

College of Engineering, Winona State University, USA

Approval of the Doctorate Dissertation

This Doctorate Dissertation is approved by the following Examining Committee Members:

1) Advisor (Committee Chair): Prof. Abdel-Hamid Ismail Mourad

   Title: Professor

   Department of Mechanical Engineering

   College of Engineering

   Signature _____   Date June 18, 2021___

2) Member: Dr. Jaber Abu Qudeiri

   Title: Associate Professor

   Department of Mechanical Engineering

   College of Engineering

   Signature _____   Date _____June 18, 2021_____

3) Member: Dr. Ahmed Hassan Noor Muhammad

   Title: Associate Professor

   Department of Architectural Engineering

   College of Engineering

   Signature _____   Date __18 June 2021_____

4) Member (External Examiner): Dr. Aravind Dasari

   Title: Associate Professor

   Department of Materials Science & Engineering

   Institution: Nanyang Technological University, Singapore

   Signature _____   Date __18 June 2021_____

This Doctorate Dissertation is accepted by:

Dean of the College of Engineering Professor James Klausner

Signature _James F. Klausner_ Date _14/11/2021_

Dean of the College of Graduate Studies: Professor Ali Hassan Al Marzouqi

Signature _Ali Hassan_ Date _14/11/2021_

Copy ____ of ____

Abstract

In this dissertation the durability of thermoset composites was investigated under sustained load. Two thermoset composites, E-glass/epoxy and E-glass/polyurethane were immersed in seawater under sustained load (10%, 15%, 20%, 25% of failure load) and varying temperature (23°C to 95°C) for the period of 15 months. Mechanical, physical and thermal properties were experimentally investigated. The effects of temperature, moisture, and immersion time on the deterioration of the composite material were studied for both composites. It was observed that the weight of the samples increased with the immersion time and temperature for both the composites. The highest increase in weight of the samples under 15% sustained load (15% of failure load) was 6.3% and 5.4% for E-glass/epoxy and E-glass/polyurethane composites respectively for the immersion period of 15 months at 65°C. The tensile strength of the E-glass/epoxy composite immersed at 65°C reduced to 89% and 82% of its original value after 15 months of immersion in seawater without load and with 15% sustained load (15% of failure load) respectively. Similarly, the tensile strength of the E-glass/polyurethane composite immersed at 65°C reduced to 66% and 65% of its original value after 15 months of immersion in seawater without load and with 15% sustained load (15% of failure load) respectively. The Differential Scanning Calorimetry (DSC) and Scanning Electron Microscope (SEM) analysis were conducted to evaluate the degradation of fiber matrix interface. Results revealed that moisture, temperature and sustained load have a deteriorative impact on the performance of the composite. It was observed that degradation mechanism accelerated at elevated temperature results in breakdown of chemical bonds between matrix and fiber at the interface. Furthermore, this experimental data was used for the development of two prediction models to predict the tensile strength of two composites for long term exposure in seawater. These prediction models were used to predict unseen data. The results of all models were in good agreement with the experimental data.

Keywords: E-glass/epoxy composite, E-glass/Polyurethane composite, Long term durability, Sustained load, Sea water, Temperature, Mechanical properties.

Title and Abstract (in Arabic)

التحقيق التجريبي والتنبؤ بالآثار طويلة المدى للأحمال المستمرة والبيئات البحرية على مركبات البوليمر المقوى بالألياف

الملخص

في هذه الأطروحة تم التحقق من متانة مركبات التصلب الحراري تحت الحمل المستمر. تم غمر مركبين متصلين بالحرارة ، الزجاج الإلكتروني / الإيبوكسي والزجاج الإلكتروني / البولي يوريثين في مياه البحر تحت الحمل المستمر (10٪ ، 15٪ ، 20٪ ، 25٪ من حمل الفشل) ودرجات حرارة متفاوتة (23 درجة مئوية إلى 95 درجة مئوية) لمدة 15 شهرًا. تم دراسة الخصائص الميكانيكية والفيزيائية والحرارية تجريبياً. تمت دراسة تأثير درجة الحرارة والرطوبة وزمن الانغماس على تدهور المادة المركبة لكلا المركبين. لوحظ أن وزن العينات يزداد مع زمن الغمر ودرجة الحرارة لكلا المركبين. كانت أعلى زيادة في وزن العينات تحت 15٪ من الحمل المستمر (15٪ من حمل الفشل) 2.5٪ و 1.9٪ لمركبات epoxy / E-glass و / E-glass polyurethane على التوالي لفترة الغمر لمدة 15 شهرًا عند 65 درجة ج. انخفضت مقاومة الشد لمركب الزجاج الإلكتروني / الإيبوكسي المغمور عند 65 درجة مئوية إلى 89٪ و 82٪ من قيمتها الأصلية بعد 15 شهرًا من الغمر في مياه البحر دون تحميل و 15٪ حمل مستمر (15٪ من حمل الفشل) على التوالي . وبالمثل ، فإن مقاومة الشد لمركب الزجاج الإلكتروني / البولي يوريثين المغمور عند 65 درجة مئوية تقلص إلى 65٪ و 62٪ من قيمته الأصلية بعد 15 شهرًا من الغمر في مياه البحر دون تحميل ومع 15٪ حمل مستمر (15٪ من حمل الفشل) على التوالى. تم إجراء تحليل المسعر التفاضلي (DSC) وتحليل المجهر الإلكتروني (SEM) لتقييم تدهور واجهة مصفوفة الألياف. أظهرت النتائج أن الرطوبة ودرجة الحرارة والحمل المستمر لها تأثير سلبي على أداء المركب. لوحظ أن آلية التحلل المتسارعة عند درجات الحرارة المرتفعة تؤدي إلى انهيار الروابط الكيميائية بين المصفوفة والألياف عند السطح البيني. علاوة على ذلك ، تم استخدام هذه البيانات التجريبية لتطوير نموذجين للتنبؤ للتنبؤ بقوة الشد لمركبين للتعرض طويل المدى في مياه البحر. تم استخدام نماذج التنبؤ هذه للتنبؤ بالبيانات غير المرئية. كانت نتائج جميع النماذج متوافقة بشكل جيد مع البيانات التجريبية.

مفاهيم البحث الرئيسية: مركب E- الزجاج / الايبوكسي ؛ مركب زجاجي / بولي يوريثين ؛ متانة طويلة المدى حمولة مستدامة مياه البحر؛ درجة حرارة؛ الخواص الميكانيكية.

Acknowledgements

I would like to express my deepest appreciation to my advisor Prof. Abdel-Hamid Ismail Mourad, for his valuable guidance, generous support, and time throughout this study. I would like to especially thank him for providing many opportunities to grow and learn.

My extended gratitude goes to Prof. Abdel-Magid Beckry, Winona State University, USA, for his co-advising on the thesis. I am especially grateful to Prof. Yaser Mohamed Greish and Dr. Mohammad Sayem Mozumder for providing guidance and support during my PhD work.

My special thanks also for Eng. AbdulSattar and Eng. Muthanna Aziz for providing the opportunity and support to work on various equipment during my PhD work. I extend my gratitude to our research team and colleagues who helped me in some technical challenges and also motivated at different stages of my work.

Above all, I would like to thank my wife, parents, family and friends for their love, prayers, and endless support throughout this experience, and for being my inspiration in completing this study.

Dedication

To my beloved wife, parents and family

Table of Contents

List of Tables

List of Figures

List of Abbreviations

A	Average Cross-Sectional Area of Specimen
DSC	Differential Scanning Calorimetry
E_a	Activation Energy
FRP	Fiber-Reinforced Polymer
FTIR	Fourier Transform Infrared Spectroscopy
GFRP	Glass Fiber Reinforced Polymers
k	Degradation Rate
KN	Kilonewton
P_i	Load at the Ith Data Point
P_{max}	Maximum Load Before Failure
R	Correlation Coefficients
SEM	Scanning Electron Microscopy
SR	Strength Retention
t	Exposure Time
T	Exposure Temperature
Tg	Glass Transition Temperature
TSF	Time-Shift Factor
W (%)	Weight Change Percentage
W_1	Weight Before Immersion
W_2	Weight After Immersion
τ	Regression Coefficient
σ_i	Tensile Stress at the Ith Data Point
σ_{ut}	Ultimate Tensile Strength

Chapter 1: Introduction

1.1 Overview

Composite materials are engineered or naturally occurring materials made from two or more constituent materials with significantly different physical or chemical properties which remain separate and distinct within the finished structure. Most composites have strong and stiff fibers in a matrix which is weaker and less stiff. The objective is usually to make a strong and stiff component with a low density.

Fiber-reinforced polymer (FRP), also fiber-reinforced plastic, is a composite material made of a polymer matrix reinforced with fibers. The fibers are usually glass, carbon, or aramid, although other fibers such as paper or wood or asbestos have been sometimes used. The polymer is usually epoxy, polyurethane or polyester thermosetting plastic.

The fiber reinforced polymer composites (FRPs) are increasingly being considered as an enhancement to and/or substitute for infrastructure components or systems that are constructed of traditional civil engineering materials, namely concrete and steel. FRP composites are lightweight, non-corrosive, exhibit high specific strength and specific stiffness, are easily constructed, and can be tailored to satisfy performance requirements. Due to these advantageous characteristics, FRP composites have been included in new construction and rehabilitation of structures through their use as reinforcement in concrete, bridge decks, modular structures, formwork, and external reinforcement for strengthening and seismic upgrade.

The main applications of the polymeric composites are in pipelines for water desalination plants, in repair and strengthening of reinforced concrete structures, water storage vessels, manufacture of leisure boats, glass fiber-reinforced polymers (GFRP)

sheet piles for continuous walls in waterfront/marine structures, GFRP columns in bridge structures and many other applications. Moreover, GFRPs have been essentially used to strengthen structures either through rods ''replacing'' reinforcing steel bars, or strips bonded to concrete as external strengthening of structural members, or confining columns.

The corrosion resistance of FRP, ease of installation, high chemical resistance, reduced architectural impact, increase of the mechanical fatigue resistance and high strength to weight ratio makes the material effective in these applications. Thus, FRP bars have been developed as a possible long- term solution to overcome the corrosion of steel in concrete structures. Due to their low cost, glass fiber reinforced polymer (GFRP) bars are used more extensively than carbon FRP bars. The global fiberglass market is projected to grow from USD 11.5 billion in 2020 to USD 14.3 billion by 2025, at a Compound Annual Growth Rate (CAGR) of 4.5% from 2020 to 2025. Figure 1 shows the glass fiber market growth rate by region from 2020-2025. The major reasons for the growth of the fiberglass market include extensive use of fiberglass in the construction & infrastructure industry and the increased use of fiberglass composites in the automotive industry are driving the growth of fiberglass market (Fiberglass Market, 2020).
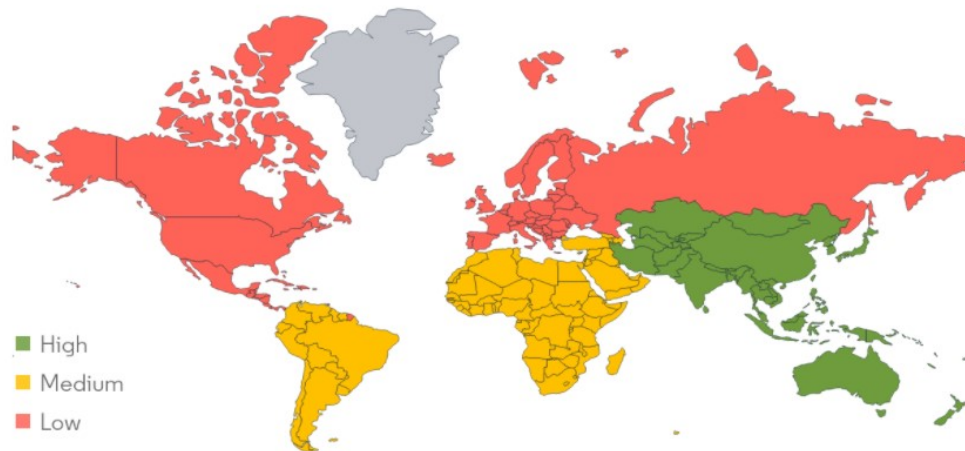
Figure 1: Glass fiber market growth rate by region 2020-2025

(Fiberglass Market, 2020)

FRPs have a linear elastic response in tension up to failure (described as a brittle failure) and a relatively poor transverse or shear resistance. They also have poor resistance to fire and when exposed to high temperatures. They lose significant strength upon bending, and they are sensitive to stress-rupture effects.

Composite materials have developed greatly since they were first introduced. However, before composite materials can be used as an alternative to conventional materials as part of a sustainable environment a number of needs remain.

• Availability of standardized durability characterization data for FRP composite materials.

• Integration of durability data and methods for service life prediction of structural members utilizing FRP composites.

• Development of methods and techniques for materials selection based on life cycle assessments of structural components and systems.

Composite materials have a broad range of industrial applications such as marine applications, aircraft applications, civil infrastructure applications etc. Marine applications include masts, hulls, decks, structural bulkheads, submarine casings, transmission shafts, propellers, offshore oil rigs and sonar domes. In aerospace applications such as aircraft components for example frames, stiffeners and rotor blades, etc. In aircraft structures, using composite materials reduces the weight and increases the strength to weigh ratio of a component and consequently improves the performance of the aircraft. In civil infrastructure applications, encloses piers and bridges by using fibers reinforced so the Fiber reinforced polymer (FRP) composite materials are being increasingly used due to their high strength/weight ratios, high stiffness/weight and corrosion resistance. Due to their superior properties; it guarantees to change various businesses and markets.

1.2 Problem Statement

Composite materials have been widely recognized for playing a major role in weight reduction over the last decades, however, the novel and unconventional nature of composites (compared to metals) has undeniably brought on their own challenges and complexities. Satisfying the high degree of reliability and safety requirements of marine and aerospace structures is a particular concern for composites, due to their unconventional complex structure, the limited information on their complex behavior due to less experience on composites compared to metals (Rana & Fangueiro, 2016), and the challenges in creating accurate and reliable prediction models. Composites are anisotropic, non-homogeneous, and exhibit complex material behavior under load, which is not always analytically predictable. Although advanced computational technology and numerical methods have played a vital role in

overcoming such challenges (Mangalgiri, 1999), the long-term durability of composites with regards to environmental degradation and impact damage is generally not understood and has therefore created an unavoidable reliance and need for excessive material testing.

During their operational life, these FRP composite structures are typically exposed to different environmental conditions, such as moisture, humidity, temperature and sustained load, which can affect their long-term mechanical, thermal and physical properties. Therefore, in order to use these materials, it is important to evaluate what adverse effects these conditions would have on the performance and durability of the composites (Hossain et al., 2011).

The impact of environmental factors such as temperature and humidity on fiber reinforced polymers behavior is a significant concern for marine and aircraft applications, since operational and storage conditions differ considerably and can add to the wear and tear of the structural components (Ray, 2006). Literature has shown that both the physical and mechanical properties of composite materials can be strongly affected when exposed to deteriorative environmental conditions involving temperature and humidity, affecting the composite performance (Akbar & Zhang, 2008). Water absorption in FRPs generally leads to swelling and plasticization of the polymer, which leads to a decrease of the glass transition temperature and deterioration of the mechanical properties (Koshima et al., 2019). Higher temperatures are also known to accelerate the moisture absorption and degradation process (Almudaihesh et al., 2020). Characterizing these effects are required and critical to prevent unexpected failures, and with the increasing applications of these materials, there is a pressing need to evaluate and quantify the extent of environmental degradation on the deviation

of mechanical, thermal and physical properties of fiber/polymer composites (Ray, 2006).

Fiber reinforced polymer composite structures are expected to experience a range of environmental conditions during their operational life. Since temperature and absorbed moisture can influence the composite performance by degrading the properties of the material and understanding the behavior is critical for predicting structural performance. Extensive research has been conducted to determine the durability of composite structures under loading, mainly through creep tests (Gates et al., 1997), or in humid environments, through immersion in distilled water (Ellyin & Maser, 2004; Gellert & Turley, 1999; Kootsookos & Mouritz, 2004b; Siriruk et al., 2009). A number of studies were also performed to investigate the short-term effect of combined loading and moisture (Abdel-Magid et al., 2005; Buck et al., 1997; Helbling & Karbhari, 2004); but data on the long-term combined effects of sea-water and sustained loading are scarce in the literature (Bank et al., 1995). Composite structures in the marine environment are subjected to both stresses from the applied loads on the structure, and environmental attack from seawater. The combined effects of these two factors are essential for the proper designing and manufacture of these structures, yet it is very difficult to simulate these combined effects in the laboratory. Small loading frames and hot water bath have been used by many researchers (Abdel-Magid et al., 2005; Helbling & Karbhari, 2008) but these are limited in scope and instrumentation. Attempts have been made to predict the long-term performance of these structures by conducting accelerated short-term tests, but these models were made for certain applications in concrete structures (Chen et al., 2007). In addition, no long-term experimental data was available to compare with these models.

The development of reliable prediction models for long-term performance of composites in marine environments requires a robust experimental set-up for short-term and long-term testing of combined real-life effects on the structures. In addition, it is essential to establish long-term experimental data against which analytical models developed from accelerated tests can be calibrated and validated. Inspection of these structures is often difficult in off-shore and submerged structures, and experience from aerospace applications indicates that internal damages of composites structures are difficult to detect. Therefore, it is significant for engineers and manufacturers to base their design of marine composites structures on reliable experimental data and tested analytical models.

1.3 Research Objectives

The objective of this study is to design and fabricate a multi-sample loading frame for sustained load application and evaluate the effects of different environmental conditions and sustained load on the structural properties of E-glass/epoxy and E-glass/polyurethane composite materials. In other words, to investigate the durability (i.e., the ability of composite material to maintain its original physical, thermal and mechanical properties) when exposed to different environmental conditions of temperature, moisture/humidity and sustained load.

The composite specimens were immersed in seawater heating chambers maintained at different temperatures varied from 23°C to 95°C for a period of time that varied from one month up to 15 months. Mechanical, physical and thermal properties were experimentally investigated and the effects of temperature, moisture, and immersion time on the deterioration of the material were studied against both E-glass/epoxy and E-glass/polyurethane composite materials.

This study will be mainly focusing on the specific objectives mentioned below:

- Design and development of a multi-sample loading frame which can accommodate 9 samples simultaneously under different environmental condition and sustained load.

- Conditioning of specimens in two groups:

  o Immersion of specimen at various temperatures (23°C to 95°C) in sea water for the duration up to 15 months without any sustained load.

  o Immersion of specimen at various temperatures (23°C to 95°C) in sea water for the duration up to 15 months with different sustained load varying from 10 to 25% of the failure strength of composites.

- Evaluate the water absorption of E-glass/epoxy and E-glass/polyurethane samples due to long-term water immersion at different immersion temperatures varies from 23°C to 95°C.

- Evaluate the impact of long-term water immersion at various temperature and sustained load on the degradation of mechanical properties of FRP composites by analyzing the tensile properties.

- Compare the effect of sustained load on the composite with the previous work in which composite samples were immersed without load in seawater at 23°C and 65°C for the duration of 90 months (7.5 years).

- Evaluate the impact of long-term water immersion at various temperature and sustained load on the thermal and chemical properties of FRP composites samples using Differential Scanning Calorimetry (DSC) and Fourier transform infrared spectroscopy (FTIR).

- Evaluate the impact of long-term water immersion at various temperature and sustained load on the physical and microstructural properties of samples by analyzing water absorption results and Scanning Electron Microscopy (SEM) images.

- Development of models to predict the mechanical properties of these materials during their design life and extended use in marine and off-shore structures

- Validation of the prediction models with the experimental results and calibration of the models to obtain a realistic prediction of properties

In addition to contributing to the science and engineering of FRP composite material, the study will play an important role in assessing and predicting the durability of FRP composites in the practical application of structures subjected to sustained loading in many applications such as marine, aerospace etc. This in turn will help manufacturers and practicing engineers to select adequate materials for long term application and will help designers and code agencies to provide proper standards for the safe application of composite in engineering infrastructures.

1.4 Research Overview

A research design is the set of methods and analyzing measures of the variable specified in the research problem during the study. Based on the research study the design model in Figure 2 has been adopted which describes the various points that need to be considered before starting the research.
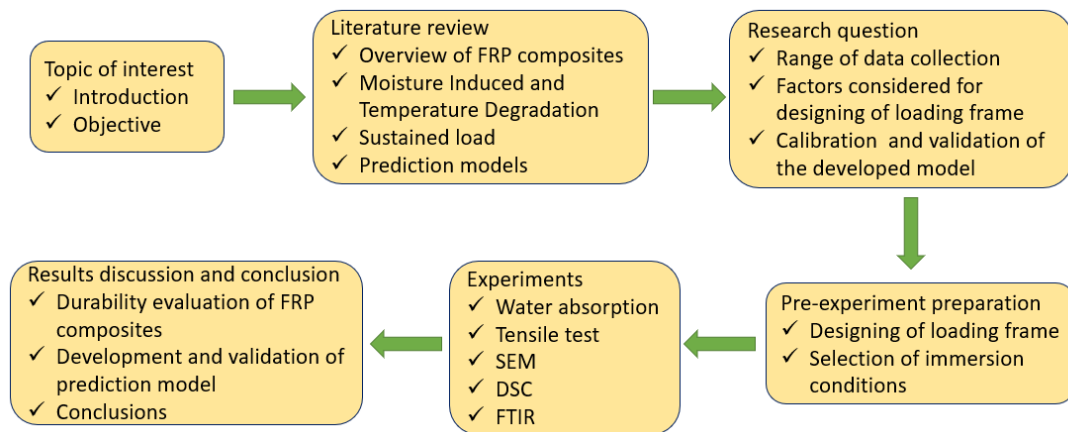
Figure 2: Overview of the research design

Figure 2 shows the flow diagram to express the procedure which has been followed to complete this work.

Figure 3 shows the flow diagram of the work and indicates the steps involved in the research. The flow of work is also expressed through a diagram shown in Figure 4.
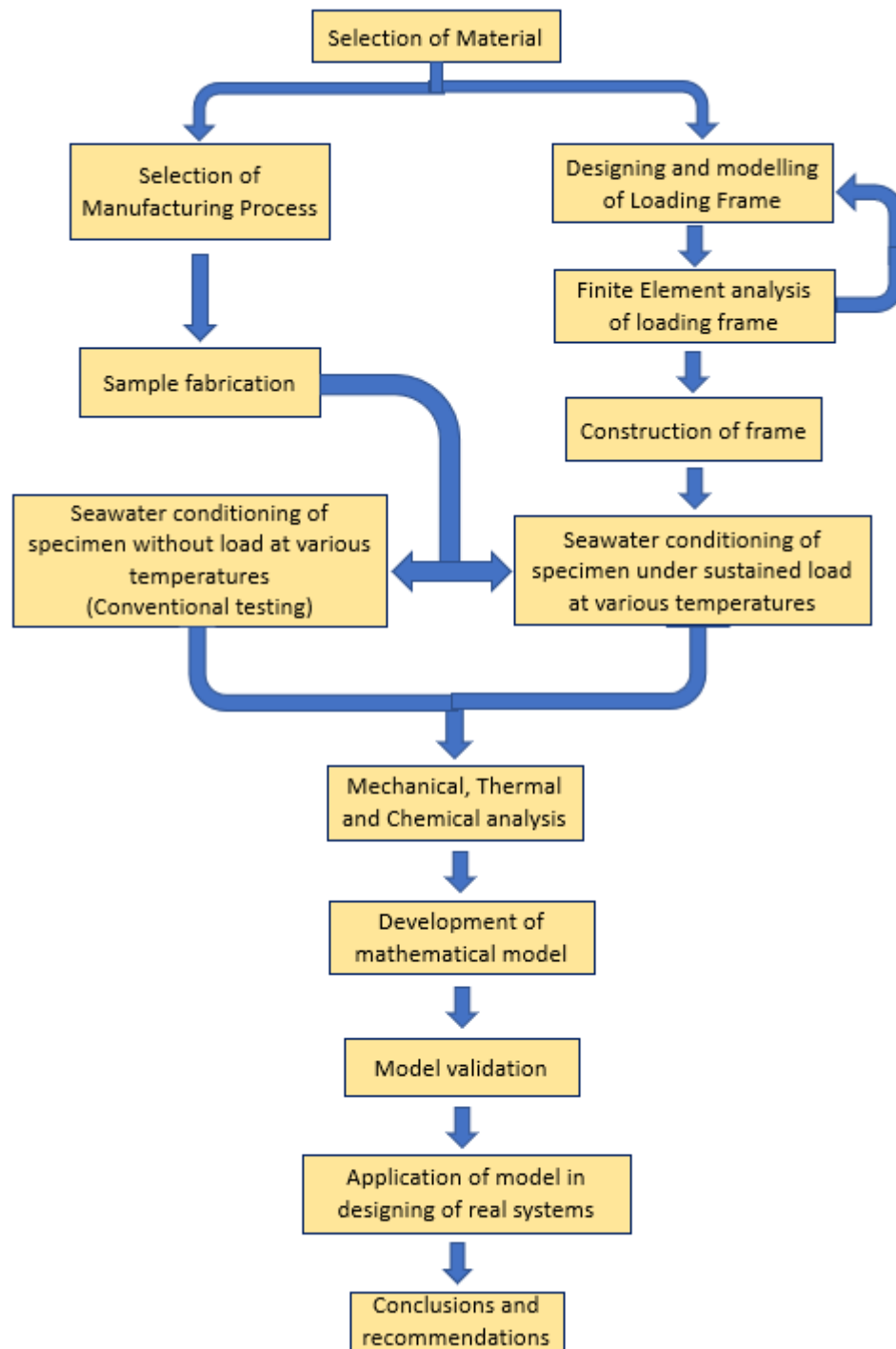
Figure 3: Process flow chart
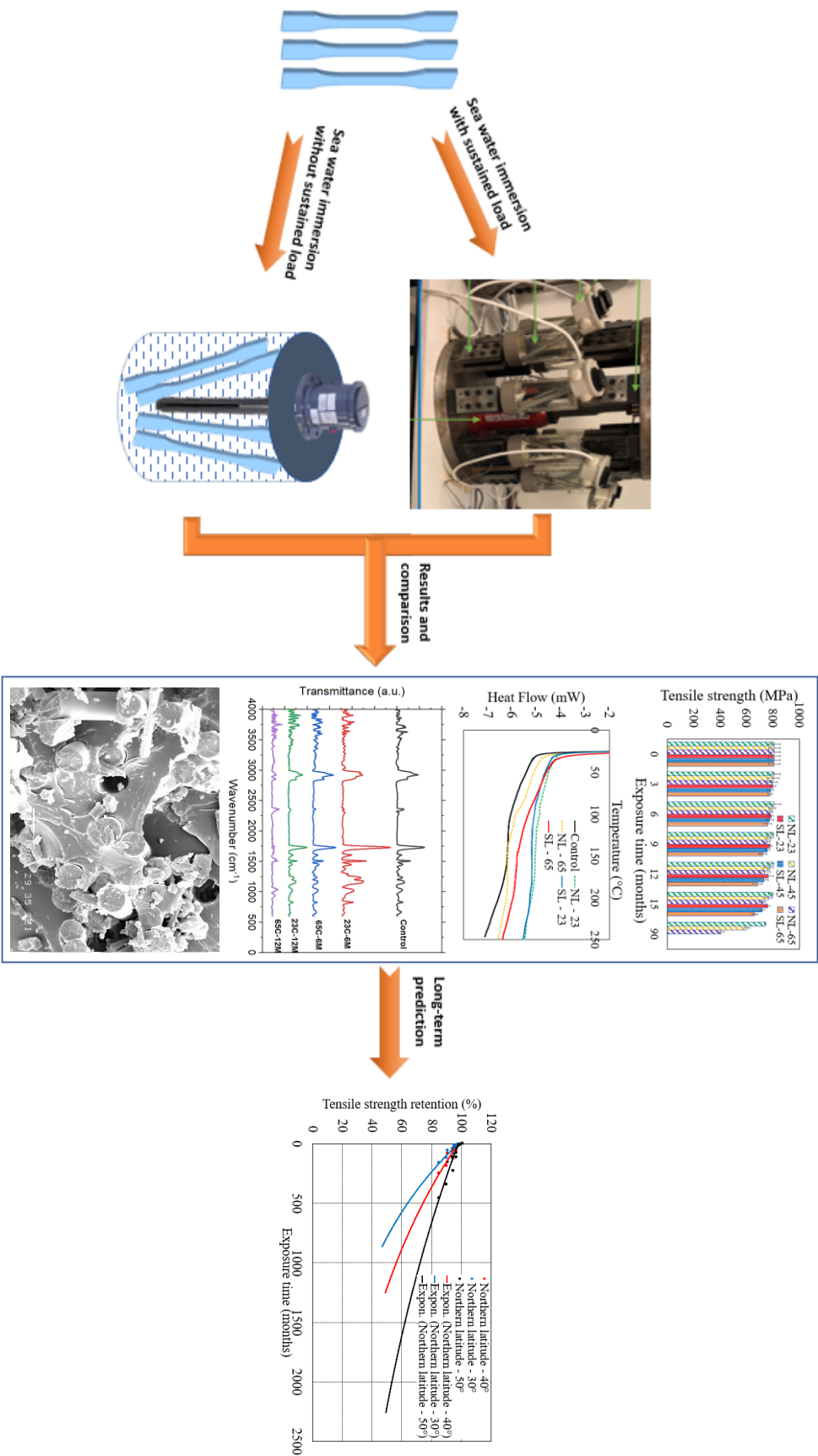
Figure 4: Research overview

1.5 Dissertation Outline

This dissertation consists of six chapters and the focus of each chapter is described in this section. The flow of the dissertation work presented in this report follows the sequence outlined herein:

Chapter 1: Introduction

This chapter discusses the overview and background of the use of composites in different applications such as marine, aircraft, civil infrastructure applications and the project's main objectives.

Chapter 2: Literature review

This chapter provides a literature review to outline and summarize the recent research conducted.

Chapter 3: Materials and research methods

This chapter provides detailed information about the materials, fabrication process, samples preparation, and characterization testing techniques used in this study.

Chapter 4: Research methodology

The information about steps followed to evaluate and predict the durability of selected FRP composites is discussed in this chapter.

Chapter 5: Design and development of loading frame

Detailed information related to the design and manufacturing of a system to immerse samples under different environmental conditions at sustained load are presented in this chapter.

Chapter 6: Results and discussion

This chapter discusses the main findings of this study, the analysis and discussion of the experimental results. Furthermore, development of prediction models and validation.

Chapter 7: Conclusion

This chapter provides a summary of the important findings and conclusions derived from the experimental results and prediction models.

Chapter 2: Literature Review

The aim of this literature review is to provide background information on the topics to be considered in this dissertation and to highlight the importance of the present research. The topics covered in this review include: 1) Overview of fiber reinforced composites; 2) Moisture induced and temperature degradation; 3) Combinations of moisture/environmental conditions and sustained loads; and 4) Prediction models

2.1 Overview of Fiber Reinforced Composites

A composite material is a material that is made from at least two constituent materials that differ significantly in their physical and chemical composition, that when combined produce a material with unique characteristics different from the individual constituent materials. The constituent materials are typically referred to as the matrix and the reinforcement. They don't blend nor lose their individual properties, they remain distinct and work together to contribute their unique features to give the composite material its desired properties which can be tailored for desired applications.

Fiber-Reinforced Polymeric (FRP) composites are made from a polymer matrix (such as epoxy or bismaleimide) that is reinforced with fibers like carbon, glass, aramid or other reinforcing material. The matrix serves as an adhesive that binds the fibers together (Mouritz, 2012), and protects the fibers from environmental exposure and transfers the load among the fibers. The fibers, in exchange, provide stiffness and strength to reinforce and strengthen the matrix and allows it to withstand cracks and fractures.

2.1.1 FRP Classifications

As shown in Figure 5, Erden & Ho, (2017) illustrated that fiber reinforced composites can be classified into four categories according to their matrix (or resin) group: Metal Matrix Composites (MMCs), Ceramic Matrix Composites (CMCs), Polymer Matrix Composites (PMCs), and Carbon/Carbon composites (C/C).
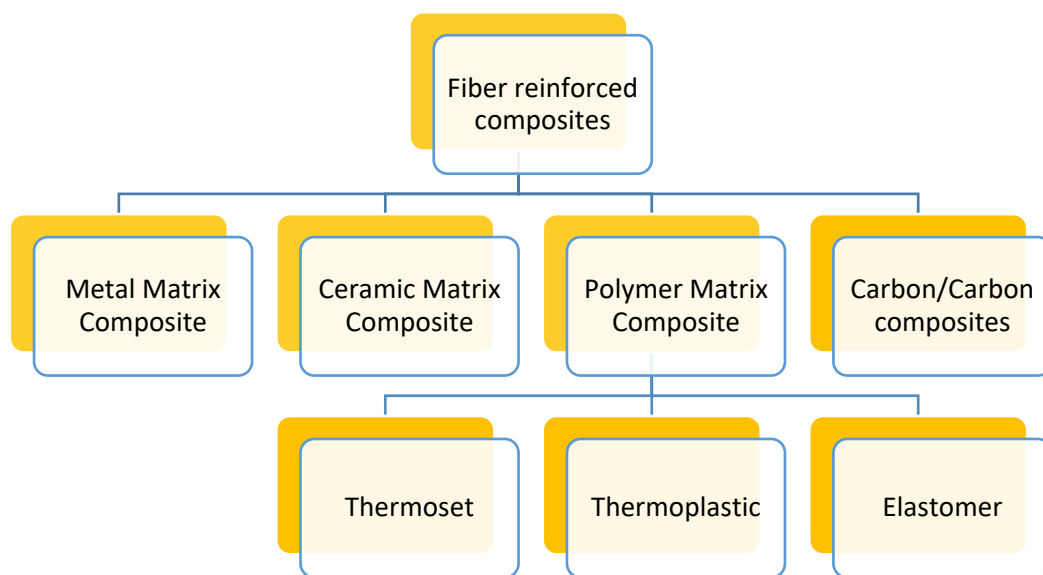
Figure 5: Classification of composites according to matrix type

2.1.2 Polymer Matrix Composites

PMCs are particularly known for their lightweight among the other matrix group types and have proven valuable across a wide range of aerospace applications. Thermosets, thermoplastics and elastomers are the three main classes of polymers. Thermosets, such as epoxy resins and bismaleimides, are the most commonly used polymers in aircraft applications due to their high mechanical performance and are used as the matrix in fiber composites and as an adhesive in structural joints and

repairs. Thermoplastics and elastomers, on the other hand, are less common in aerospace applications. Elastomers lack the required stiffness and strength for aerospace applications, as shown in Figure 6. Thermosets demonstrate better mechanical performance (strength, stiffness, and creep resistance) compared to thermoplastics as shown in Figure 6, since it has molecular chains that are crosslinked which prevent the chains from sliding under stress and therefore increase the mechanical properties (Mouritz, 2012).
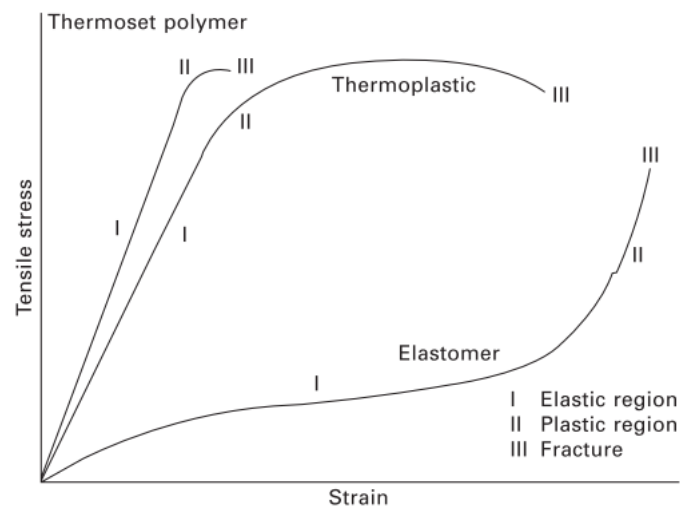
Figure 6: Typical stress–strain curves for a thermoplastic, thermoset and elastomer polymers

(Mouritz, 2012)

As shown in Figure 7, the elastic modulus of most polymers declines sharply with elevated temperatures (above 100–150°C), and therefore their use in composite applications must be limited to lower temperatures. Bismaleimides, cyanates, and polyimides are polymer systems that can operate at elevated temperatures (below 200–220°C). Thermosets do not experience melting at elevated temperatures, due to the crosslinking of the molecular chains and therefore they can retain their structural

rigidity and shape, however thermosets experience decomposition when further heated (Mouritz, 2012).
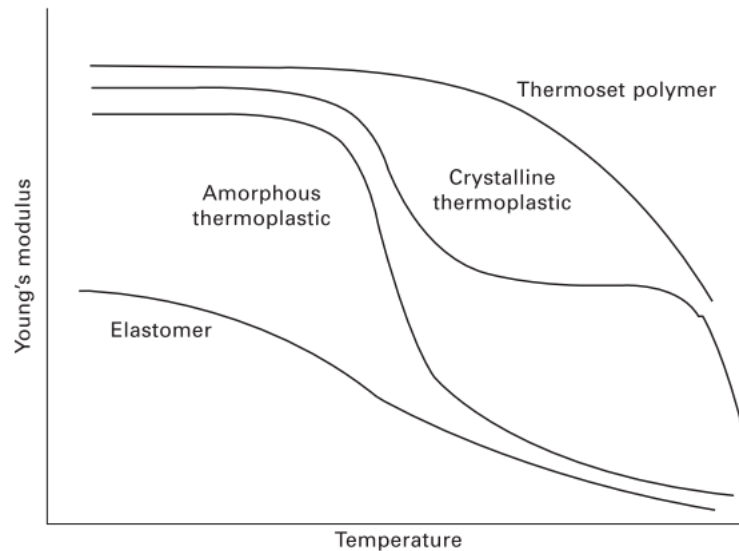
Figure 7: Variation of Young's modulus with temperature

(Mouritz, 2012)

2.1.3 Reinforcements

Fiber reinforcements are classified as natural and synthetic fibers as shown in Figure 8. Carbon, glass, and aramid fibers are considered synthetic fibers, and consist of tens to thousands of single filaments of different diameters and strengths. Fibers generally come in the form of a fabric or cloth, which can be further classified as woven, nonwoven, braided or knitted. Woven fabrics are produced by interlacing two sets of yarns (warp and weft), and the method in which the yarns are interlaced defines the style of weave like: plain, satin, twill, etc, which has an effect on the properties of the fabric, such as smoothness and durability (Erden & Ho, 2017).
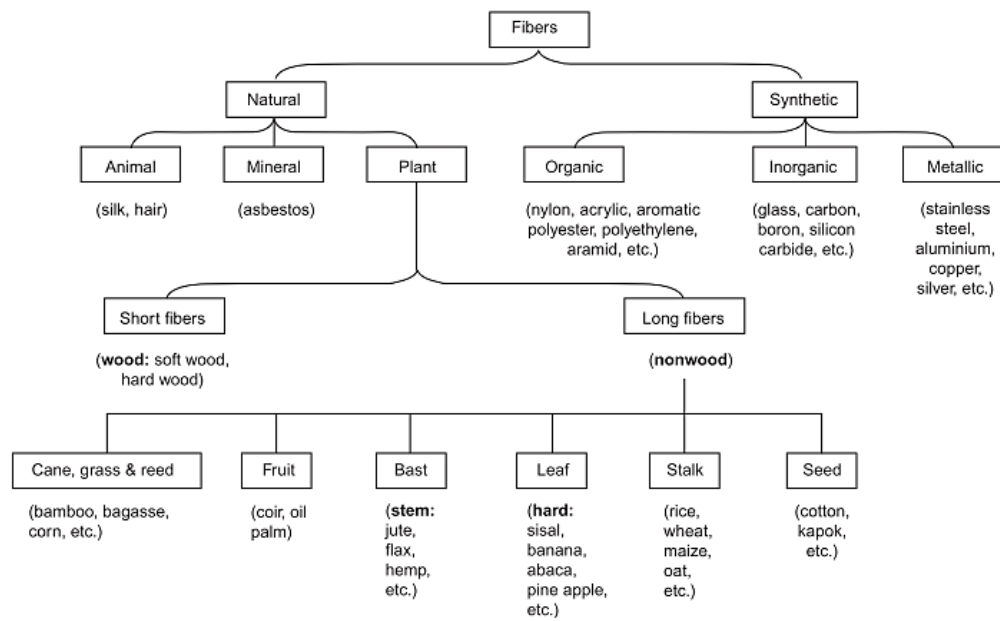
Figure 8: Classifications of fibers
(Erden & Ho, 2017)

2.2 Moisture Induced and Temperature Degradation

Environmental conditions are considered as an accelerating factor for the degradation of composite materials. The degradation takes place due to two effects, the first is Moisture/solution effect and the second is the thermal effect. The moisture/solution effects include tap water, deionized water, sea water, alkaline and acidic solutions. There have been a large number of experimental evidence in the literature that demonstrated the unfavorable effects of combined moisture and temperature on the physical and mechanical properties of polymeric composite materials, influencing the composite's performance and limiting its functionality (Akbar & Zhang, 2008; Paiva et al., 2005; Khan et al., 2010; Patel, 1999; Sun et al., 2011; Vieille et al., 2012).

The moisture absorption of composite materials depends on factors such as temperature, fiber orientation, fiber volume fraction, fiber type and sizing, matrix type,

contact area, void content, and water types such as sea water, or demineralized water (Akbar & Zhang, 2008; Almudaihesh et al., 2020). The extent of deterioration that takes place in fiber reinforced polymers due to environmental exposure is associated with the amount of moisture absorbed, which occurs through diffusive and/or capillary processes (Ray, 2006; Reis et al., 2018). Diffusion is considered a key process under which moisture penetrates polymeric composites and is known to be a matrix-dominated phenomenon in which water is mainly diffused in the matrix (Akbar & Zhang, 2008; Ray, 2006), while moisture diffusion through the fibers is considered negligible (Li et al., 2016; Murthy et al., 2010). The capillary process involves moisture being drawn into voids and microcracks at the fiber/matrix interfaces, in which the cracks provide a transport system for moisture penetration (Li et al., 2016; Patel & Case, 2002).

The downside of polymer-based composites is the deterioration of the polymer matrix and the fiber/matrix interface when subjected to moist conditions by reacting with water in a hydrolysis process that has an effect on their mechanical performance (Almudaihesh et al., 2020; Kootsookos & Mouritz, 2004a). The influence of water absorption is known to affect the mechanical properties of thermoset polymers, demonstrated by both reversible and irreversible changes (Almudaihesh et al., 2020; Ray, 2006).

Plasticization, swelling and degradation of the fiber/matrix interface are among the adverse effects of absorbed water. Moisture absorption has a plasticizing effect and induces plastic deformation in the matrix, which results in lowering of the glass transition temperature (Tg) of the matrix (Akbar & Zhang, 2008; Ray, 2006) due to the disruption of the hydrogen bonds in the epoxy resin (Li et al., 2016). This effect is

generally reversible when the absorbed water is removed, however, exposure to water at elevated temperatures can cause irreversible impacts, due to the chemical degradation of the matrix and to the deteriorative effect on the fiber/resin interface (Akbar & Zhang, 2008; Kootsookos & Mouritz, 2004a) which increases internal voids and promotes microcrack formation (Akbar & Zhang, 2008).

Swelling is due to the induced differential strain resulting from the significant difference of the amount of moisture absorbed by the matrix resin relative to that of the reinforcement fibers (Ray, 2006). Polymers are known to swell when they absorb moisture, while the reinforcement typically does not, and therefore the reinforcement inhibits the swelling of the matrix and causes internal strains and stresses in the polymeric composite (Akbar & Zhang, 2008). Swelling can stimulate the propagation of microcracks in the composite which may accelerate the absorption of water into the composite (Li et al., 2016; Starke, 1996).

The structural integrity and lifetime performance of FRP composites are highly dependent on the stability of the fiber/matrix interfacial region, since it is most likely to control and influence the overall mechanical behavior of the composites (Ray, 2006) (Khan et al., 2010). The strength of the interface determines the applied stress transmissibility to the load-carrying fibers, which is a function of the level of adhesion at the fiber/matrix interface (Akbar & Zhang, 2008), which is adversely affected when exposed to the environment due to the plasticization of the matrix, chemical and mechanical degradation (Ray, 2006). Increased temperatures can cause significant reductions in the strength and stiffness of the epoxy. Such reductions can begin to occur at temperatures well below Tg. The reduction in the mechanical properties may

be permanent at high enough temperatures. Moreover, the effects are magnified with increased time-at-temperature and moisture content (Paiva et al., 2005; Patel, 1999).

In this section, some literatures have been discussed to show the effect of a harsh environment on the durability of composite. Renaud and Greenwood (2005) investigated the effect of different environments as tap water, air, salt water, de-ionized water and hydrochloric acid on two different GFRP composites under constant tensile stress. They used an extrapolation method to predict the maximum stress limits of the specimens after 50 years at different environmental conditions. It was predicted that the maximum stress limit of traditional E-glass composite at 23°C equal 44% of ultimate strength in the air, 30% in salt water, 17% in tap water, 16% in deionized water, 15% in cement extract pH 12.6 and 1% in 1N hydrochloric acid. On the other hand, the maximum stress limit of advantex glass composite at 23°C will be 46% of ultimate tensile strength in air, 42% in salt water, 38% in tap water, 40% in deionized water, 25% in cement extract (pH 12.6) and 13% in 1N hydrochloric acid. It was observed that the least aggressive environment combined with constant tensile stress was air followed by salt, tap water and deionized water, cement extract of pH 12.6 and hydrochloric acid on GFRP composites. Chen Y. et al (Chen et al., 2007) compared the effect of two pH values (pH 13.6 and 12.7) of alkaline solution. The solution consists of sodium hydroxide (NaOH), potassium hydroxide (KOH) and calcium hydroxide ($Ca(OH)_2$). It was observed that the solution of pH 13.6 is more severe than the solution of pH 12.7. Consequently, the most severe environment was acid solutions and the least one was air. They also studied the effects of dry and wet cycles and thawing and freezing cycles.

The thawing and freezing combined with solutions have a little degradation effect on FRP bars in contrast, the wetting and drying cycles combined with tap water or alkaline solutions have more effect, but the continuous immersion has more severity compared to both. In addition to the wetting and drying cycles combined with sea water at different temperatures (30°C, 40°C and 50°C), the ultimate tensile strength decreased by 2.5% at 30°C, 6.4% at 40°C and 6% at 55°C but the continuous salt water immersion had more significant changes in tensile strengths of GFRP composites. It is observed that the tensile retention of GFRP exposed to continuous salt water immersion is 0.74 after 70 days at 60°C compared to wet and dry cycles equal 0.86 after 72 days and thawing and freezing cycles equal 1.04 after 300 cycles.

The thermal effect has dominance in accelerating the degradation of composite materials such as temperature variations and cycles. Al-Kuwaiti and Mourad (2015), investigated the effect of different environmental conditions on the mechanical behavior of plain woven laminated Carbon/Epoxy composites by studying the water absorption and degradation in mechanical properties. The specimens were divided into four groups; group one was exposed to no water and tested at room temperature, group two were exposed to no water and tested at high temperature (93°C), group three were exposed to hot water (71°C) for (19 days) and tested at room temperature and the last group were exposed to hot water immersion for (32 and 100 days) and tested at hot temperature (93°C). Specimens were tested in tension to predict the mechanical properties; however, the tensile modulus hadn't significantly changed except at groups three and four by 4.6% and 5.1%. The tensile strength had a significant change especially in groups three and four by 17.2% and 18.3% so that the highest degradation impact was under the combined effect of hot water immersion and testing at high temperature.

Based on the previous researches, it was observed that the environmental conditions including different solutions at elevated temperatures have significant effect on the mechanical properties of composite materials than at room temperatures. It is also illustrated that the effect of combination between environmental conditions and under sustained stress on composite materials also has a substantial effect on mechanical properties of composites. Masmoudi et al. (2003) presented an experimental setup for accelerated ageing tests for the durability of fiber-reinforced polymer (FRP) composites. The composites are composed of 73% E-glass fibers and vinyl-ester resin. The setup used combinations of environmental exposure and a sustained load on the specimens and it is used two series of glass fiber-Reinforced Polymer (GFRP) bars. The bars were exposed to two different environments such as alkaline solution and de-ionized water at different temperatures varying from 45°C to 63°C and exposed to sustained load varying from 20 to 29% of the ultimate tensile strength to accelerate degradation for 104 days duration. 13 to 15% reduction in tensile strength was observed for both the two series of GFRP bars after 104 days exposure. The same environmental conditions on GFRP bars have no effect on the modulus of elasticity.

Silva et al. (2014) studied the durability of GFRP laminates with epoxy resin based on accelerated tests by exposing the composites to salt water at different temperatures 30°C, 50°C and 65°C of duration 5000 hours. Until 1500 hours and in the three cases (30°C, 40°C and 55°C) the modulus behavior suggests that the prevailing damage mechanism is swelling. Then, between 1500h and 2500h plasticization processes were predominant especially for specimen aged under 30°C. In elastic modulus behavior suggested that plasticization phenomenon happened between 1500 to 2500 hours in all temperatures especially for specimens at 30°C.

Chakraverty et al. (2015) exhibited the effect of sea water immersion of glass fiber reinforced polymers (GFRP) composites with epoxy resin for duration of one year for studying its effect on mechanical properties of GFRP such as ILSS, stress and strain at rupture, elastic modulus and glass transition temperature. The stress and strain at rupture were determined showing that the decrement of both properties by increasing the sea water immersion period so the stress at rupture reduced to 21% of as-cured sample after 6 months and 16% after 1 year and somewhat recovery in stress at rupture values while strain at rupture decreased by 12% of as-cured sample and 20% after 1 year of sea water immersion so these decrements in values of stress and strain at failure due to the plasticization and swelling in composite material. Subsequently, the variation in elastic modulus decreased in first two months and then slightly increased and decreased again reaching the minimum decrement by 25% and in the last value decreased by 5% in compared to the initial value so the higher initial decrement of modulus and the increasing of strain value were due to the plasticization in matrix and ability of the matrix to move against each other while the final increase in the last stage might be the swelling which improves the mechanical adhesion between the matrix and fiber. Bhise (2002) studied the effect of alkaline solution (NaOH) immersion of GFRP bars with vinyl-ester resin at three different temperatures (30, 45 and 57°C) for duration of 180 days. It was observed that the change in modulus of elasticity was in the range of 10% at elevated temperature and alkalinity while the strength loss was 50% after immersion of 180 days at 57°C.

Based on the work of some researches (Bhise, 2002; Chakraverty et al., 2015; Masmoudi et al., 2003; Mourad et al., 2010; Silva et al., 2014), the trend of elastic modulus is almost constant even if there were some changes up or down due to swelling or plasticization phenomena. Bhise (2002) observed that there is a change in

modulus of elasticity about 10% at an elevated temperature after 180 days. In conclusion, the environmental conditions have a slight effect on the elastic modulus of the composites.

2.3 Combinations of Moisture/Environmental Conditions and Sustained Loads

There are many conditions that lead to the failure of composite materials so one of the severe conditions is composites under sustained load. These loads are classified into tensile, compressive and flexural loads. The researchers always try to reach the most severe conditions to monitor the behavior of composite through its mechanical properties. The most applied experimental work is concentrated on creep tests (sustained load – environmental conditions) especially in civil engineering.

Masmoudi et al. (2003) presented an experimental work to study the combination of sustained load (tensile load) varied from 20 to 29% of the ultimate tensile strength and exposure to alkaline solution and de-ionized water at temperatures varied from 45°C to 63°C for 104 days exposure on GFRP composites. Tensile test was done for GFRP specimens and 13 to 15% reduction in tensile strength was observed for both the two series of GFRP bars after 104 days exposure. Al-Tamimi (2013) investigated in his report the durability of bonding between the external CFRPs with an epoxy resin and the concrete in which the CFRPs were exposed to combination sets of environmental exposure conditions such as loading effects, humidity and moisture, high thermal effects and ageing tests. The specimens are divided into four groups so loaded specimen between 5 KN and 10 KN in dry mode and others are same loaded in splash mode subsequently, the higher sustained load with an exposure type of environment had more chance for failure. It was concluded that the harsher environment the more failure is occurred. Other author concentrated on combination

of thermal effect by fire degradation and compressive load on GFRP composites panels and it is showed the load effective on survival of GFRP degraded by fire. Creep test is considered to warrant consideration for structures undergoing prolonged loads such as hull-girders, concentrated machinery loads, or for submersibles subjected to prolonged external pressure. Creep strain of immersed GFRP composites was significantly higher than for the atmospherically aged laminates where ageing had been accompanied by flexure loading at set deflections (Gellert & Turley, 1999).

Li et al. (2017) studied the combined effect of different environment and sustained load on mechanical characteristics of FRP composite utilizing a system showed in Figure 9. The samples were immersed under unstressed state, and 30% and 60% of the ultimate failure load of the control sample. Glass fiber reinforced polymer (GFRP) specimens, were exposed to three different environmental conditions; freeze–thaw cycles, hygrothermal aging, and wet–dry cycles. The freeze–thaw conditioning was performed in fresh water at a rate of one cycle per day between -17°C ± 2°C and + 8°C ± 2°C. For comparison, 50, 100, 200, and 300 freeze–thaw cycles were used. For hygrothermal exposure, samples were immersed at high temperature (50 ± 2°C) and humidity (93 ± 3% RH) for the duration of 30, 90, 180, 360 days. An offshore wet–dry environment was simulated by immersion samples in 5% NaCl simulated seawater for 12 hours followed by accelerated blow-drying for12 hours per cycle. For comparison, 30, 90, 180, and 360 wet–dry cycles were used. The reduction in tensile strength of the CFRP specimens after 300 freeze–thaw cycles, when compared to the tensile strength of control sample, were 3.3%, 6.6%, and 12.0% at 0, 30%, 60% loading levels, respectively. This reduction was 16.0% and 22.8% for the GFRP specimens at 0 and 30% loading levels, respectively. The tensile strength of CFRP specimens reduced by 6.3%, 10.6%, and 15.7% in 0, 30%, and 60% loading levels respectively

after 360 days of hygrothermal exposure. However, the tensile strength reduced by 16.6% and 27.9% in 0 and 30% loading levels, respectively for the GFRP specimens. Similar to freeze–thaw and hygrothermal exposure, the tensile strength of samples conditioned with wet–dry cycles reduced with exposure time and loading level. For CFRP specimens, the tensile strength reduced by 7.5% to 10.4% and 12.1% for 0,30% and 60% for loading levels respectively after 360 wet–dry cycles whereas this respective reduction was 18.0% and 24.1% in 0 and 30% loading level for GFRP specimens.
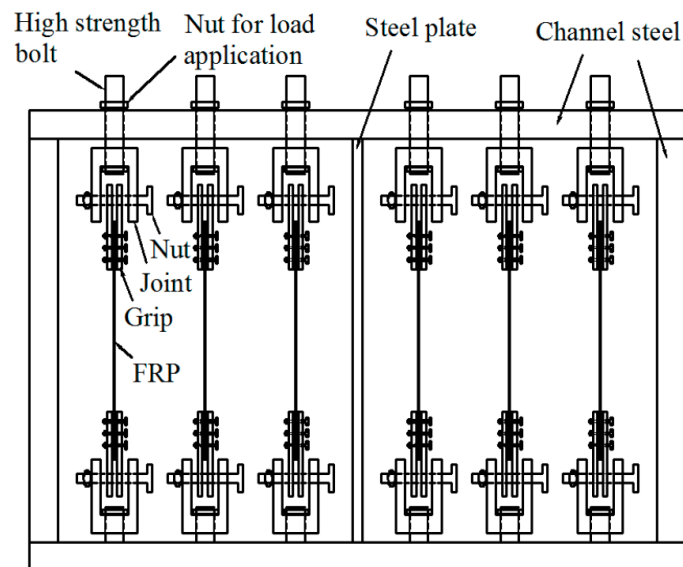
Figure 9: Schematic diagram of sustained loading apparatus
Li et al. (2017)

Abdel-Magid et al. (2005) evaluated the mechanical properties of E-glass/epoxy composite material. The samples were immersed in water at room temperature and at 65°C for the period of 500, 1000, and 3000 hours as shown in Figure 10. The sustained tension was kept constant to 20% of the ultimate strength of the material. The results show that the tensile strength of the samples reduced by 5% and 14% for the conditioning at room temperature for 500 hours and 1000 hrs

respectively. However, the respective decrease was 18% and 35% for the immersion at 65°C in 1000 hrs and 3000 hours.
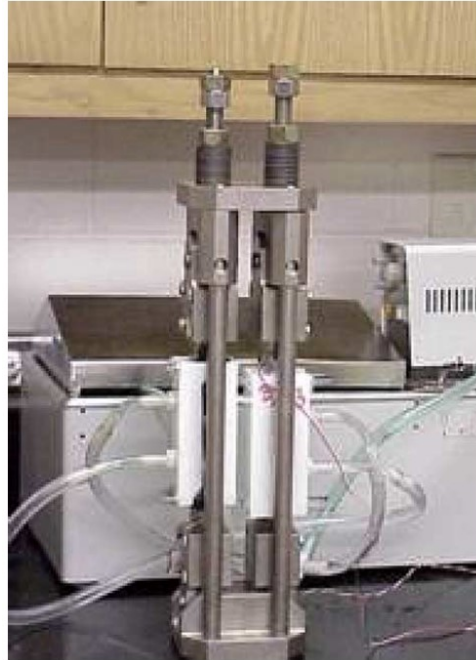
Figure 10: Constant load fixture and hot water bath.
(Abdel-Magid et al., 2005)

Wu et al. (2015) determined the tensile properties of unstressed and stressed carbon-fiber-reinforced polymer (CFRP) bars and glass fiber-reinforced polymer (GFRP) bars. The stress level was maintained between 10% and 60% of the tensile stress of the composite using an arrangement showing in Figure 11. In this study, four types of harsh environments were selected: de-ionized water, alkaline solution, acid solution, and salt solution, at 25°C, 40°C, and 55°C. The corrosive environment had minor and negligible effects on the degradation of composite for the sustained-load level load of 20%. For a stress level of 40%, degradation process was noticeably accelerated. The failure of the bars occurred due to creep load at the stress level of 60% and it accelerated by the simulated harsh environment.
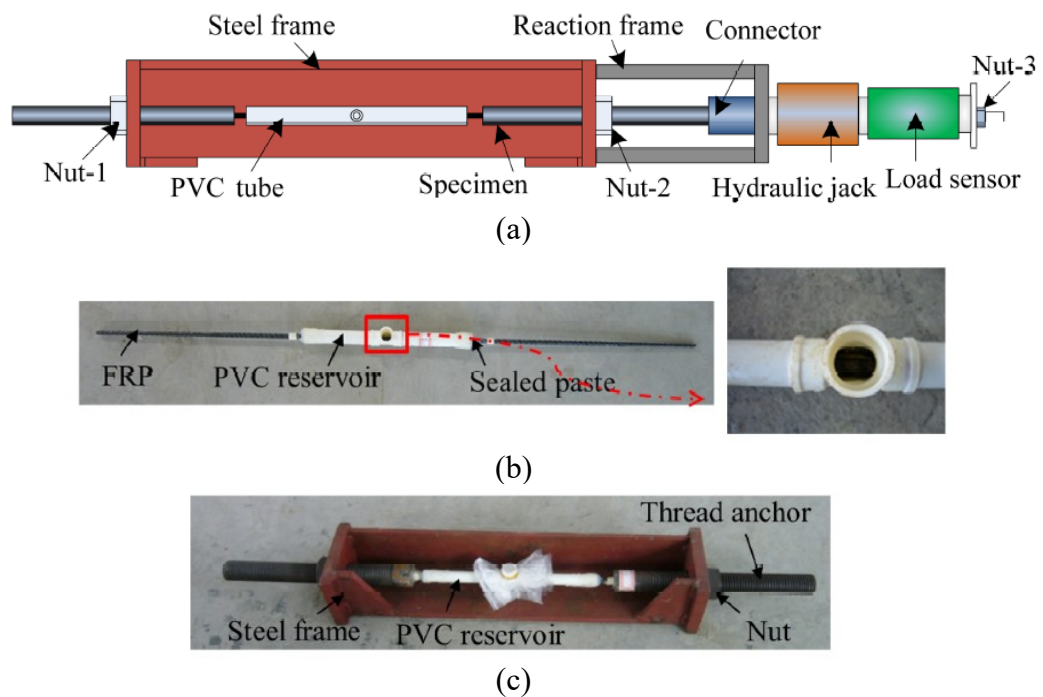
Figure 11: Specimen preparation: (a) device for axial-load application; (b) installed PVC reservoir; (c) prepared stressed specimen
(Wu et al., 2015)

The effects of moisture on the mechanical properties was investigated by Kafodya et al. (2015) on the CFRP samples conditioned in water and seawater at room temperature under sustained bending strain. The bending strain was maintained between 30% and 50% of the ultimate tensile strain of the samples as shown in Figure 12. The specimens were removed for the tensile test after 2, 4, 12 and 20 weeks of immersion. The decrease in the tensile strength was about 18% for water immersed and 13% in the seawater immersed samples for the strain level of 50%. The unstrained samples show slight decrease in the strength, about 9% and 12% for water and seawater immersed samples, respectively.

Figure 12: Bending fixture for CFRP plates.
(Kafodya et al., 2015)

Karbhari et al. (2007) determined the effects of sustained bending strain and moisture on durability of E-glass/vinylester composites. The specimens were conditioned with 0, 16.9, 35.9, 44.3, 51.2, and 57.5% of ultimate strain at a 23°C in water for different period of conditioning (4, 8 16, 32, 48, 80, and 112 weeks). The moisture uptake and the diffusion coefficient increased with an increase in the level of sustained bending strain. The tensile test results show decrease in tensile strength by 32.5% for unstressed specimens and 48% for the samples with highest level of bending strain after 112 weeks of exposure.

Zhang and Deng (2019) evaluated the durability of GFRP bars under sustained compressive load using a specially designed system shown in Figure 13. The samples were exposed at different compressive strength levels (0%, 20%, and 40%) for the period of 16, 60, and 90 days at different temperature (40°C, 60°C, and 80°C) in salt water and alkaline solution. After immersing in the salt solution at 80°C for 90 d, the strength retentions of the specimens with stress levels of 0%, 20% and 40% were 67%,

62% and 55% respectively. After immersing in the alkaline solution at 80°C for 90 d, the strength retentions of the specimens with stress levels of 0%, 20% and 40% were 44%, 36% and 24% respectively.
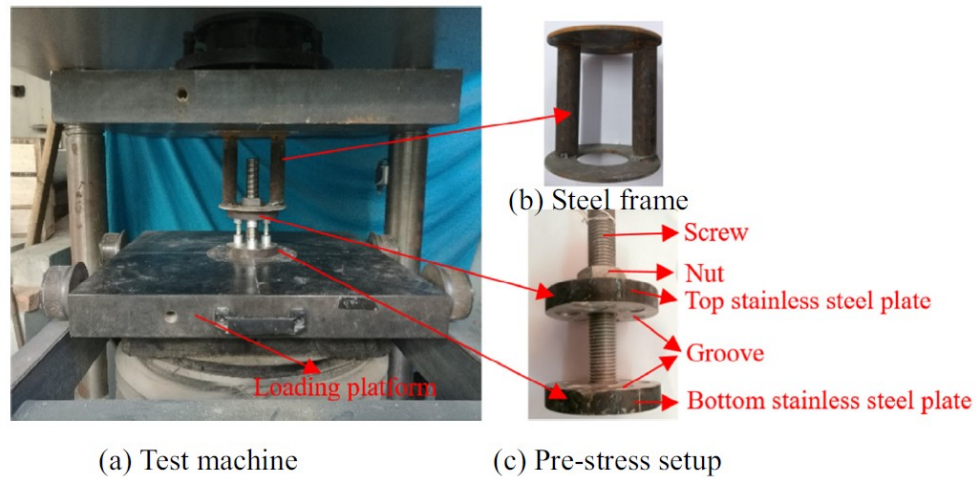
Figure 13: Imposing the sustained stress on the GFRP specimens.
(Karbhari et al., 2007)

The long-term performances of epoxy and polyurethane based CFRP plates were evaluated by Hong et al. (2017). The samples were conditioned in water/seawater under sustained bending (0%, 30%, and 58% of the tensile strain), shown in Figure 14. The strength of unstrained epoxy-based CFRP composite reduced to 90.8% and 89.2% for the samples immersed in water and seawater respectively at 60°C for 6 months. However, slight degradation was observed for unstrained PU-based CFRP samples. The strain level had significant impact of the tensile strength of both composite and it reduced by 12.1% and 13.8% in water and seawater immersed PU-CFRP composite with 58% of strain level at 60°C respectively. On the contrary, the respective reduction was 21.0% and 23.3% in water and seawater at 60°C.
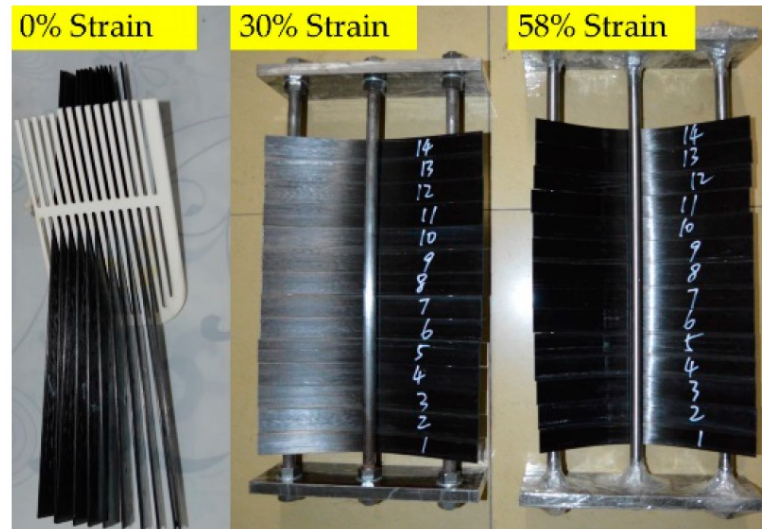
Figure 14: CFRPs under sustained 0%, 30%, and 58% bending strains, respectively.
(Hong et al., 2017)

2.4 Prediction Models

Some researchers conducted experimental work to evaluate the effect of the environmental condition on the mechanical, chemical and physical performance of composite materials subjected to short and long exposure time from approximately one year to 4 years. Therefore, prediction of the durability parameters is considered one of the important issues. The work on both durability assessment and its prediction need more attention.

There are various types of prediction models available in the literature for the prediction of the durability of composite materials for long term of exposure to particular conditions and these conditions may be included environmental conditions effect, sustained loads or both. One of these common methods is Arrhenius model which describes the degradation rate of the material as a function of temperature as presented by Equation (1):

$$K = A\, e^{\frac{-E_a}{RT}} \qquad\qquad (1)$$

This equation is expressed as follows by Chen et al. (2006), where "k" is the reaction rate or degradation rate (1/Time), "A" is constant of a material and degradation process, "E_a" is the activation energy or the minimum energy needed for molecules to form a reaction, "R" is the universal gas constant (8.3143 J/mol K) and "T" is the temperature in kelvin. The assumption used to utilize this approach is that the single dominant mechanism of degradation neither varies with the temperature range of accelerated ageing nor with time, but the rate of degradation increases with the increasing of temperature (Chen et al., 2006; Silva et al., 2014).

This model is often used when the temperature is the dominant factor of the accelerated ageing process. The Arrhenius equation can be written in other forms presented by Equations (2) & (3):

$$\frac{1}{K} = \frac{1}{A} e^{\frac{E_a}{RT}} \tag{2}$$

or

$$\ln\left(\frac{1}{K}\right) = \frac{E_a}{RT} - \ln(A) \tag{3}$$

From Equation (2) it can be interpreted that "K" is as the inverse of time needed for the material property to reach a certain value. Dejke (2001) explained concept of time shift factor which is the ratio between times required for certain decrease in the mechanical property at different temperatures are proportional to the inverse of degradation rate "K".

It can be observed that the natural logarithm of (1/K) provide the time for the property to reach specific value is a linear function with (1/T) with the slope of E_a/R (Chen et al., 2006; Silva et al., 2014). Chen et al. (2006) presented procedures for

predicting the durability of GFRP reinforcing bars embedded in concrete structure are based on Arrhenius relation and the accelerating aging tests are based on short term data. The GFRP reinforcing bars were exposed to simulated concrete solution at different temperatures 20°C, 40°C and 60°C. They used Equation (4) which is based on the Arrhenius relation by Phani and Bose (1987) by assuming that the GFRP bars degraded completely at infinite exposure time.

First Model $\qquad$ $SR(\%) = SR(t) = 100\,e^{-Kt}$ $\qquad$ (4)

Where "SR" is the percentile tensile strength retention of composite material which is residual of tensile strength divided by the original tensile strength and "t'" is the time of exposure.

Bank et al. (2003) presented another equation based on Arrhenius model which assumed that the retention strength approached to infinity at time equals zero as shown in Equation (5).

Second Model $SR(\%) = a\log(t) + b$ $\qquad$ (5)

Here, a and b are the regression constants and t is the exposure time. This model is also used for the prediction of durability of composite materials.

Davalos et al. (2012) derived an equation to predict the degradation of GFRP bars based on moisture absorption, as shown in Equation (6).

Third Model $\qquad$ $SR\,(\%) = (1 - j\,t^{\alpha+1})^2$ $\qquad$ (6)

Here, j is a factor accounting for solution concentration, temperature and other experimental conditions, α is a material constant and t is the immersion time.

Uomoto and Katsuki (1995) introduced a new model to predict the penetration of alkali into GFRP rods with time by using Fick's first law and assuming that the penetrated area is circular. The tensile strength of an area that has not been penetrated by the alkali is measured, but the tensile strength of a penetrated area has zero value; also, the tensile strength of the nonpenetrated area was similar to the tensile strength before the GFRP bar was exposed to the alkali, as shown Equation (7) below.

Fourth Model $$\qquad SR(\%) = 100 * \left(1 - \frac{\sqrt{2*D*C*t}}{R_o}\right)^2 \qquad\qquad (7)$$

D, C, t, and R_o are the diffusion coefficient (mm^2/h), alkaline concentration (mol/L), curing time (h) and radius of the GFRP rods, respectively.

Wang et al. (2015) described a new model that combines the effect of sustained loads and immersion time. This model is based on the Arrhenius equation coupled with a fracture mechanics principle, as shown in Equation (8).

Fifth Model $$\qquad SR(\%) = 100 \exp\left(-\frac{t}{\tau}\right) \exp(K\sigma) + \alpha \exp\left(-\beta(1-\mu)^2\right) \quad (8)$$

In this equation, t is exposure time, τ is the inverse of the degradation rate K, β, μ and α are regression constants, and σ is the ratio between the sustained stress and the ultimate stress of an unconditioned FRP composite.

In the light of the above, there are many points that have not been discussed in the literature and need more attention such as long-term exposure and sustained load. Therefore, the main objective of this research is to design and fabricate the multi-sample loading frame and conduct experimental work to assess the durability of two different composite materials. These are E-glass/epoxy and E-glass/polyurethane composites. This study includes the effects of sustained loading and environmental

degradation due to seawater and high temperature. In addition, to evaluate the durability of the composite, prediction models were developed to predict the tensile strength of two composites for long term exposure in seawater. These prediction models were used to predict unseen data. The results of all models were in good agreement with the experimental data.

Chapter 3: Research Methodology

The following steps have been followed to evaluate the composite durability experimentally and developing prediction models.

Task 1: Tensile sample preparation

Task 2: Construction of loading frame

Task 3: Long-term conditioning and testing

Task 4: Development of analytical models

Task 5: Calibration of analytical models with experimental data

3.1 Task 1. Tensile Sample Preparation

In this study, unidirectional E-glass/epoxy composite reinforced with 52 vol % of glass fiber and E-glass/polyurethane reinforced with 58 vol% of glass fiber were utilized. The samples were prepared from the panels in the manufacturing lab at Winona State University, USA. Samples with an average thickness of 3 mm were cut and tabbed according to ASTM D 3039 (D3039 ASTM, 2008). The dimensions of the specimen are given in Table 1 and Figure 15(a).

Table 1: Tensile specimen geometry

Parameters	Dimensions
Specimen length, L	250 mm
Specimen width, b	15 mm
Specimen thickness, h	3 mm
Gauge length, S	150 mm
Tab length, L_{tab}	50 mm
Tab thickness, h_{tab}	4 mm
Tab bevel angle	90^0

The specimens have GFRP end-tabs bonded onto both ends as shown in Figure 15(b) to give uniform load distribution and to promote failure in the loading-direction.

(a)

E-glass/epoxy

E-glass/polyurethane

(b)
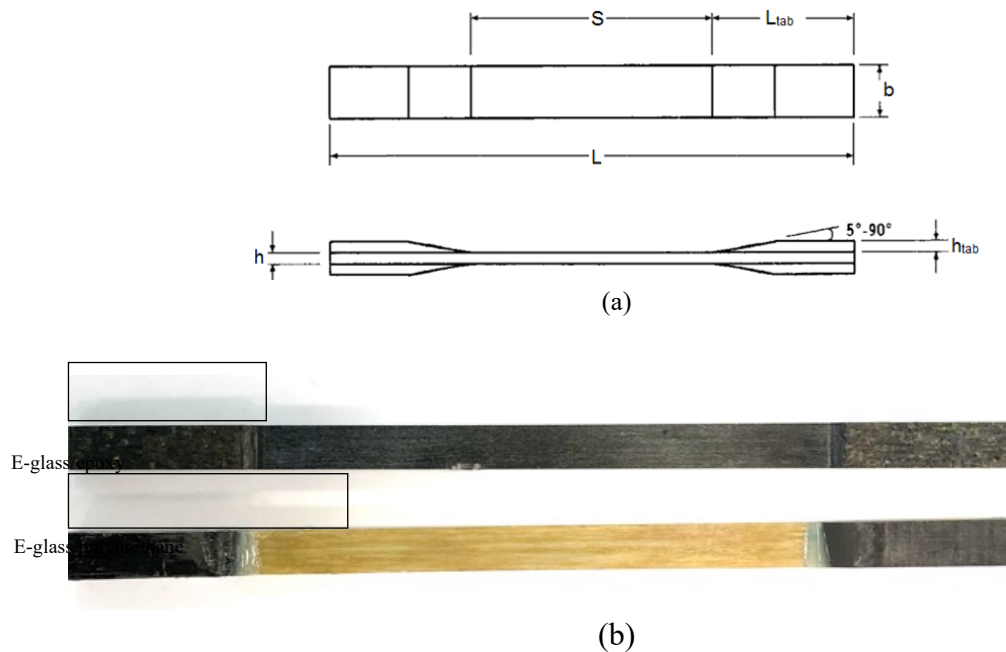
Figure 15: Tensile test specimen (a) line diagram of the sample (b) actual Sample

3.2 Task 2. Construction of Loading Frame

A robust loading frame was specially designed and fabricated in the Mechanical Engineering Lab at the UAE University (shown in Figure 16). The frame can load nine specimens simultaneously with a load capacity that will impart stresses in the range of 10% to 50% of the specimens' strength. The frame consists of chambers to allow specimens to be submerged in seawater while being loaded. The chambers are connected to a regulated heating bath to condition the specimens at various temperatures. The frame is connected to a laptop computer through data acquisition system to record the data (load and temperature) with time. Total of five loading frames were fabricated which can load 9 samples simultaneously.
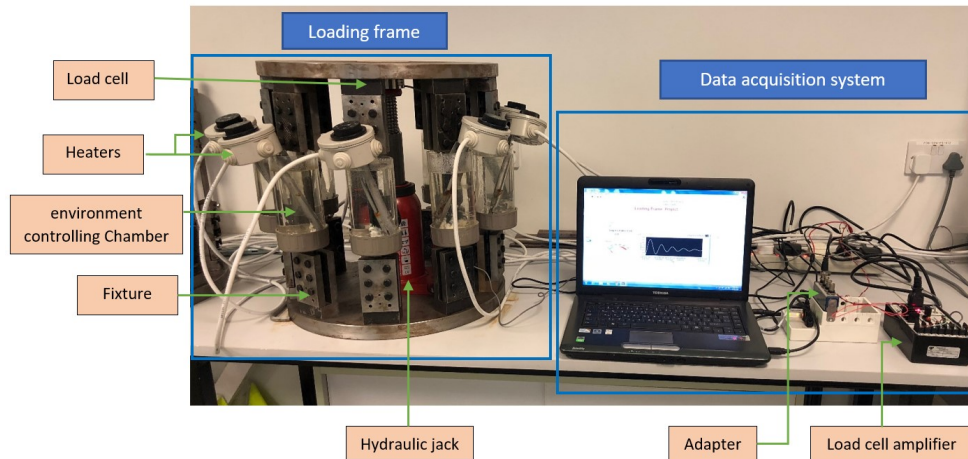
Figure 16: Designed and manufactured loading frame to investigate the durability of the composite

3.3 Task 3. Conditioning and Testing

Specimens have been conditioned in the materials lab in the mechanical engineering department at the UAE University and tested after every three months. Specimens conditioned for 15 months in seawater at room temperature (23°C), 45°C and 65°C. All samples were loaded to a stress level of 15% of the static strength of the material. Specimens weighed before the submersion in seawater and weighted again after removal from the seawater to determine the rate and amount of water absorption in the materials. The specimens were also inspected before and after conditioning for apparent damage to the surface. MTS testing machine was used to perform tensile tests according to ASTM Standard D-3039 to obtain the tensile properties of control and conditioned specimens (D3039 ASTM, 2008). Failure analysis performed using scanning electron microscope and FTIR to investigate the damage at the interface. Furthermore, the data was analyzed to evaluate the combined effect of seawater, temperature and sustained load on the selected composites. The conditioning and testing program is shown in Table 2.

Table 2: Long-term conditioning and testing of specimens (tested 3 samples at the interval of 3 months)

FRP Material	Conditioning	Duration (month)
E-Glass/Epoxy	SW, without load, 23°C	15
	SW, without load, 45°C	15
	SW, without load, 65°C	15
	SW, 15% strength, 23°C	15
	SW, 15% strength, 45°C	15
	SW, 15% strength, 65°C	15
E-Glass/polyurethane	SW, without load, 23°C	15
	SW, without load, 45°C	15
	SW, without load, 65°C	15
	SW, 15% strength, 23°C	15
	SW, 15% strength, 45°C	15
	SW, 15% strength, 65°C	15

SW = seawater

3.4 Task 4. Development of Prediction Models

Prediction models were developed for each material using accelerated testing and time - temperature superposition. The temperature used as the accelerating agent where specimens were conditioned and loaded at higher temperature. The changes in property curves plotted and shifted along the time scale to obtain a master curve. An equation for the master curve was established to predict the long-term properties of the materials at various stress levels. This method has been successfully used to predict long-term creep properties of composite materials (Gates & Feldman, 1996).

Higher temperature also used as the accelerating agent for durability in the marine environment where loaded specimens immersed in seawater with temperatures ranging from 45°C to 95°C. Accelerated tests were conducted for one month and changes in properties with time and temperature within the elastic range graphed

for each material. Time-temperature superposition used to shift the curves along the time scale to obtain master curves for long term-properties. An equation was developed for the master curves to predict the tensile strength of each material at any given time during its design life. The following schedule mentioned in Table 3 and Table 4 will be used for the accelerating tests:

Table 3: Accelerating test parameters for time-temperature superposition

FRP Material	Conditioning	Duration (month)	Temperature (°C)
E-Glass/Epoxy	SW, at 15% strength	3	23, 55, 65, 75, 85, 95
E-Glass/polyurethane	SW, at 15% strength	3	23, 55, 65, 75, 85, 95

Table 4: Effect of Loading

FRP Material	Conditioning	Duration (month)	Load Level (% Strength)
E-Glass/Epoxy	SW, const. Temp at 65°C	3	0%, 10%, 15%, 20%, 25%
E-Glass/polyurethane	SW, const. Temp at 65°C	3	0%, 10%, 15%, 20%, 25%

3.5 Task 5. Calibration of Prediction Models with Experimental Data

The prediction modes consisting of equations developed for the master curves calibrated and validated with the data obtained in Task 3. The master curves and the equations for tensile strength were compared with the experimental data; to determine the accuracy of the model and extrapolate the model's prediction with confidence beyond the 15 months.

Chapter 4: Materials and Research Methods

4.1 Materials

In this study structural properties of two types of Fiber reinforced polymer composites were analyzed. Two different polymeric material were used as matrix to fabricate the FRP composite: Epoxy and Polyurethane. For both composites, fiber E-glass was selected as a reinforcement. The E-glass/epoxy composite fabricated by reinforcing E-glass fiber to the epoxy resin using continuous lamination process. The volume of the fiber was fixed to 52% for all glass/epoxy composite samples. However, E-glass/polyurethane composite reinforced with 58 vol % of glass fiber were utilized. The E-glass/epoxy and E-glass/polyurethane composite panels were purchased form Gordon Composites Inc, USA and Creative Pultrusions Inc, USA respectively. These panels were cut, tabbed and sealed from the edges to avoid seawater penetration to the shoulders of the specimen. The samples preparation task was performed at Composites Materials Technology Center (COMTEC) at Winona State University (WSU), USA.

4.2 Testing Methods

4.2.1 Water Absorption

To determine the mass change behavior due to water immersion, the tensile samples were withdrawn from the water, wiped dry to remove surface moisture, and then the weight was recorded to the nearest 0.0001 g, as shown in Figure 17.

The percentage weight change of the composite samples (W) can be calculated by Equation (9) (Kootsookos & Mouritz, 2004a):

$$W\ (\%) = \frac{W_2 - W_1}{W_1} \times 100 \qquad (9)$$

Where,

W (%) = Weight change percentage, (%)

W_2 = Weight after immersion, g

W_1 = Weight before immersion, g
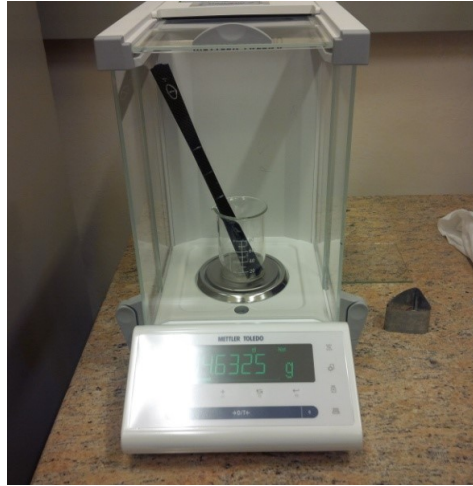
Figure 17: Sensitive scale with 4 decimal place resolution

4.2.2 Tensile Test

Tensile test was performed at room temperature (RT) on control and conditioned cured samples in accordance with ASTM D-3039, as shown in Figure 18. The tensile test was carried out using MTS Universal Testing Machine with 100 kN load cell at a crosshead displacement of 2 mm/min. The ultimate tensile strength σ_{ut} and tensile stress σ_i were calculated as per Equations (10 and 11):

$$\sigma_{ut} = \frac{P_{max}}{A} \tag{10}$$

$$\sigma_i = \frac{P_i}{A} \tag{11}$$

Where,

σ_{ut} = Ultimate tensile strength, MPa

P_{max} = Maximum load before failure, N

σ_i =   Tensile stress at the ith data point, MPa

P_i =   Load at the ith data point, N

A =   Average cross-sectional area of specimen, mm^2
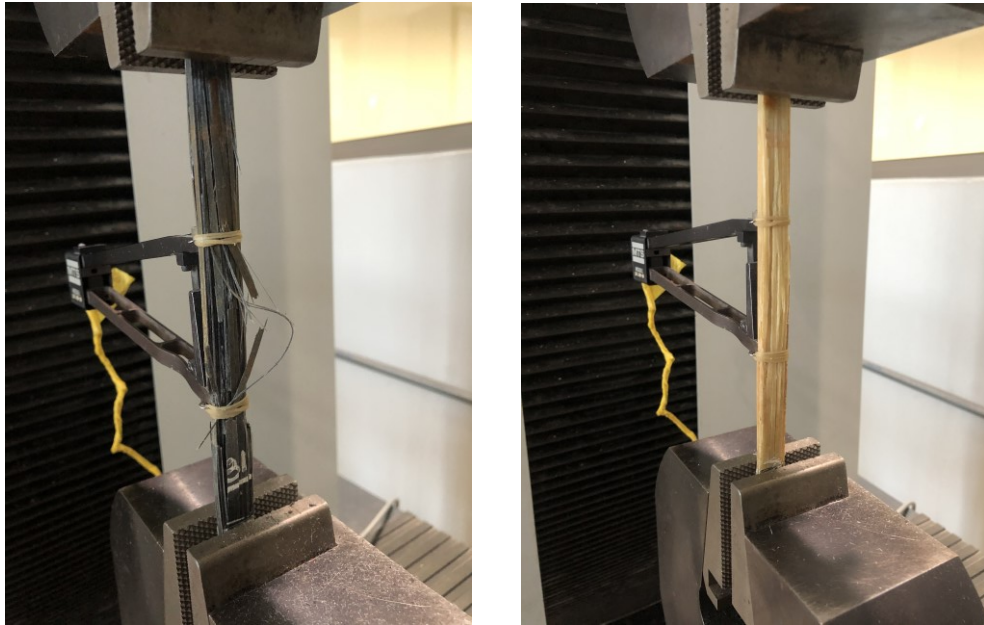
(a)   (b)

Figure 18: Tensile sample a) E-glass/epoxy sample b) E-glass/polyurethane sample

4.2.3 Differential Scanning Calorimetry (DSC)

Differential scanning calorimetry (DSC) tests were performed on control and conditioned samples to determine the glass transition temperature using the TA instrument Q200 series as shown in Figure 19. The test was conducted in an inert environment using nitrogen gas. The experiment was run from 25°C to 250°C with a heating rate of 10.0°C/min. Three samples for each condition were considered to determine the glass transition temperature.

Figure 19: Differential scanning calorimetry: TA instrument Q200 series

4.2.4 Scanning Electron Microscope (SEM)

The fracture surfaces of the tensile samples were examined for visible signs of fiber/resin degradation due to the long-term exposure using a Scanning electron microscope (SEM) on control and conditioned samples. The scanning electron microscope used was JEOL JSM-5600, as shown in Figure 20(a).
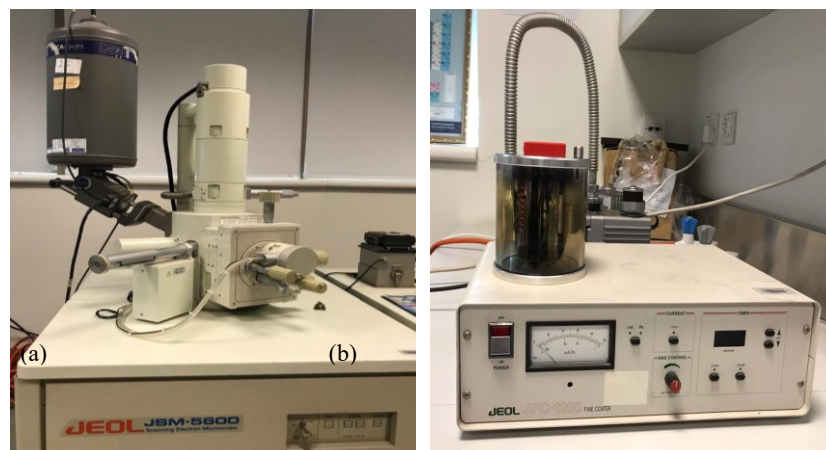
Figure 20: Equipment used for SEM test. (a) JEOL JSM-5600 scanning electron microscope (b) JEOL JFC-1200 fine coater

A small chunk of fibers from the failure surface of the samples were cut and fixed vertically on the SEM specimen stub using double-sided conductive carbon tape

and were coated with a gold layer using JEOL JFC-1200 fine coater, as shown in Figure 20 (b).

4.2.5 Fourier Transform Infrared Spectroscopy (FTIR)

The Fourier transform infrared spectroscopy (FTIR) was performed on JASCO FT/IR-4700 FTIR spectrometer, shown in Figure 21, at room temperature in the transmission mode. FTIR spectra were logged in between 600 cm^{-1} and 4000 cm^{-1} at a resolution of 2 cm^{-1} with 10 scans. Before testing the samples, Background spectra were taken in the empty chamber to eliminate the influence of moisture and CO_2 in air.

Figure 21: Fourier transform infrared spectroscopy (FTIR)

Chapter 5: Design and Development of Loading Frame

5.1 Loading Frame System

The motive of this part of the dissertation was to design and manufacture a rigid and innovative testing device to measure the durability of fiber reinforced polymer (FRP) composite materials in various environments. This device can be used to study the effect of different environmental conditions such as different temperatures and humidity under sustained loads for a long duration. These environmental conditions represent a practical and important life aspect that affect directly the degradation of composite materials which is taken into consideration in various industrial sectors that deals with polymeric and composite materials applications such as aerospace, automotive, construction, energy and medical field. The loading frame system consist of four subsystems: 1) Mainframe system; 2) Loading system; 3) Heating system; 4) Data acquisition system.

5.1.1 Mainframe System

It is the main structure of the loading frame which includes the top and bottom plate and fixture to grip the specimen. Stainless steel selected as the material for the loading frame as it is easily available and have high strength, uniformity, elasticity, and ductility. Also, it does not deteriorate with time, and most importantly steel is safe for heavy load application.

For the frame design, several options were explored to load multiple samples simultaneously. From all alternatives, loading frame with circular disc was selected which can accommodate nine samples simultaneously, shown in Figure 22. In this research three samples were tested for each condition to replicate the results. This

design helped in removal of samples in multiple of three. This shape is lighter compared to square design frame and less complex compared to nonagon design
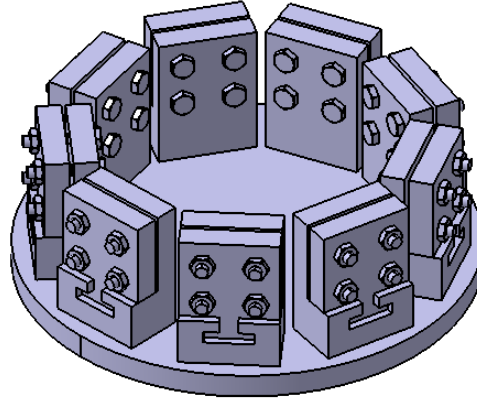
Figure 22: Selected frame design

During the selection of fixture, three designs (Simple jaw, L-shape jaw, Eyebolt jaw) were compared based on ease of fabrication, specimen slipping probability etc. Based on the comparison, L-shape jaw fixture was selected for the loading frame. The L-shape jaw fixture is shown in Figure 23. This type of fixture is easy to fabricate and it can hold the specimen accurately without slipping of the specimen. It is divided in two parts; lower jaw and upper jaw. In this fixture lower jaw is always fixed to the bottom or top plate by means of bolts, however, upper jaw can move and grip the specimen tightly.
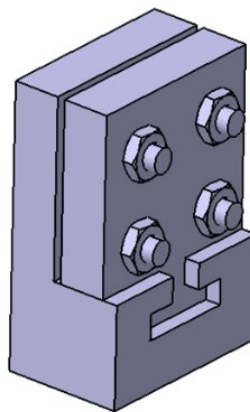
Figure 23: Selected fixture alternative

5.1.2 Loading System

5.1.2.1 Hydraulic Jack

The loading system consist of hydraulic jack and the load cell. The main objective of the hydraulic jack is to provide required force to condition the samples under sustained load over long period of time.

As it is shown in Table 5, five main bottle hydraulic jack alternatives were suggested based on its ability to achieve the required specification. The selection of the final alternative was based on extensive study to ensure the existence of all essential features that will enable the jack to perform its intended function properly. The selected device must include all required features which are the hydraulic jack ability to provide the maximum required load capacity that was calculated to be 20 tons, affordable cost, availability in the market, fulfill geometric constraints, ease of performance and efficient connectivity with other system devices.

Alternative (1) is being produced by Mega company which is a Spanish brand that offers good devices with affordable prices. However, the main disadvantage is that the closed height of the jack exceeds the limited available height for jack installation inside the loading frame. Also, the deice has relatively large base dimension compared to other alternatives which is not recommended since it occupies more space. Based on the project design requirements it is preferred to reduce the overall device weight through minimizing the size as much as possible.

Table 5: Bottle Hydraulic Jack Alternatives

Alternative	1	2	3	4	5
Product Image					
Brand	Mega	ENERPAC	HYDRAFORE	ATD	ATD
Model Number	MG-20	RCH-206	YG-20100K	ATD-7387	ATD-7386
Load Capacity	20 Ton	20 Ton	20 Ton	20 Ton	20 Ton
Country	Spain	US	US	US	US
Lift / Jack Type	Bottle	Bottle	Bottle	Bottle	Bottle
Mechanism Type	Hydraulic	Hydraulic	Hydraulic	Hydraulic	Hydraulic
Frame Material	Steel	Aluminum	Steel	Hard-cast steel	Hard-cast steel
Product Weight (kg)	12.1	14.1	10	9.53	11.8
Dimensions (mm)					
Product Weight (kg)					
Max. Lift Height	459	461	323	285.75	473.1
Closed Height	384	306	223	165.1	241.3
Product Width	144	98	98	149.2	149.2
Product Length	221	98	98	162	162
Market					
Price (AED)	400	3750	1169	240	248.2

Alternative (2) has several advantages such as being produced by ENERPAC which is a leading US brand in the industry of high-pressure hydraulic devices and this ensures the product good quality. Also, the circular geometry of the hydraulic jack body allows exposing more area to the applied load making the system more stable by having a uniform distributed load. The downside of purchasing this jack alternative is its expensive price which doesn't even include the pump, hose and gauge. Therefore, additional payment will be required to complete the jack kit

Alternative (3) resembles the same features of alternative (2) but with a cheaper price which makes it a more suitable alternative to be selected. Unfortunately, the downside of this alternative is that the company doesn't supply the entire jack kit which will require us to purchase the pump, hose and gauge separately from another brand that will eventually add extra payment to the total jack cost. In addition to that, the possibility of hydraulic oil leakage will increase due to combining several parts together from different brands which will make the system quite messy and more difficult to maintain easy usage.

Alternative (4) and (5) have effective small base dimensions compared to other alternatives which makes them more practical options. However, alternative (4) main disadvantage is having a short maximum lift height which will require designing a higher base which will result in raising the total manufacturing price. For this work, ATD-7386 bottle hydraulic jack was selected from available options.

5.1.2.2 Load Cell

Based on the selected design of mainframe system, compression type load cell was selected to measure the applied load. Different alternatives of compression load cell were suggested based on the desired capacity of 20 tons. After analyzing and studying the available different types of compression load cells in the market, these six alternatives were highly recommended.

As it is shown in Table 6, alternatives (1), (2) and (5) have sufficient capacity of 25 tons, and their small dimensions make them fit in very small spaces. Therefore, these alternatives are very practical in such application because our system has a very restricted space for installing the load cell. However, they are not easily available in the market especially in the gulf region.
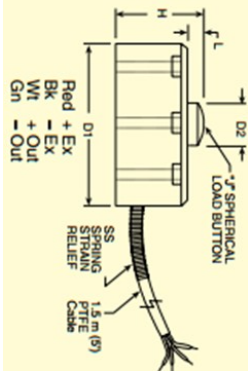
On the other hand, alternatives (3), (4) and (6) can be supplied to the whole of the GCC countries by Dealer Company called PETRA which makes them better choices comparing to the previous ones. Moreover, they meet the load capacity requirement of having at least 20 tons. Another factor must be taken into consideration is the dimension constraint. To clarify, the compression load cell must have a relatively small outer diameter because of the restricted available area in the system. However, alternatives (3) and (4) have larger outer diameter comparing to alternative (6).

Eventually, the process of selection was based on certain factors which are geometric constraints, easy availability in the market, easy installation and cost effective as well. Therefore, it was decided to select alternative (6) CSP-M Compression Load Cell to be our preferable alternative since it perfectly meets all the previous discussed requirements.

Table 6: Compression Load Cell Alternatives

Alternative	Information					
	1	2	3	4	5	6
Load cell Type	Miniature Industrial Compression Load Cell with Through-Body Mounting Holes	Miniature Load Cell Industrial Compression Load Cell	CRI C3 Compression Load Cell	BM14A Compression Load Cell	CSP-M Compression Load Cell	Load Button Load Cell
Product Image						
Frame Material	Stainless Steel	Stainless Steel	Stainless Steel	Stainless Steel	Stainless Steel	Stainless Steel
Country	United Kingdom	United Kingdom	Spain	Netherlands	United States	United States
Load Capacity	25 ton	25 ton	20 ton	25 ton	25 ton	25 ton
Model Number	LCGB-50K	LCGD-50K	CRI-C3	BM14A	FSH04033	CSP-M
Dealer	OMEGA	OMEGA	PETRA	PETRA	FUTEK	PETRA
Brand	OMEGA	OMEGA	SCELL	Zemic	FUTEK	Vishay Precision Group
D1	76	76	128	73	75.7	72
D2	20	20	35	31.8	19.8	32
H	38	38	54	82.5	38.1	83
L	4.6	4.6	14	6.5	4.6	6.5
Price (AED)	1873.18	1762.99	1300	1700	1300	1400

Dimensions (mm)

5.1.3 Heating System

Heating system consist of heating bath and heaters. In this system nine heating bath used for the nine samples i.e., each specimen has its own heating bath/chamber and heater. This arrangement provides more accuracy in the results and safety as if something goes wrong in any heating bath (i.e., burning of chamber, leakage of fluid), the test on the other specimens will not be affected, Also, it is available in the market with different sizes.

The selection of a proper heating element for the testing device depends on, dimensions of the heater, temperature range, environment conditions, cost, and delivery availability. The require dimension for the heating element is to have the height less than the specimen's height and to a have the diameter smallest size possible to fit the heating bath. Few alternatives for the heaters are shown in Table 7. In addition, the required temperature range should be from room temperature to 100 °C. The heaters should be corrosion resistant and can handle chemical changes in the water.

Table 7: Heating element Alternatives

Heaters Alternative	1	2	3
Heater Name	Suburban Water Heater Element	Cartridge Heater (Rod Heater)	Dernord Immersion Water Heater
Heater Picture			
Heater Specification	• Conductors bonded together for ease in handling • All copper strand core with PVC coating • Manufactured to highest quality standards 100% copper conductor • Temperature rating of 80 degree C at 60 V or less,	• High watt density design • Vibration resistant • High thermal conductivity • Uniform heat transfer • High electric strength • Maximum watts accommodated in small length • Designed as per customer specification • Longer life	• High Watt Density Stainless Steel Immersion Water Heater Element • Provides 2000 W 120 V of power • Stainless steel surface has electropolish • Listed to the safety standards • Supplied with silicon sealing washer which is flexible and waterproof
Heater Dimension	254x81.28x50.8 mm	As required	254x30.48x20.32 mm
Dealer Name	Amazon	Dubai Heater	Amazon
Brand Name	Suburban	Dubai Heater	Dernord
Heater Price	74 AED	180 AED	114 AED

The rod type heater was utilized and purchased from Dubai heaters (local supplier). These heaters could be fabricated with required dimensions and temperature ranges with high quality. Also, it is economical, waterproofed and applicable in different pH level. This heating element comes with a digital control system to indicate and control the temperature of heater.

5.1.4 Data Accusation System

The loading frame is connected to a data acquisition device for receiving electrical signals of sustain load measurements and store in microcontroller. This microcontroller processes the data and transmits the digital signals representing the sustain load measurements to a load monitoring device or laptop. The various graphs can be plotted to monitor the applied load with the time.

5.2 Assembly of Loading Frame

This section shows the assembly/position of various parts of the loading frame. CATIA software was used to create schematic drawings and the 3D model of the system. Table 8 indicates the list of components designed for this system.

Table 8: Design components

Number	component
1	Top and bottom plate
2	Upper jaw
3	Lower jaw
4	Frame's bolt
5	Fixture's bolt
6	Fixture's nut
7	Load cell's upper mounting
8	Load cell's lower mounting
9	Load Cell's upper mounting bolt
10	Load Cell's upper mounting nut

For the proper explanation and position of each part, assembly drawings are represented from Figure 24 to Figure 28.

Figure 24: Model of load cell and it's mounting

Figure 25: 3D model of load cell and hydraulic jack

Figure 26: Model showing top frame and upper mounting assembly

Figure 27: Final concept 3D model
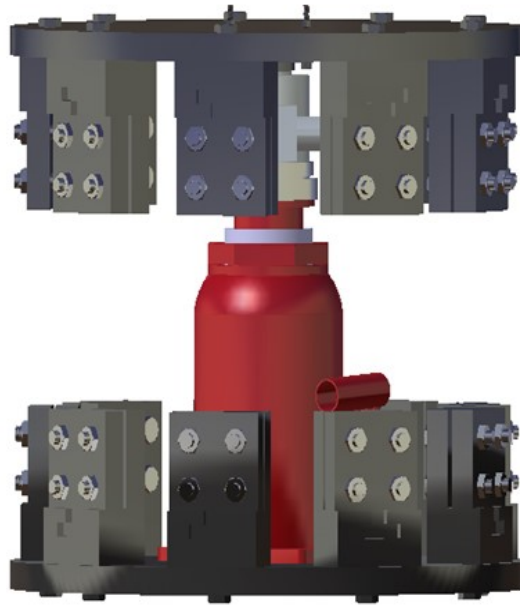
Figure 28: Final concept 3D model assembly

5.3 Claims of the System

This versatile loading frame can be used in research and development section of all companies, dealing with composite materials such as marine, aircraft, civil infrastructure, automobile, oil and gas companies etc. This system can also be utilized in research centers and academic institutions. Figure 29 shows the loading frame with the data acquisition system. The loading frame is loaded with a total of 9 specimens under sustained load. The setup allows all specimens to be conditioned at different environments (e.g., high temperature, salt water etc). The environmental conditions and effects can be monitored and controlled by connected data acquisition system.

The loading frame has following features:

1. The loading frame is comprised of 9 sub-frames and can accommodate 9 test specimens; each sub-frame structure is independent of the others.

2. The loading frame utilizes a compression load cell (secured between the top plate and the hydraulic jack) for measuring the applied load transferred to the specimen using hydraulic jack.

3. The loading frame is equipped with heaters located inside the environmental chambers.

4. The loading frame is connected to a data acquisition device for:

   a) Receiving electrical signals of sustain load measurements

   b) Converting the received electrical signals into digital signals, and

   c) Transmitting the digital signals representing the sustain load measurements to a load monitoring device.

5. Regulators can be connected to the environment controlling chambers to obtain the desired environmental conditions within the environment controlling chambers.

6. The load monitoring device comprises microprocessor for receiving and monitoring the sustain load measurements of the one or more test specimens.
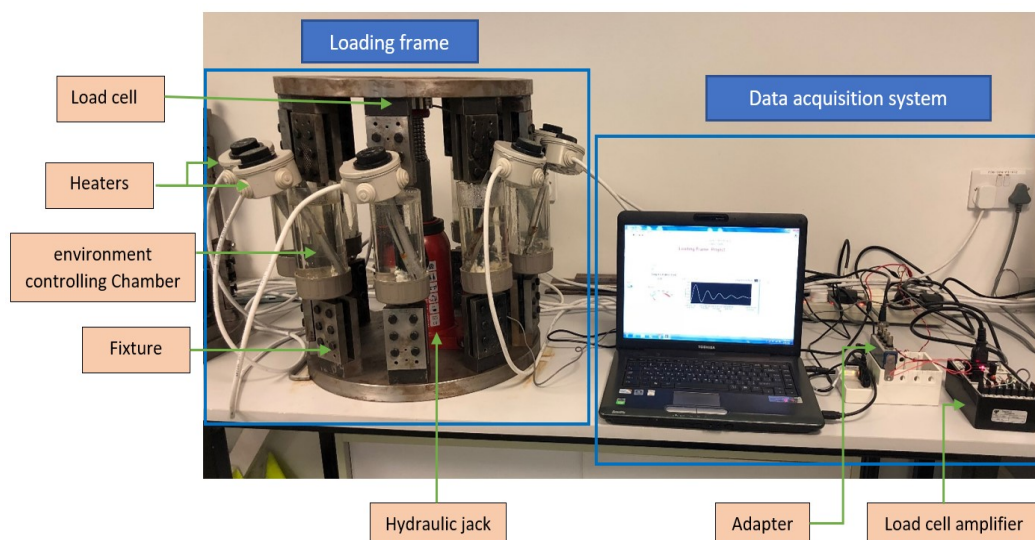
Figure 29: Experimental set-up used by principal investigators for composites durability

Chapter 6: Results and Discussion

Tensile specimens of 3 mm average thickness were prepared from E-glass/epoxy and E-glass/polyurethane composite material according to ASTM Standard D-3039 (Materials, 2006) for conditioning and testing. The cut edges of the specimens were sealed by a thin layer of adhesive prior to conditioning. The specimens were conditioned by immersion in three tanks of seawater from the Arabian Gulf. The tanks were maintained at three different temperatures (23°C, 45°C, and 65°C). To determine the effect exposure duration under sustained load, the samples were immersed with 15% sustained load (15% failure load) for the immersion period varied from 3 to 15 months using loading frame which was designed and manufacture for sustained load application in this work. Furthermore, comparison was performed between the samples immersed without load and with sustained load. In addition to determine the effect of seawater exposure duration, individual effect of different temperatures and sustained load was investigated to analyze the degradation of composite materials in seawater environment. At least three replicate specimens of each material were removed from their respective conditioning chamber every three months to conduct the tensile test. Results of control (unconditioned) and conditioned samples are presented and discussed in the following sections.

6.1 Water Absorption Test

The weight of specimens was taken before immersion into the water at different temperatures. Specimens were removed from water tank after every three months to determine the change in the weight. Table 9 and Table 10 shows the percentage change in the weight of the E-glass/epoxy and E-glass/polyurethane specimen after different

Table 9: Absorbed water content (%) in E-glass/epoxy composite

| Exposure time (months) | E-glass/epoxy | | | | | |
| | No-load (NL) | | | Sustained load (SL) | | |
	23°C	45°C	65°C	23°C	45°C	65°C
3	0.9 ± .21	1.7 ± .21	2.8 ± .18	1.05 ± .21	1.8 ± .16	2.9 ± .11
6	1.4 ± .22	1.9 ± .19	3 ± .21	1.4 ± .18	2.2 ± .12	3.3 ± .09
9	1.7 ± .11	2.7 ± .11	3.8 ± .11	1.9 ± .11	2.9 ± .14	4.1 ± .15
12	2.6 ± .19	3.4 ± .12	5.1 ± .17	2.8 ± .15	3.7 ± .21	5.5 ± .18
15	3.1 ± .14	3.9 ± .07	5.7 ± .14	3.4 ± .1	4.3 ± .2	6.3 ± .21
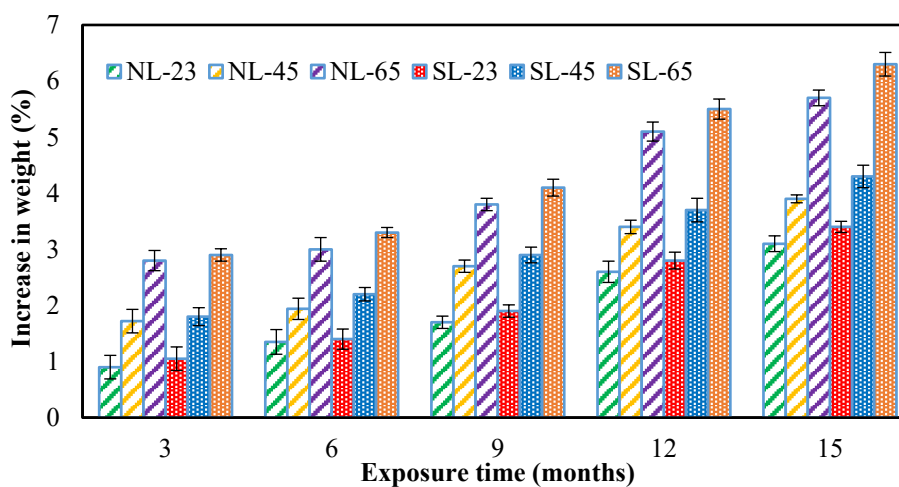
(a)
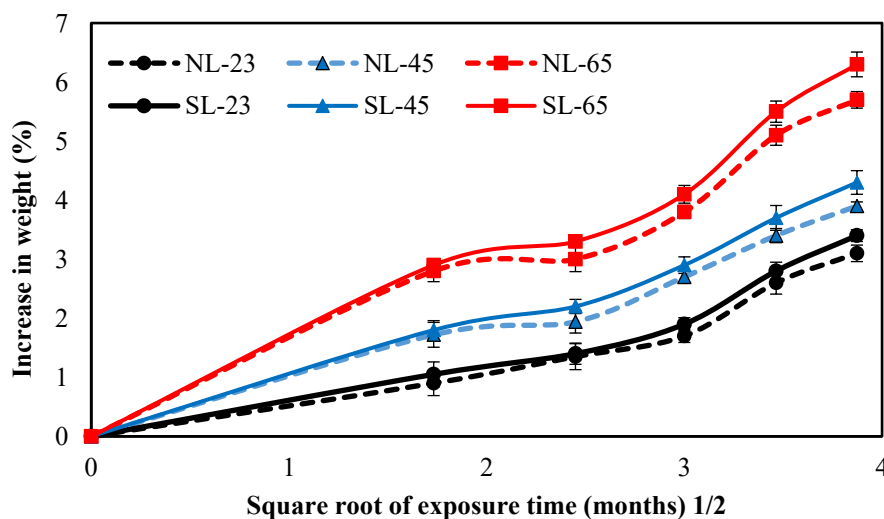
(b)

Figure 30: Variation in weight of E-glass/epoxy composite with conditioning duration and temperature

periods of immersion. An increase in the weight of the specimen was observed at 23°C, 45°C, and 65°C for E-glass/epoxy specimens shown in Figure 30(a). The water absorption or increase in weight was 3.1%, 3.9% and 5.7% for samples immersed without sustained load after the immersion of 15 months at 23°C, 45°C, and 65°C respectively. However, the weight of samples immersed with sustained load (15% of failure load) increased by 3.4%, 4.3%, and 6.3% after the immersion of 15 months at 23°C, 45°C and 65°C, respectively.

An increase in the weight of the specimen was observed at 23°C, 45°C, and 65°C for E-glass/polyurethane specimens shown in Figure 31(b). The water absorption or increase in weight was 3.6%, 4.3% and 5.1% for samples immersed without sustained load after the immersion of 15 months at 23°C, 45°C and 65°C respectively. However, the weight of samples immersed with sustained load (15% of failure load) increased by 3.8%, 4.5%, and 5.4% after the immersion of 15 months at 23°C, 45°C and 65°C, respectively.

Table 10: Absorbed water content (%) in glass/polyurethane composite

Exposure time (months)	E-glass/polyurethane					
	No-load (NL)			Sustained load (SL)		
	23°C	45°C	65°C	23°C	45°C	65°C
3	1.6 ± .11	2.1 ± .09	3.1 ± .19	1.7 ± .12	2.2 ± .09	3.2 ± .12
6	1.9 ± .09	2.4 ± .11	3.3 ± .12	2 ± .09	2.6 ± .11	3.6 ± .11
9	2.6 ± .12	3 ± .15	3.8 ± .08	2.7 ± .14	3.3 ± .18	4.1 ± .06
12	3.2 ± .14	3.8 ± .17	4.7 ± .18	3.3 ± .13	4 ± .08	4.9 ± .12
15	3.6 ± .17	4.3 ± .2	5.1 ± .13	3.8 ± .14	4.5 ± .11	5.4 ± .09
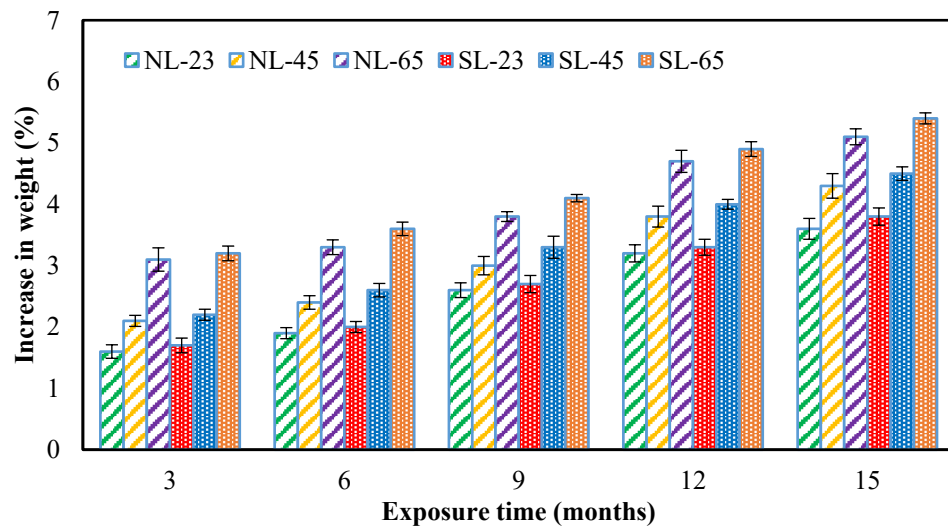
(a)
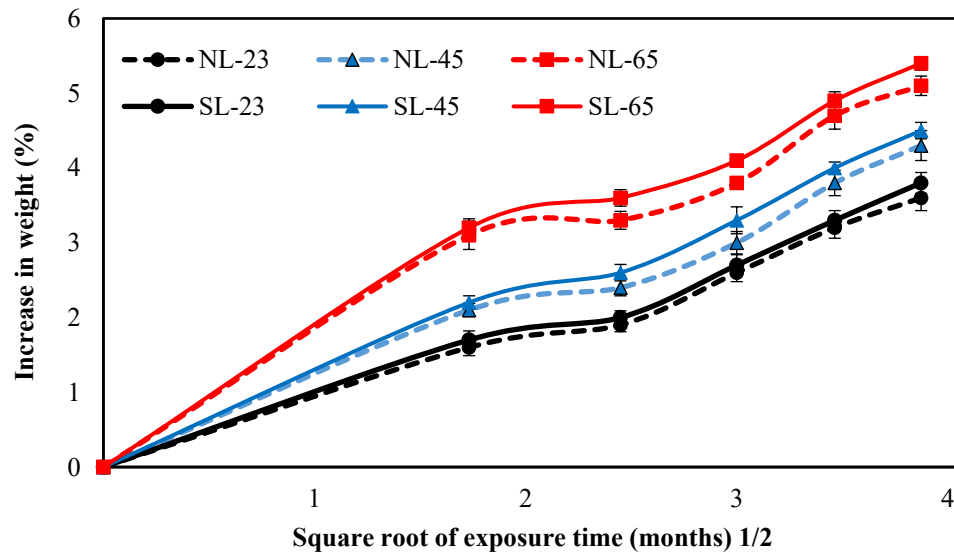
(b)

Figure 31 : Variation in weight of E-glass/polyurethane composite with conditioning duration and temperature

If we see the curves shown in Figures 30(b) and 31(b), it possesses three stages: linearly increasing at the first stage, slightly dropping at the second stage, and dramatically increasing at the third stage. Furthermore, the first stage also conforms to the typical Fickian diffusion process and the higher the exposure temperature is, the higher the diffusion rate is. The second stage should be mainly attributed to the resin

degradation (e.g. the hydrolysis of resin and dissolution of small molecular monomer) of the FRP surface during exposure to seawater, and the loss of resin could counteract and even exceed the moisture diffusion rate. Consequently, the third stage started as the sufficient defects allow more moisture permitted into the matrix, and the moisture diffusion contents dramatically increased due to the significant capillarity.

The results show that water absorption was higher in samples immersed with sustained load as compared to without load samples, and this could be due to the stretching of micro-voids presents in the samples immersed under sustained load. The micro-voids may elongate due to the stretching/tension developed in the samples immersed under sustained load which increased the absorption of water molecules. However, the general increase in weight, for both groups, is due to the water absorption that occurs through diffusive and/or capillary processes. Diffusion is considered a key process under which moisture penetrates polymeric composites and is known to be a matrix-dominated phenomenon in which water is mainly diffused in the matrix (Akbar & Zhang, 2008; Ray, 2006). The capillary process involves moisture being drawn into voids and microcracks at the fiber/matrix interfaces, in which the cracks provide a transport system for moisture penetration (Li et al., 2016; Patel & Case, 2002).

Moreover, for all exposure times, it was observed that higher absorption occurs at higher exposure temperatures, for both composites, which therefore indicates that higher temperatures accelerate the absorption process, which could be due to the deteriorating effect of temperature in generating higher degradation (such as micro-voids), which in turn induces higher absorption. Similar findings were reported in the literature, where higher temperatures are observed to have more influence in

accelerating the moisture absorption and degradation process in polymers (Almudaihesh et al., 2020).

As seen in the literature, the extent of deterioration that takes place in fiber reinforced polymers due to environmental exposure is associated with the amount of moisture absorbed (Ray, 2006; Reis et al., 2018), therefore it is important to highlight that the highest increase in weight due to water absorption reported was 5.7% and 5.1%, in the E-glass/epoxy and E-glass/polyurethane specimen immersed without load at the exposure temperature of 65°C for the exposure period of 15 months.

6.2 Tensile Properties

6.2.1 Effect of Exposure Time

6.2.1.1 E-glass/Epoxy Material

The tensile test was conducted after removal of the samples from the seawater immersion. Figure 32 shows the conditioned samples before and after tensile test. Tensile strength, of control and conditioned samples of E-glass/epoxy are shown in Table 11. Figure 33 shows the tensile strength of the no-load and sustained load immersed specimen at different temperature.

<p style="text-align:center">(a)   (b)</p>
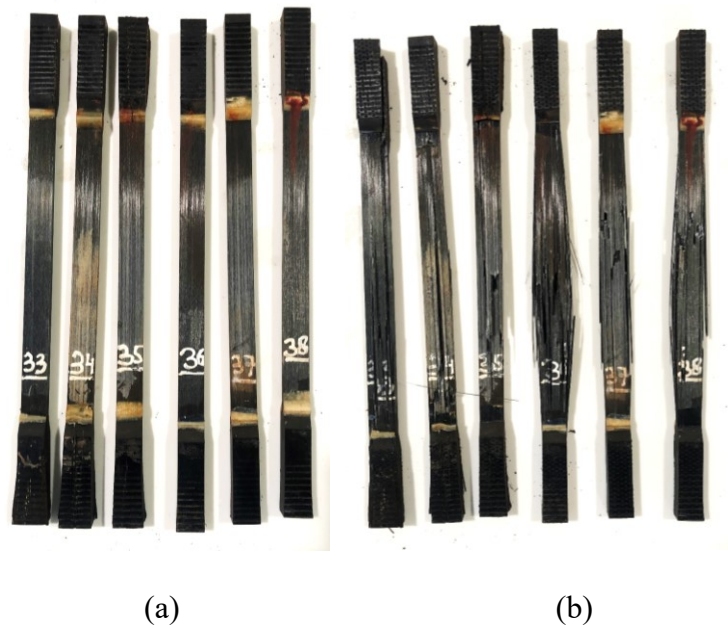
Figure 32: E-glass/epoxy composite samples a) before tensile test b) after tensile test

The tensile strength of no-load immersed specimen reduced only by 1.1% at the immersion of 15 months at 23°C whereas the drop in the strength was higher comparatively at 65°C for the same duration of time. The strength reduced by 11% from 811 MPa to 721 MPa. Sample immersed at 45°C had the intermediate effect on the durability of composite and it reduced to 94.5%. The tensile test results for the samples immersed without load for 90 months are also added to Table 11 and Figure 33 (Mourad et al., 2019). It shows that the tensile strength of E-glass/epoxy composite reduced by 8.2%, 25.7% and 49.9% after immersions of 90 months without load at 23°C, 45°C, and 65°C respectively.

Tensile strength of samples immersed with 15% sustained load reduced by 6.2% and 11.3% at the immersion of 23°C and 45°C whereas a significant decrease in the tensile strength was noted at 65°C for 15% sustained load specimen and it reduced by 18.2% from 811 MPa to 663 MPa. The reduction in the tensile strength for no-load immersed specimens was gradual at all temperatures. The tensile strength for samples

immersed under sustained load at 65°C reduced gradually by 6.3% from 811 MPa to 760 MPa within 6 months and continued to 663 MPa with comparatively faster rate in the remaining 9 months. The observation shows that the tensile strength reduction was 64% higher compared to no-load immersed samples for the exposure duration of 15 months at 65°C.

Table 11: Tensile strength of E-glass/epoxy samples conditioned in seawater without load and with sustained load (15% of failure strength) at 23°C, 45°C and 65°C for the period of 15 months

Exposure time (months)	Tensile strength (MPa)					
	No-load (NL)			Sustained load (SL)		
	23°C	45°C	65°C	23°C	45°C	65°C
0	811 ± 45	811 ± 45	811 ± 45	811 ± 45	811 ± 45	811 ± 45
3	809 ± 47	804 ± 43	796 ± 38	799 ± 22	782 ± 21	778 ± 18
6	807 ± 52	797 ± 25	778 ± 22	788 ± 29	776 ± 28	760 ± 32
9	806 ± 48	783 ± 32	751 ± 27	780 ± 11	757 ± 22	724 ± 29
12	803 ± 43	774 ± 41	734 ± 47	768 ± 35	731 ± 34	684 ± 36
15	802 ± 38	766 ± 28	721 ± 24	761 ± 18	719 ± 17	663 ± 21
24	778 ± 87	687 ± 35	502 ± 51	-	-	-
36	775 ± 9	659 ± 31	484 ± 22	-	-	-
60	770 ± 53	646 ± 43	424 ± 53	-	-	-
72	758 ± 22	625 ± 30	413 ± 27	-	-	-
84	750 ± 34	612 ± 42	409 ± 85	-	-	-
90	744 ± 6	602 ± 21	406 ± 27	-	-	-
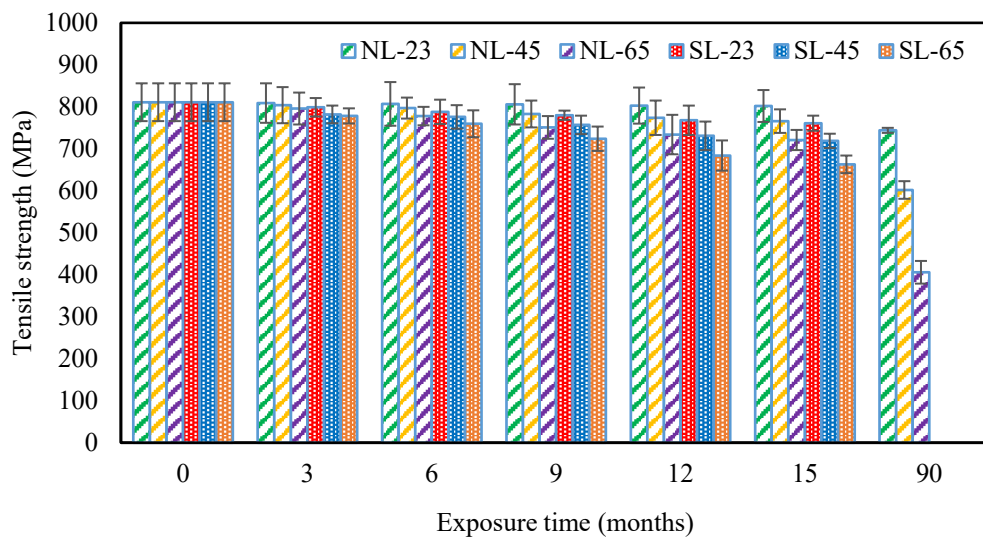
Figure 33: Tensile strength of E-glass/epoxy composite after the immersion of 15 months

The glass fiber shares most of the load applied to the laminates, and the fiber/matrix interface plays an important role in load transmission (Hughes, 1991). Therefore, the deterioration of the fiber/matrix interface due to water immersion led to a decrease in the fiber/matrix interface load transmission efficiency; as a result, the mechanical properties of the composite deteriorated. Previous studies have shown a similar behavior in which the strength decreases immediately after immersion and gradually decreases to saturation depending on the amount of water absorbed in the sample (Garcia-Espinel et al., 2015; Murthy et al., 2010). Therefore, it was suggested that the deterioration of the mechanical properties greatly depended on the deterioration of the fiber/matrix interface resulting from water immersion.

Table 12 and Figure 34 indicates that seawater immersion has slightly affected the elastic modulus of the samples conditioned at 23°C, 45°C, and 65°C. The elastic modulus varied from 37.1 GPa to 37.8 GPa, 37.2 GPa and 34.8 GPa for specimen immersed for 15 months at 23°C 45°C, and 65°C respectively. The tensile modulus of the composite reduced for the immersion of 90 months under all environmental

conditions which indicate a reduction of the stiffness of the composite for long term immersion.

Table 12: Tensile Modulus of E-glass/epoxy samples conditioned in seawater without load and with sustained load (15% of failure strength) at 23°C, 45°C and at 65°C for the period of 15 months

Exposure time (months)	Tensile modulus (GPa)					
	No-Load (NL)			Sustained load (SL)		
	23°C	45°C	65°C	23°C	45°C	65°C
0	37.1 ± 2.5	37.1 ± 2.5	37.1 ± 2.5	37.1 ± 2.5	37.1 ± 2.5	37.1 ± .03
3	37.8 ± 2	37 ± 1.7	35.4 ± 1.7	39.9 ± .9	40.1 ± .7	40.5 ± .4
6	35.1 ± 3	34.7 ± 2.1	33.6 ± .6	41.2 ± .7	39.5 ± 1.3	42.3 ± 1.7
9	36 ± 1.8	35.5 ± 1.5	34 ± 1.2	40.5 ± .9	40.2 ± 1.2	42.6 ± 2
12	38.2 ± 2.5	37.2 ± 2	35.4 ± 3.1	37.5 ± 2.1	39.7 ± 1.8	41.7 ± 1.1
15	37.8 ± .08	37.2 ± 1.5	34.8 ± 1.5	41.3 ± 1.2	38.9 ± 1.1	42.5 ± .8
18	33.8 ± 1.7	35.4 ± 1.4	36.9 ± 1.1	-	-	-
24	32.2 ± 1.7	32.6 ± 1.3	33.0 ± 0.9	-	-	-
36	37.8 ± 3.2	37.5 ± 1.8	37.1 ± 0.4	-	-	-
60	37.3 ± 1.5	37.6 ± 1.6	37.8 ± 1.8	-	-	-
72	37.7 ± 2.2	38.5 ± 1.8	39.4 ± 1.4	-	-	-
84	38.8 ± 0.8	36.2 ± 1.1	33.7 ± 1.4	-	-	-
90	35 ± 1.3	36.1 ± 1.2	36.9 ± 0.9	-	-	-

The tensile modulus increased for all samples immersed under sustained load from 37.1 GPa to 41.3 GPa, 38.9 GPa and 42.5 GPa. for specimen immersed for 15 months at 23°C 45°C, and 65°C respectively. The percentage increase was 8.6, 4.8, 14.6 respectively. The elastic modulus of the FRP specimen depends on the modulus of fibers. The immersion in seawater environment may not have any severe effect on the durability of the fibres, the modulus of GFRP has not suffered any obvious change after immersion (Wang et al., 2017).
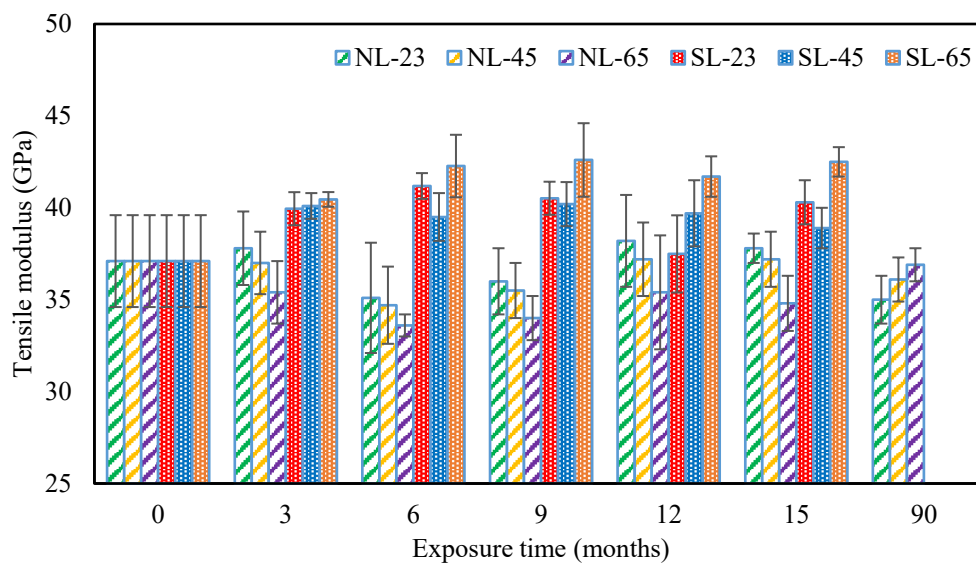
Figure 34: Tensile modulus of E-glass/epoxy composite after the immersion of 15 months

Figure 35 and Table 13 show the failure strain of the E-glass/epoxy composite after immersion in seawater at 23°C, 45°C, and 65°C for the duration of 15 months. Figure 35 shows that after the 6 months of exposure to sea water without load at room temperature and 45°C, the failure strain increased progressively from 2.2% to 2.4% and then decreased to 2% after 15 months of immersion. Sample immersed at 65°C observed with similar behavior of increase and then decrease in failure strain. The failure strain peaks for these samples to 2.4% after 3-month followed by a fall to 2.1% after 15 months. The tensile strain of the composite reduced for the immersion of 90 months under all environmental conditions which indicate a significant decrease in tensile strength for immersion at 65°C. It reduced by 15.9%, 30%, and 50% after the immersions of 90 months without load at 23°C, 45°C, and 65°C respectively.

Table 13: Tensile strain of E-glass/epoxy samples conditioned in seawater without load and with sustained load (15% of failure strength) at 23°C, 45°C and at 65°C for the period of 15 months

Exposure time (months)	Tensile Strain to Failure (%)					
	No-Load			Sustained load		
	23°C	45°C	65°C	23°C	45°C	65°C
0	2.2 ± .03	2.2 ± .03	2.2 ± .03	2.2 ± .03	2.2 ± .03	2.2 ± .03
3	2 ± .12	2.1 ± .1	2.4 ± .15	2 ± .05	2.0 ± .05	2 ± .05
6	2.4 ± .01	2.4 ± .15	2.3 ± .2	1.9 ± .12	1.95 ± .09	1.85 ± .07
9	2.1 ± .09	2.2 ± .09	2.2 ± .09	1.96 ± .08	1.9 ± .1	1.8 ± .12
12	2.1 ± .23	2.1 ± .15	2.2 ± .05	2.01 ± .13	2 ± .04	1.67 ± .06
15	2 ± .2	2 ± .07	2.1 ± .1	1.9 ± .06	1.9 ± .07	1.65 ± .08
18	2.3 ± 0.1	1.92 ± 0.14	1.5 ± 0.18	-	-	-
24	2.5 ± 0.38	2.02 ± 0.275	1.5 ± 0.17	-	-	-
36	2 ± 0.49	1.85 ± 0.26	1.3 ± 0.03	-	-	-
60	2.0 ± 0.25	1.75 ± 0.165	1.1 ± 0.08	-	-	-
72	1.98 ± 0.03	1.81 ± 0.05	1.1± 0.07	-	-	-
84	1.9 ± 0.27	1.67 ± 0.26	1.2 ± 0.25	-	-	-
90	1.85 ± 0.05	1.54 ± .05	1.1 ± 0.04	-	-	-

For the samples immersed under sustained load, the failure strain gradually decreased from 2.2% to 1.9% for the immersion at 23°C and 45°C. However, the decrease in failure strain was from 2.1% to 1.65% after immersion at 65°C. These observations indicate plasticization of the matrix due to seawater absorption which results increase in tensile strain and decrease in tensile modulus; however, after an increase in exposure duration, the matrix becomes more rigid and brittle causing a decrease in failure strain and an increase in tensile modulus. It is more noticeable under sustained load at 65°C when the tensile strain reduced to 1.65% after 15 months of immersion. Strait et al. (1992) observed an increase in impact energy of E-glass/epoxy due to initial plasticization at the early phase of seawater immersion and Merah et al. (2010) reported brittle fracture reduction in failure strain after prolonged exposure to seawater.
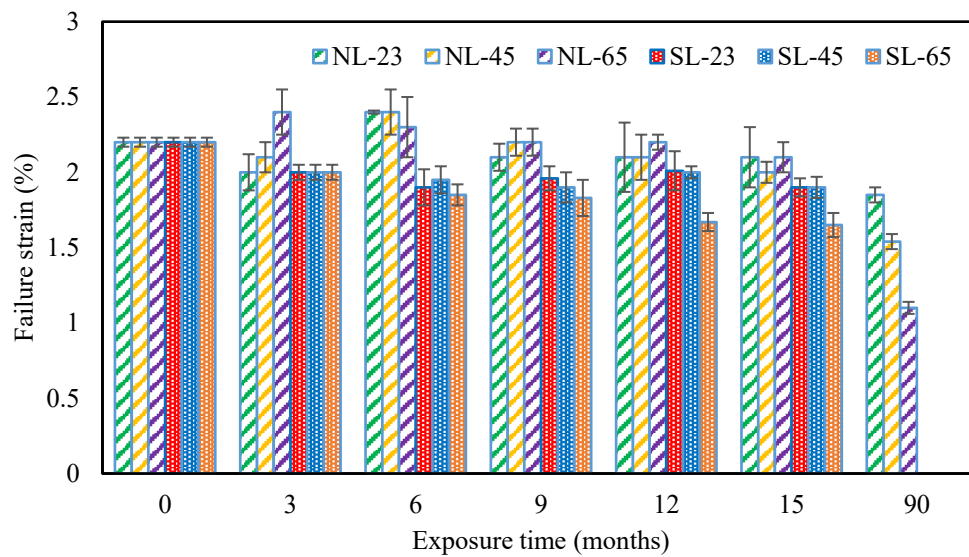
Figure 35: Failure strain of E-glass/epoxy composite after the immersion of 15 months

The results shows that the effect of sustained load was not significant on the tensile strength of the composite. It can be explained through fiber straightening due to the applied stress. As each specimen is subjected to 15% of its ultimate tensile stress, the fibers align themselves in the direction of the load just as an amorphous polymer aligns itself under applied stress. The schematic in Figure 36(a) shows the material with the typical fiber misalignment during processing, and the composite material with the aligned fibers due to the applied stress is shown in Figure 36(b). This alignment of fibers makes the material more efficient in carrying the load, thus increasing the strength and enabling the material to approach its theoretical strength, as predicted by the rule of mixture, after short periods of pre-stress when tested to failure. Similar behavior was observed by Abdel-Magid et al. (2005) after short duration of creep loading.

(a)

(b)
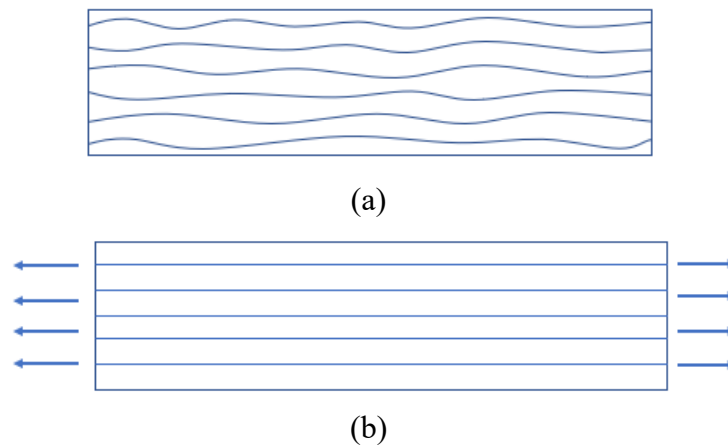
Figure 36: Fiber alignment due to applied stress: (a) before load application; (b) after loading.

For specimens conditioned in water at 45°C and 65°C, the water must have penetrated through the fiber/matrix interphase. The presence of water at the interphase causes the covalent chemical bonds between the silane coupling agent and the glass surface to transform into strong physical interactions via formation of hydrogen bonds between the glass surface, water molecules and the network of silane coupling agents. Previous works on formation of silane network on glass fibers have shown that the siloxane network does not cover the glass fiber continuously as a monolayer film. It rather forms islands of three-dimensional network on glass fiber. This is demonstrated schematically in Figure 37(a) where the fiber is shown to be bonded to the matrix at certain spots. We speculate that the presence of water in the matrix and at the interface in conjunction with the axial load may increase the effective contact area/region between fiber and matrix, in which strong physical interactions can create adhesion between fiber and matrix. This is shown in Figure 37(b). In this figure, it is shown that although the chemical bonds between fiber and matrix are broken, the presence of water has created a region where larger surfaces of fiber and matrix (compared to the unconditioned case) participate in the adhesion process. This larger contact area/region

allows the load to transfer to the fiber more effectively thus maintaining the strength. It also makes composite more brittle and stiff results increase in the modulus and decrease in the failure strain for specimens conditioned. The reduction in composite properties due to temperature and moisture has also been observed by (Ellyin & Maser, 2004; Helbling & Karbhari, 2004).

(a)   (b)
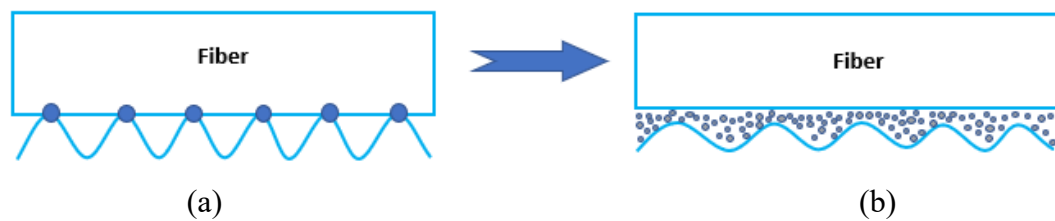
Figure 37: Hydrogen bonds forming at elevated temperature (a) control specimens, (b) conditioned specimens

Further analysis of the effect of seawater on E-glass/epoxy at extended durations is given by comparing the stress-strain behavior of the control sample and samples conditioned for 6 months and 15 months at different temperatures. The stress strain graphs in Figures 35 show the variation in mechanical properties, from the control material after 6 months and 15 months of immersion in seawater at 23°C without load and with sustained load. For specimens immersed in seawater at 23°C without load, the tensile strength reduced by 0.5% and 1.1% after 6 months and 15 months respectively and this respective reduction was 2.8% and 6.2% after immersion of 6 months and 15 months under sustained load. In Figure 38(b), it is shown that the slope of the specimen conditioned at room temperature with and without sustained load is more than the control samples which indicates the increase of modulus of the composite. The modulus of the composite decreased by 5.4% after 6 months of sea water immersion without load but it increased by 11% for the composite immersed

under sustained as shown in Figure 38(a). With further increase of immersion time to 15 months, the modulus of the composite increased by 1.9% for seawater immersion without load and 8.6% for composite immersed under sustained as shown in Figure 38(b). The graphs also show the corresponding change in strain-at-failure, decreasing by 4.5% and 13.6% after 15 months without and with sustained load respectively.
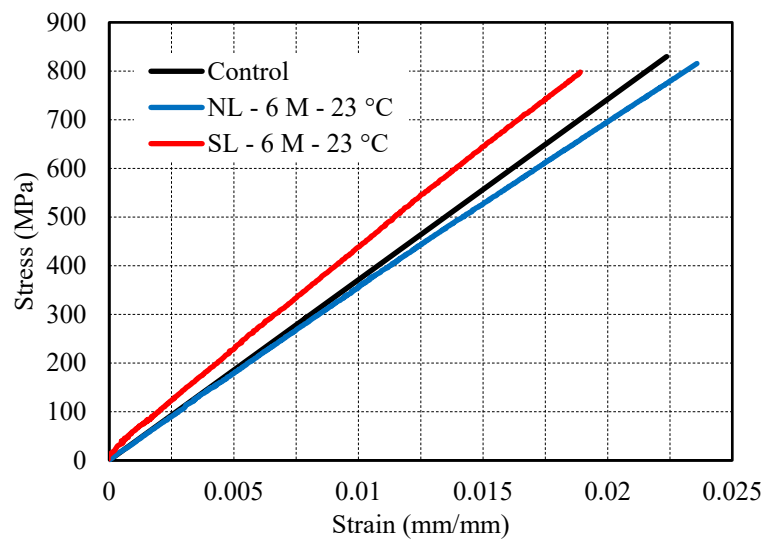
(a)
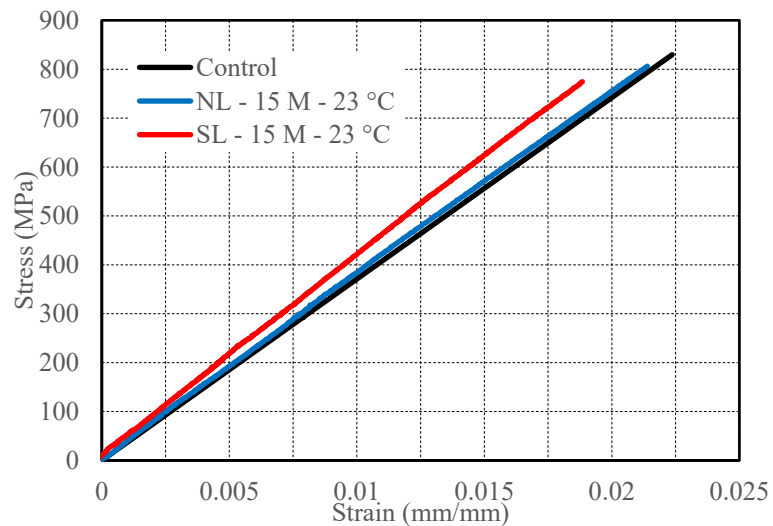
(b)

Figure 38: Stress-strain behavior of E-glass/epoxy specimen immersed in seawater at 23°C for (a) 6 months (b) 15 months
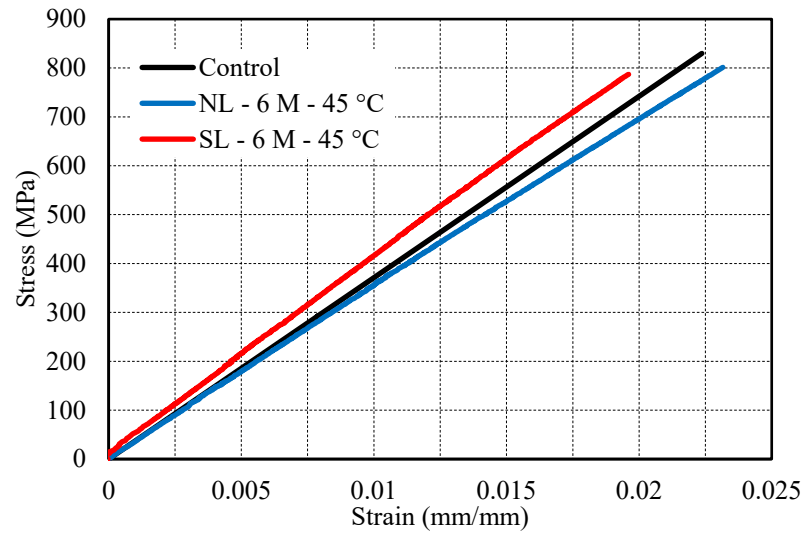
(a)
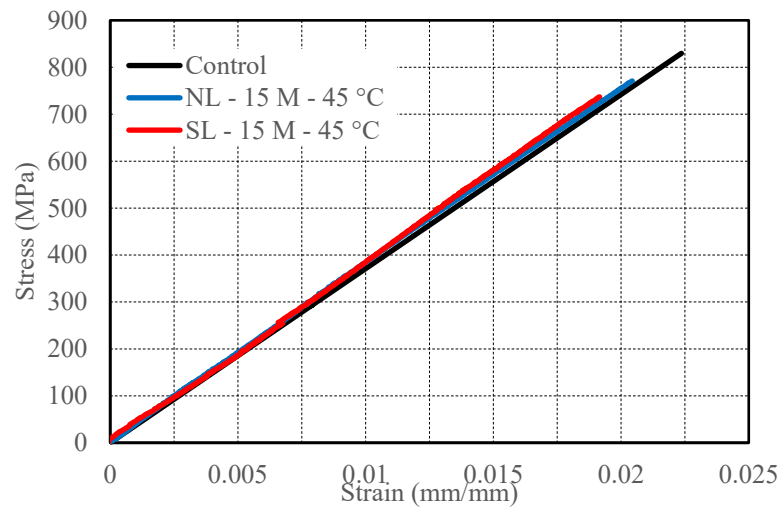
(b)

Figure 39: Stress-strain behavior of E-glass/epoxy specimen immersed in seawater at 45°C for (a) 6 months (b) 15 months

The stress strain graphs in Figure 39 show the variation in mechanical properties, from the control material after 6 months and 15 months of immersion in seawater at 45°C without load and with sustained load. For specimens immersed in seawater at 45°C without load, the tensile strength reduced by 1.7% and 5.5% after 6 months and 15 months respectively and this respective reduction was 4.3% and 11.3% after immersion of 6 months and 15 months under sustained load. Similar to 23°C

immersion without load, the modulus of the composite decrease after 6 months and then increased for immersion of 15 months. The increase in modulus was 0.3% and 4.9% after immersion of 15 months without and with sustained load respectively. The failure strain reduced by 9% and 13.6% after 15 months without and with sustained load respectively.
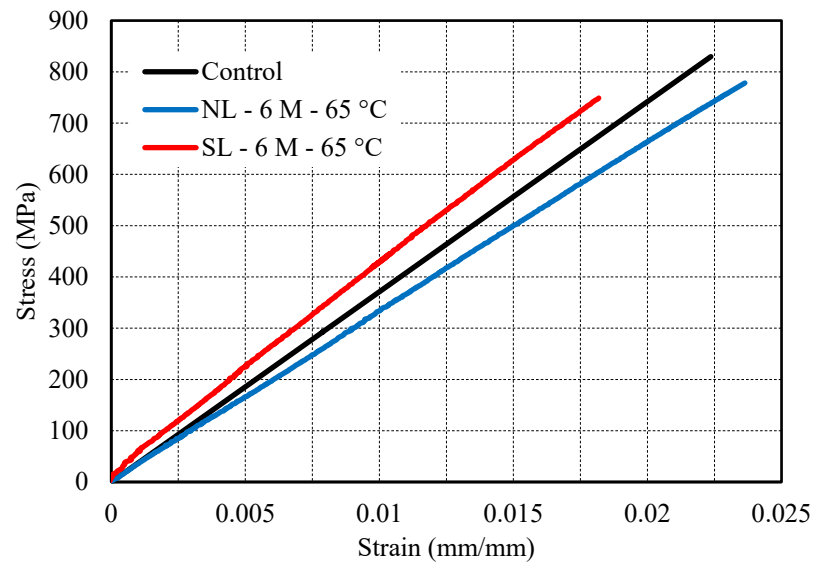
(a)
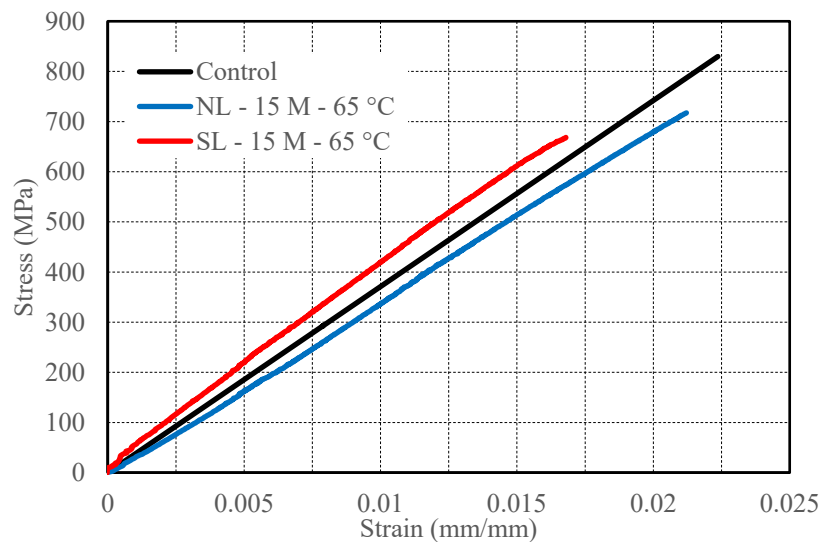
(b)

Figure 40: Stress-strain behavior of E-glass/epoxy specimen immersed in seawater at 65°C for (a) 6 months (b) 15 months

The stress-strain graphs in Figures 40 show the variation in mechanical properties, from the control material after 6 months and 15 months of immersion in seawater at 65°C without load and with sustained load. For specimens immersed in seawater at 65°C without load, the tensile strength reduced by 4.1% and 11.1% after 6 months and 15 months respectively and this respective reduction was 6.3% and 18.2% after immersion of 6 months and 15 months under sustained load. In Figure 40, it is shown that the slope of the specimen conditioned without load is reduced compared to control samples. The decrease in modulus was 9.4% and 6.2% after immersion of 6 months and 15 months respectively. However, samples conditioned with sustained load had a higher slope compared to the control samples. The increase in modulus was 13.9% and 14.6% after immersion of 6 months and 15 months respectively. Sligh reduction was observed in failure strain for the sample immersed without load which was about 4.5% in 15 months. The failure strain of the samples significantly affected by seawater immersion at 65°C under sustained load and it reduced by 25% in 15 months.

6.2.1.1 E-glass/Polyurethane Material

The tensile test was conducted after removal of the samples from the seawater immersion. Figure 41 shows the conditioned samples before and after tensile test.

(a)   (b)
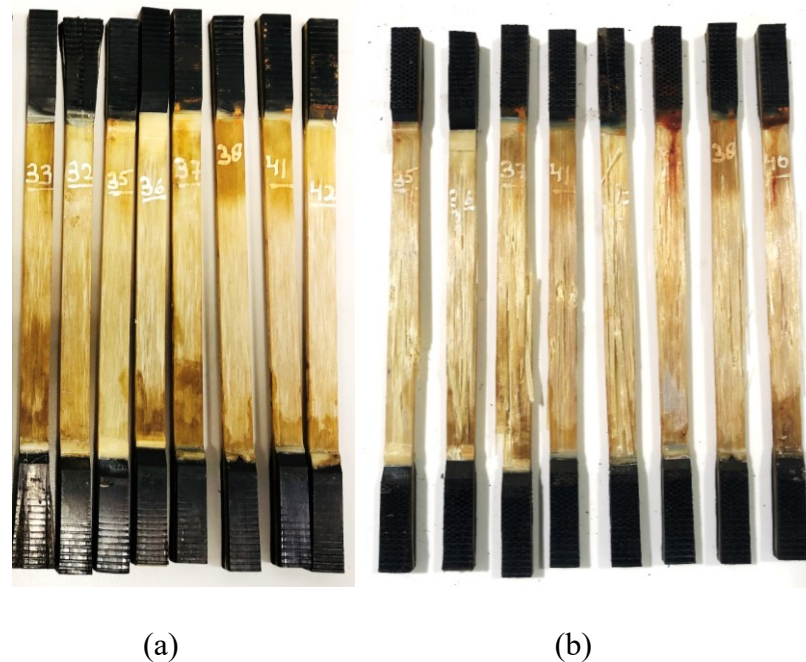
Figure 41: E-glass/polyurethane composite samples a) before tensile test b) after tensile test

The tensile strength of the E-glass/polyurethane composite is shown in Table 14 and Figures 42 below. The strength of E-glass/polyurethane material decreased continuously during the 15 months of exposure to seawater for all immersion conditions. The tensile strength reduced by 18.5% from 891 MPa to 726 MPa for the samples immersed at 23°C without load. This reduction was 25.7% and 34.1% for the samples immersed at 45°C and 65°C respectively. The tensile test results for the samples immersed without load for 90 months are also added to Table 14 and Figure 42 (Mourad et al., 2019). It shows that the tensile strength of E-glass/polyurethane composite reduced by 40.4%, 50.9% and 65.2% after immersions of 90 months without load at 23°C, 45°C, and 65°C respectively.

Table 14: Tensile strength of E-glass/polyurethane samples conditioned in seawater without load and with sustained load (15% of failure strength) at 23°C, 45°C and at 65°C for the period of 15 months

Exposure time (months)	Tensile Strength (MPa)					
	No-Load (NL)			Sustained load (SL)		
	23°C	45°C	65°C	23°C	45°C	65°C
0	891 ± 53	891± 53	891 ± 53	891 ± 53	891 ± 53	891 ± 53
3	861 ± 32	803 ± 35	734 ± 38	762 ± 48	731 ± 41	688 ± 31
6	847 ± 28	752 ± 37	631 ± 45	752 ± 58	688 ± 43	609 ± 51
9	781 ± 21	709 ± 25	627 ± 28	711 ± 15	654 ± 23	580 ± 17
12	734 ± 17	683 ± 31	609 ± 34	664 ± 14	613 ± 13	569 ± 4
15	726 ± 20	662 ± 18	587 ± 33	649 ± 21	603 ± 9	551 ± 11
18	693 ± 55	620 ± 38	568 ± 21	-	-	-
24	644 ± 32	577 ± 19	511 ± 6	-	-	-
36	576 ± 9	519 ± 18	370 ± 27	-	-	-
60	564 ± 19	483 ± 32	322 ± 45	-	-	-
72	554 ± 24	456 ± 25	319 ± 9	-	-	-
84	549 ± 36	448 ± 15	312 ± 6	-	-	-
90	531 ± 41	437 ± 29	310 ± 2	-	-	-

The tensile strengths of the E-glass/polyurethane composite after immersion in seawater at 23°C, 45°C, and 65°C with 15% of sustained load for the duration of 15 months was reduced to 649 MPa, 603 MPa and 551 MPa, respectively. The reductions percentage are 27.2, 32.3 and 35.2 respectively. The observation shows that the tensile strength reduction was 10.6% higher compared to no-load immersed samples for the exposure duration of 15 months at 65°C. The degradation in strength is mainly due to the diffusion of hot water into the matrix which in turn causes degradation at the fiber/matrix interface, as reported by Dogan and Atas (2016).
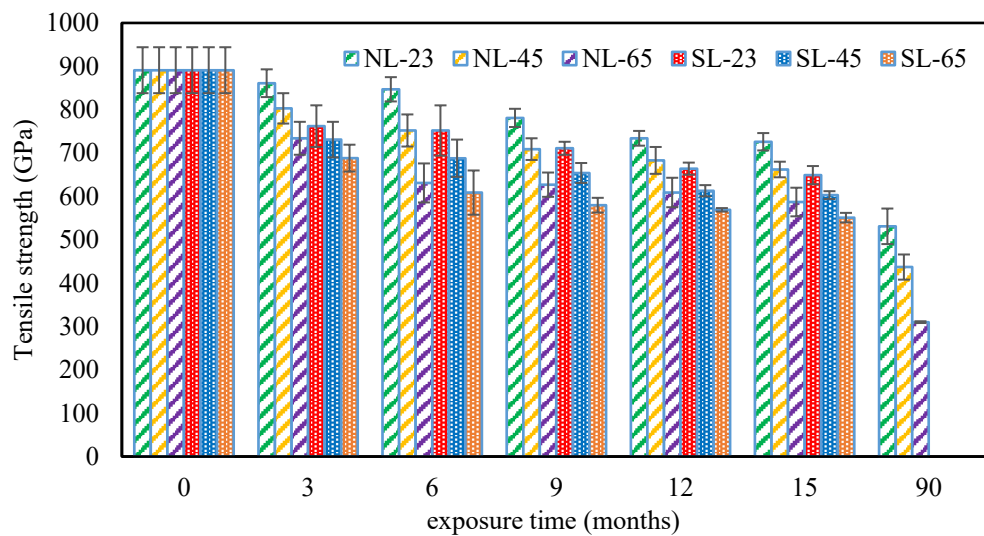
Figure 42: Tensile strength of E-glass/polyurethane composite after the immersion of 15 months

Unlike the continuous decrease in strength, the tensile modulus of the material varied within a limited range of ±1.5 GPa from the original control value of 41.8 GPa. The lowest measured average was nearly 40.8 GPa and the highest measured average was nearly 43.2 GPa during the 15 months of immersion without load in seawater at 23°C, 45°C and 65°C, as shown in Table 15 and Figure 43 below. The tensile modulus of the composite increased for the immersion of 90 months under all environmental conditions which indicate that the composite became stiffer with an increase of immersion duration. The variation in tensile modulus was comparatively higher for samples immersed under sustained load. The modulus increased from 41.8 GPa to 48.2 GPa, 46.2 GPa, and 44 GPa for the samples immersed in seawater at 23°C, 45°C and 65°C. This increase in percentage was 15.3, 11, and 5.5 respectively.

Table 15: Tensile modulus of E-glass/polyurethane samples conditioned in seawater without load and with sustained load (15% of failure strength) at 23°C, 45°C and 65°C for the period of 15 months

Exposure time (months)	Tensile modulus (GPa)					
	No-Load (NL)			Sustained load (SL)		
	23°C	45°C	65°C	23°C	45°C	65°C
0	41.8 ± 1.4	41.8 ± 1.4	41.8 ± 1.4	41.8 ± 1.4	41.8 ± 1.4	41.8 ± 1.4
3	41.6 ± .8	41.2 ± 1.4	42.5 ± 1.9	46.2 ± 1.8	48.7 ± 1.9	50.1 ± 2.1
6	40.8 ± 1.9	40.8 ± 2.1	41 ± 2.5	50.1 ± 2	47.6 ± 2.3	46.8 ± 4.6
9	41 ± 1.2	41 ± 1.6	41.2 ± 1.8	50.2 ± 1.5	48.4 ± 1.9	45.8 ± 2.5
12	41.7 ± 1.4	41.5 ± 1.8	41.5 ± 2.1	44.3 ± 2.4	45.5 ± 3.5	46.8 ± 3.6
15	43.2 ± 1.5	41 ± 2.1	41.3 ± 2.4	48.2 ± 2.1	46.4 ± 2.5	44 ± 2.8
18	41.6 ± 1.55	42.0 ± 2.1	42.5 ± 2.6	-	-	-
24	36.8 ± 0.32	37.9 ± 1.4	38.9 ± 2.4	-	-	-
36	45.7 ± 1.8	46.2 ± 1.8	46.6 ± 1.9	-	-	-
60	46.7 ± 2.2	46.8 ± 3.2	46.9 ± 2.2	-	-	-
72	44.4 ± 1.6	45.6 ± 0.8	46.8 ± 0.1	-	-	-
84	44.3 ± 0.9	44.9 ± 1.6	45.5 ± 2.3	-	-	-
90	45.2 ± 1.1	43.7 ± 1.1	42.8 ± 0.8	-	-	-
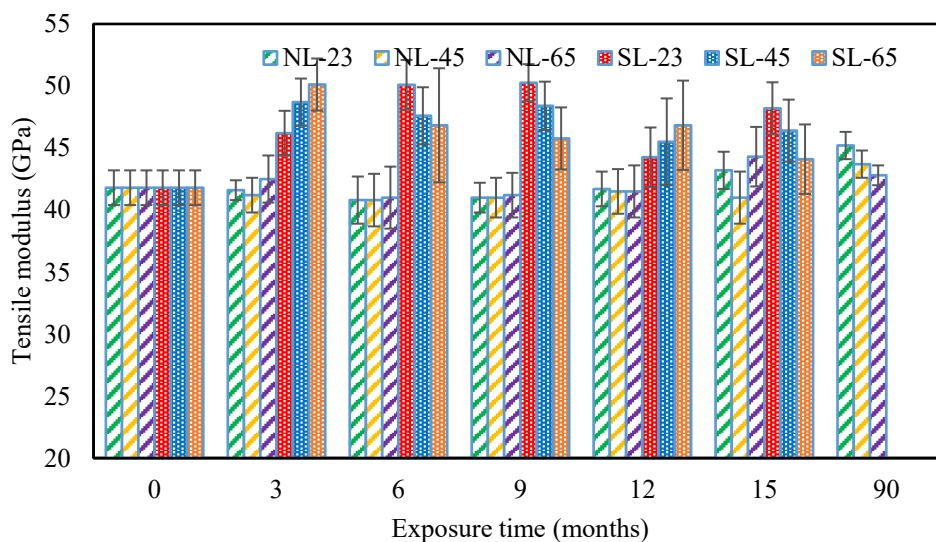
Figure 43: Tensile modulus of E-glass/polyurethane composite after the immersion of 15 months

It is shown in Table 16 and Figure 44 that the strain-at-failure increases slightly from 2.1% for the control samples to 2.3% after 6 months, and then decreases continuously until it reaches 1.8% after 15 months of exposure to seawater at 23°C.

At the elevated temperature of 45°C and 65°C the strain-at-failure of the E-glass/polyurethane decreases continuously from the original value of 2.1% to 1.6% and 1.3% after 15 months as shown in Table 16. These 14%, 24%, and 38% respective drops in strain-at-failure indicate that the polyurethane matrix becomes more brittle and more rigid than the epoxy matrix with extended exposure to seawater. The tensile strain of the composite reduced for the immersion of 90 months under all environmental conditions. It reduced by 41.4%, 53.3%, and 65.2% after the immersions of 90 months without load at 23°C, 45°C, and 65°C respectively.

Similar reduction in the tensile failure observed for immersion under sustained load at all immersion temperatures. The failure strain reduced from 2.1% to 1.35%, 1.3%, and 1.25% for immersion at 23°C, 45°C, and 65°C respectively. This reduction in failure strain may explain the slight increase in the modulus of the E-glass/polyurethane composite as shown in Figure 43.

Table 16: Tensile strain of E-glass/polyurethane samples conditioned in seawater without load and with sustained load (15% of failure strength) at 23°C, 45°C and at 65°C for the period of 15 months

Exposure time (months)	Tensile Strain to Failure (%)					
	No-Load (NL)			Sustained load (SL)		
	23°C	45°C	65°C	23°C	45°C	65°C
0	2.1 ± .18	2.1 ± .18	2.1 ± .18	2.1 ± .18	2.1 ± .18	2.1 ± .18
3	2.14 ± .2	1.9 ± .3	1.7 ± .2	1.65 ± .3	1.5 ± .2	1.3 ± 03
6	2.3 ± .1	2 ± .15	1.55 ± .3	1.5 ± .07	1.45 ± .3	1.5 ± .2
9	2.1 ± .25	1.9 ± .2	1.6 ± .15	1.4 ± .07	1.35 ± .11	1.3 ± .15
12	2 ± .3	1.85 ± .3	1.5 ± .2	1.4 ± .09	1.35 ± .07	1.3 ± .07
15	1.8 ± .3	1.6 ± .2	1.3 ± .1	1.35 ± .1	1.3 ± .09	1.25 ± .06
18	3.1 ± .6	2.1 ± 0.36	1.3 ± 0.13	-	-	-
24	2.8 ± 0.48	2.3 ± 0.28	1.3 ± 0.08	-	-	-
36	2 ± 0.09	1.53 ± 0.11	1.06 ± 0.12	-	-	-
60	1.7 ± 0.37	1.39 ± 0.22	0.99 ± 0.07	-	-	-
72	1.5 ± 0.03	1.37 ± 0.17	0.97 ± 0.30	-	-	-
84	1.26 ± 0.07	1.02 ± 0.08	0.7 ± 0.08	-	-	-
90	1.23 ± .02	0.98 ± .07	0.73 ± .02	-	-	-
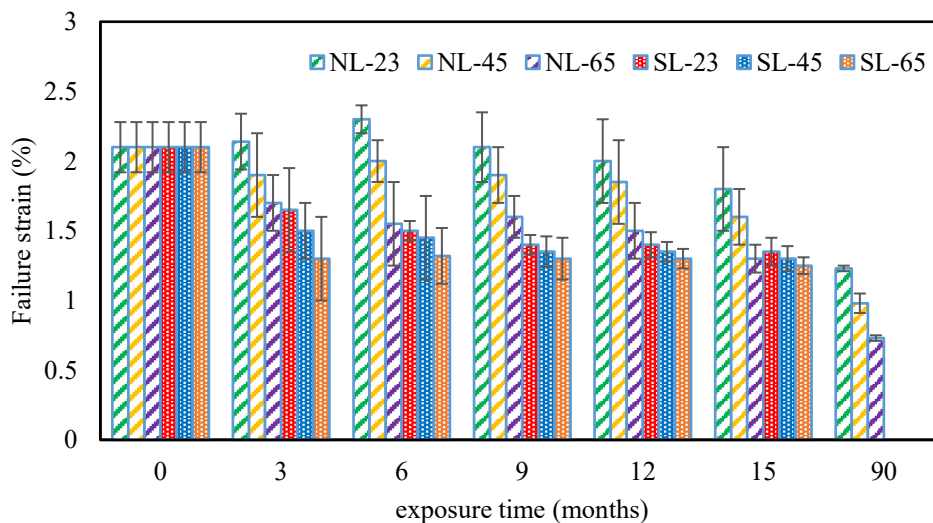
Figure 44: Failure strain of E-glass/polyurethane composite after the immersion of 15 months

The stress-strain graphs in Figures 45 show the variation in mechanical properties of E-glass/polyurethane composite, from the control material after 6 months and 15 months of immersion in seawater at 23°C without load and with sustained load. For specimens immersed in seawater at 23°C without load, the tensile strength reduced by 17.6% and 18.5% after 6 months and 15 months respectively and this respective reduction was 25.4% and 27.2% after immersion of 6 months and 15 months under sustained load. In Figure 45, it is shown that the slope of the specimen conditioned without load at 23°C slightly reduced in immersion of 6 months and increased after 15 months. The slope was higher than control samples for the immersion of samples under sustained load. The modulus of the composite first reduced by 2.3% after 6 months of seawater immersion without load then increased by 3.3% for 15 months of immersion. For immersion under sustained load, the modulus increased by 19.9% and 15.3% for the 6 months and 15 months respectively. The graph shows that the failure strain reduced for both conditioned and it was 14.3% and 35.7% for without and with sustained load after an immersion period of 15 months respectively.
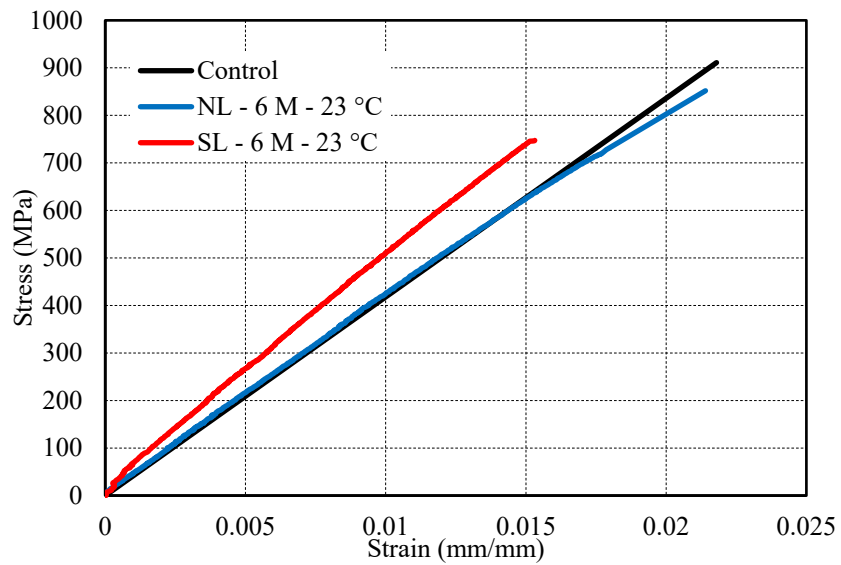
(a)
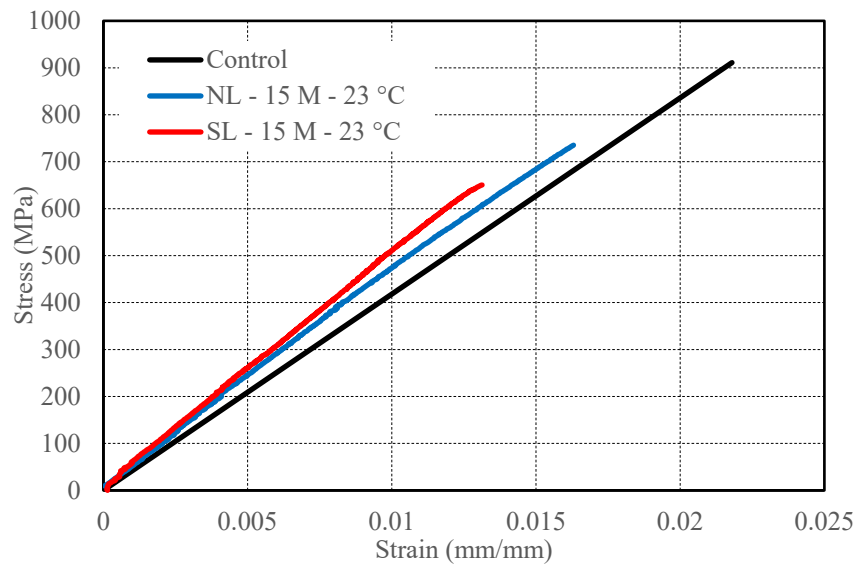
(b)

Figure 45: Stress-strain behavior of E-glass/polyurethane specimen immersed in seawater at 23°C for (a) 6 months (b) 15 months

The stress strain graphs in Figures 46 show the variation in mechanical properties of E-glass/polyurethane, from the control sample after 6 months and 15 months of immersion in seawater at 45°C without load and with sustained load. For specimens immersed in seawater at 45°C without load, the tensile strength reduced by 15.6% and 25.7% after 6 months and 15 months respectively and this respective

decrease was 22.85% and 32.3% after immersion of 6 months and 15 months under sustained load. The modulus of the samples reduced by 2.4% and 1.9% after 6 months and 15 months respectively and this respective increase was 13.9% and 11% after immersion of 6 months and 15 months under sustained load. The failure strain of the samples reduced by 23.8% and 38.1% after 15 months without and with sustained load respectively.
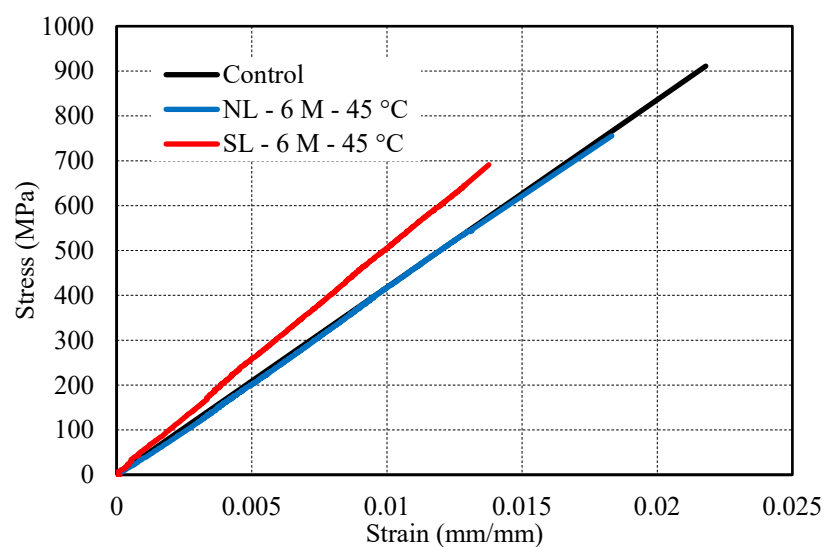
(a)
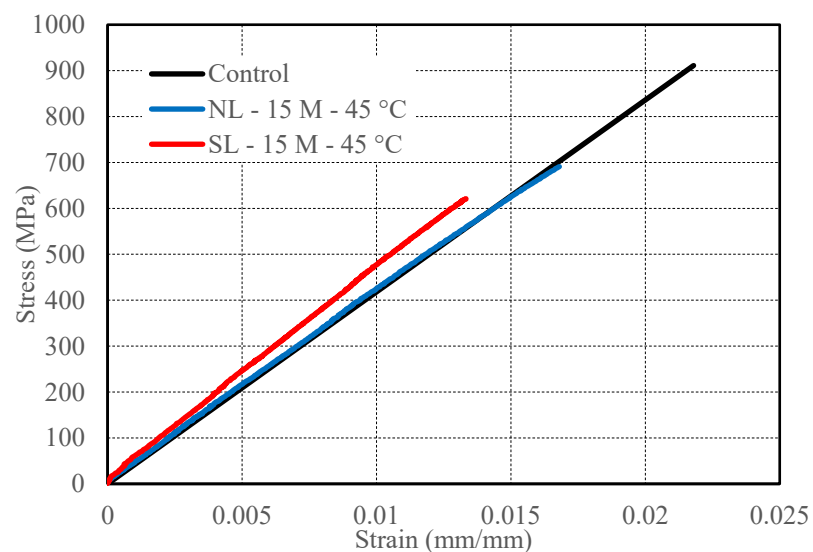
(b)

Figure 46: Stress-strain behavior of E-glass/polyurethane specimen immersed in seawater at 45°C for (a) 6 months (b) 15 months
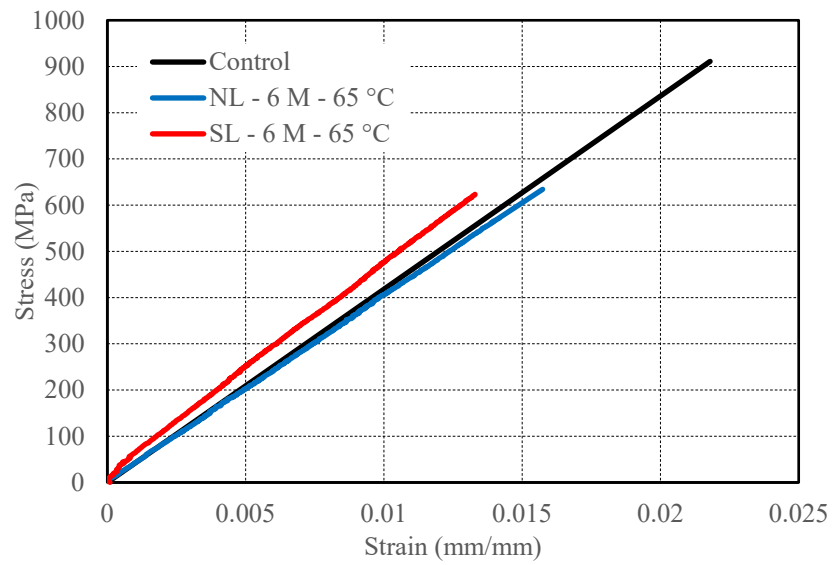
(a)
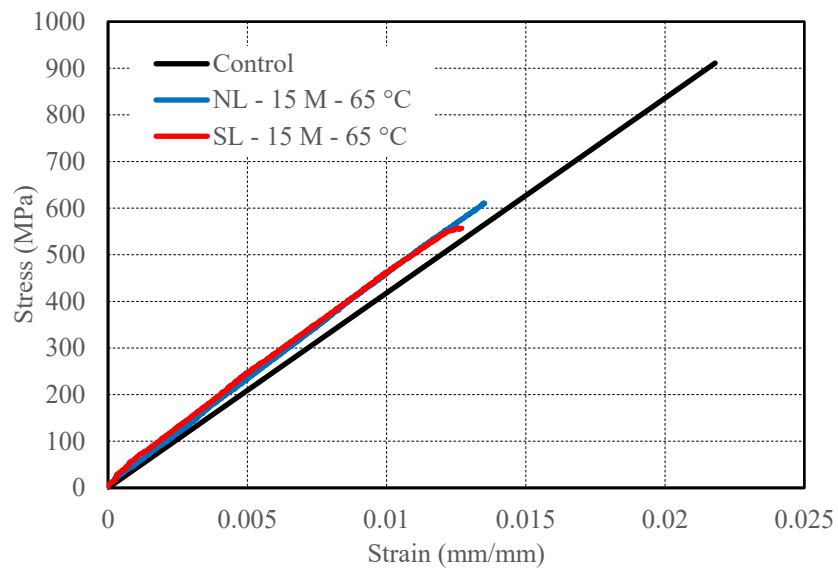
(b)

Figure 47: Stress-strain behavior of E-glass/polyurethane specimen immersed in seawater at 65°C for (a) 6 months (b) 15 months

The stress-strain graphs in Figures 47 show the variation in mechanical properties, from the control material after 6 months and 15 months of immersion in seawater at 65°C without load and with sustained load. For specimens immersed in seawater at 65°C without load, the tensile strength reduced by 29.2% and 34.1% after 6 months and 15 months respectively and this respective reduction was 31.7% and

38.22% after immersion of 6 months and 15 months under sustained load. In Figure 47, it is shown that the slope of the specimen conditioned without load is reduced by 1.9% compared to control samples in 6 months of immersion and then increased by 6% after 15 months of immersion. The increase in modulus was 12% and 5.5% after immersion of 6 months and 15 months respectively with sustained load. The failure strain was significantly reduced for both conditions and it was 38.1% and 40.1% after 15 months of immersion without and with sustained load respectively.

6.2.2 Effect of Temperature on the Tensile Properties

The accelerated tests were conducted to analyze the effect of harsh conditions on the durability of both composites. Samples were immersed in seawater maintained at different temperature (23 - 95 °C) under 15% of sustained load for the duration of one month. The tensile properties of both composites are noted in Table 17.

Table 17: Tensile properties of E-glass/epoxy and E-glass/polyurethane samples conditioned in seawater at different temperature with sustained load (15% of failure strength) for the period of 1 month

Exposure temp (°C)	E-glass/epoxy			E-glass/polyurethane		
	Stress	strain	modulus	Stress	strain	modulus
Control	811 ± 45	2.2 ± .03	37.1 ± 2.5	891 ± 53	2.1 ± .18	41.8 ± 1.4
23	802 ± 37	2 ± .11	41.8 ± 2.5	787 ± 43	1.7 ± .1	51.7 ± 3.8
55	795 ± 42	1.92 ± .07	45.7 ± 2.1	736 ± 31	1.4 ± .07	53.1 ± 2.1
65	791 ± 15	2 ± .04	43.5 ± 3.2	683 ± 35	1.35 ± .04	52.3 ± 1.7
75	748 ± 51	1.8 ± .11	44.5 ± 2.5	664 ± 23	1.43 ± .11	50.3 ± 2.5
85	718 ± 49	1.33 ± .06	42.3 ± 0.7	657 ± 14	1.54 ± .15	50.1 ± 2
95	697 ± 53	1.28 ± .03	45.6 ± 3.8	649 ± 24	1.35 ± .17	52.8 ± 1.2

Figure 48 shows the tensile strength of E-glass/epoxy and E-glass/polyurethane composite immersed at different temperature. The tensile strength of both composites reduced with an increase of immersion temperature for the same period of

conditioning. The strength of the E-glass/polyurethane dropped gradually with an increase of temperature but at a higher rate compared to the E-glass/epoxy composite. The tensile strength of E-glass/epoxy composite reduced by 1.1%, 1.9%, and 2.4% with immersion at 23°C, 55°C, and 65°C but the rate was higher after 65°C. The tensile strength reduced from 2.4% to 8%% with 10°C increase in temperature. It could be due to combined effect of moisture and plasticization of the composite. The reduction in the tensile strength was 8%, 11.5%, and 14% with immersion at 75°C, 85°C, 95°C respectively.

For E-glass/polyurethane this reduction was 11.7%, 17.4%, 23.3%, 25.5%, 26.3%, and 27.2%, at 23°C, 55°C, 65°C, 75°C, 85°C, and 95°C respectively. The decrease in tensile strength of E-glass/polyurethane was higher compared to E-glass/epoxy composite at all temperatures. The decrease in the tensile strength was 96% and 94% higher in E-glass/polyurethane composite compared to E-glass/epoxy composite immersed at 23°C and 95 °C respectively.

Figure 48: Tensile strength of E-glass/epoxy and E-glass/polyurethane composite after the immersion of 1 month at different temperature

Figure 49 shows the tensile modulus of E-glass/epoxy and E-glass/polyurethane composite after the immersion of one month at different temperature. The modulus of both the composite increased compared to the control sample. The maximum increase for E-glass/epoxy composite was approx 5GPa Whereas this increase was 12 GPa for E-glass/polyurethane composite. The increase in modulus indicates the increase in the stiffness of the composite, which in mostly depends on the fibers of the composite, due to the immersion of samples at high temperature. The high temperature immersion degraded the matrix phase and stiffened the fibers of the composite.

Figure 49: Tensile modulus of E-glass/epoxy and E-glass/polyurethane composite after the immersion of 1 month at different temperature

The failure strain of E-glass/epoxy and E-glass/polyurethane composite after the immersion of one month at different temperature is presented in Figure 50. The graph indicates that the failure strain significantly affected with increase in the immersion temperature. The tensile strain of E-glass/epoxy and E-glass/polyurethane reduced to 1.28% and 1.35% respectively for the immersion of one month at 95 °C.

The high temperature immersion results increase in the brittle behavior of the composite and failure of the samples at small strain.

Figure 50: Failure strain of E-glass/epoxy and E-glass/polyurethane composite after the immersion of 1 month at different temperature

6.2.3 Effect of Load on the Tensile Properties

The accelerated tests were conducted to analyze the effect of sustained load on the durability of both composites. Samples were immersed in seawater maintained at 65°C under sustained load varied from 10% to 25% of failure strength of the sample for the duration of one month. The tensile properties of both composites are noted in Table 18.

Table 18: Tensile properties of E-glass/epoxy and E-glass/polyurethane samples conditioned in seawater at 65°C under different sustained load for the period of one month

Sustained load (%)	E-glass/epoxy			E-glass/polyurethane		
	Tensile strength (MPa)	Failure strain (%)	Tensile modulus (GPa)	Tensile strength (MPa)	Failure strain (%)	Tensile modulus (GPa)
Control	811 ± 45	2 ± .03	37.1 ± 2.5	891 ± 53	2.1 ± .18	41.8 ± 1.4
10	798 ± 28	2.4 ± .06	44.5 ± 2.2	724 ± 38	1.3 ± .07	52.3 ± 1.1
15	791 ± 15	2 ± .04	43.5 ± 3.2	683 ± 35	1.35 ± .04	52.2 ± 1.7
20	785 ± 12	1.85 ± .08	46.4 ± 1.8	511 ± 29	1.3 ± .13	52.2 ± 1.1
25	771 ± 33	1.95 ± .1	41.7 ± 1.2	494 ± 34	1.1 ± .16	56.6 ± 0.7

Figure 51 shows the tensile strength of E-glass/epoxy and E-glass/polyurethane composite immersed under different sustained load at 65°C for the immersion of one month. The tensile strength of both composites reduced with an increase of sustained load for the same period of conditioning. The tensile strength of E-glass/polyurethane composite reduced steeply with increase of sustained load whereas it reduced gradually for E-glass/epoxy composite. The tensile strength of E-glass/epoxy composite reduced by 1.6%, 2.5%, 3.2%, and 4.9% with sustained of 10%, 15%, 20% and 25% respectively for immersion at 65°C. For E-glass/polyurethane this reduction was 18.7%, 23.3%, 42.6% and 44.6% with sustained of 10%, 15%, 20% and 25% respectively. The significant decrease in the tensile strength of the composite could be due the presence of porosity or micro-cracks in the samples and degradation of fiber/matrix interface at 65°C immersion under elevated sustained load. The increase in sustained load may cause stretching of the micro-voids and cracks, hence premature failure of the composites.
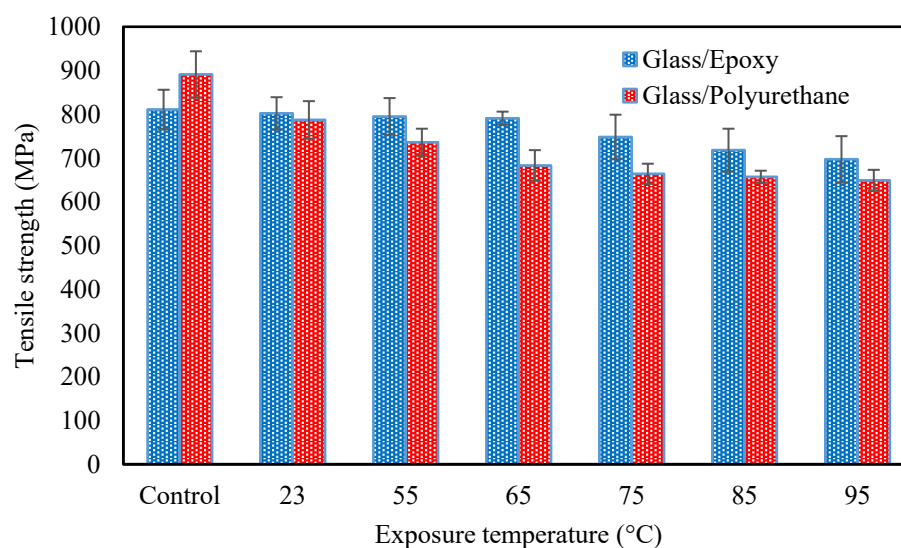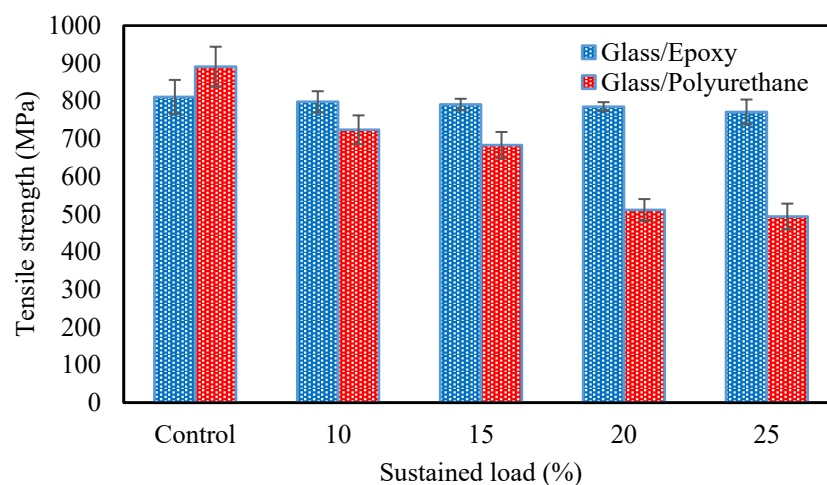

Figure 51: Tensile strength of E-glass/epoxy and E-glass/polyurethane composite after the immersion of 1 month under different load
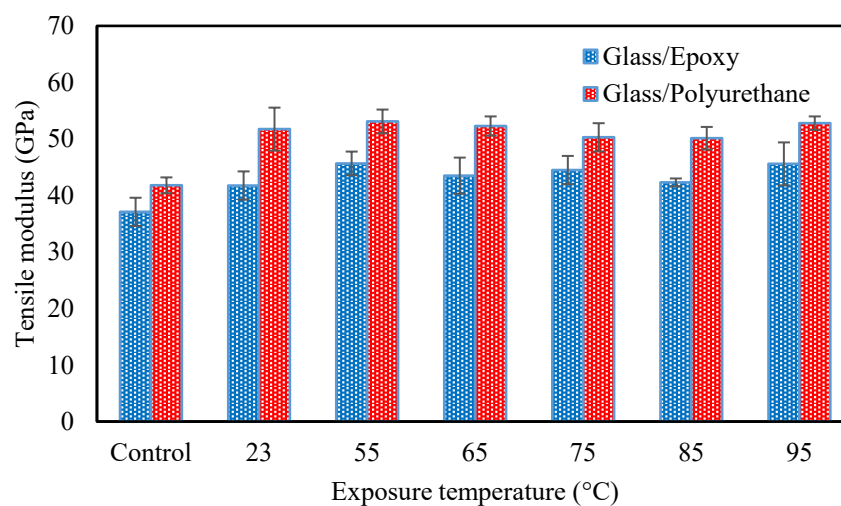
Figure 52 shows the tensile modulus of E-glass/epoxy and E-glass/polyurethane composite after the immersion of one month at different sustained load. The modulus of both the composite increased compared to the control sample. The maximum modulus for E-glass/epoxy and E-glass/polyurethane composite was 46.4 GPa and 56.6 GPa for the immersion with 20% and 25% sustained load respectively. The tensile modulus reduced by 12.4% from 37.1 GPa to 41.7 GPa for E-glass/epoxy composite and by 35.4% from 41.8 GPa to 56.6 GPa for E-glass/polyurethane composite immersed at 65°C with 25% sustained load.

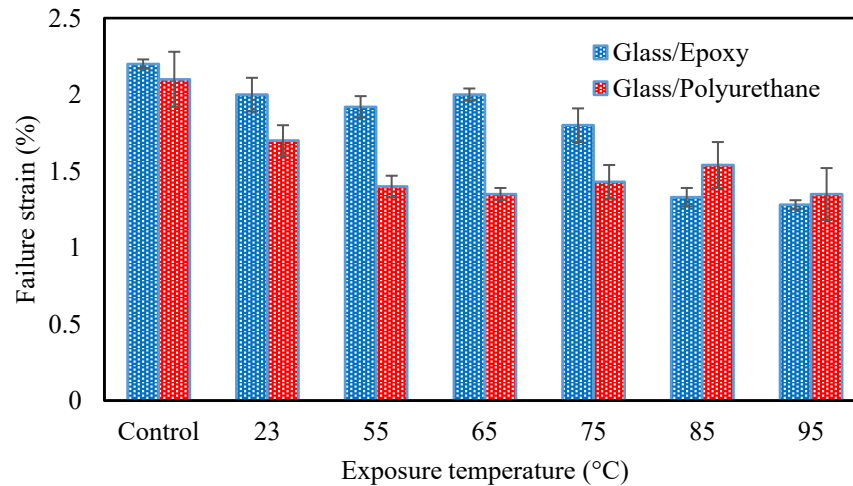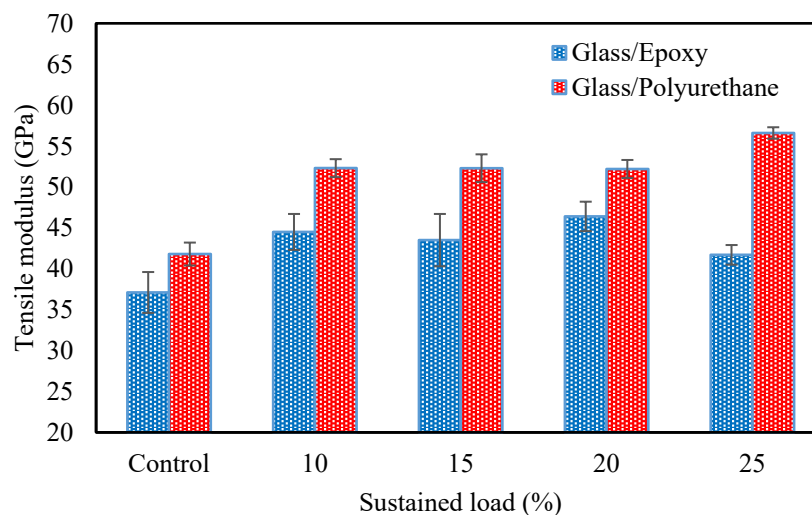Figure 52: Tensile Modulus of E-glass/epoxy and E-glass/polyurethane composite after the immersion of 1 month under different load

The failure strain of E-glass/epoxy and E-glass/polyurethane composite after the immersion of one month at different temperature is presented in Figure 53. The graph indicates that the failure strain significantly affected with increase in the sustained load. The tensile strain reduced by 11.4% from 2.2% to 1.95% for E-glass/epoxy composite and by 47.6% from 2.1% to 1.1% for E-glass/polyurethane composite immersed at 65°C with 25% sustained load.
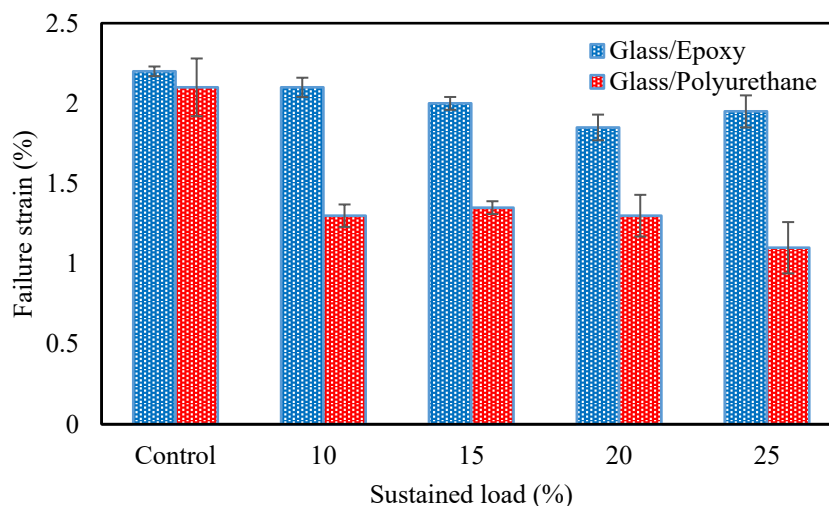
Figure 53: Failure strain of E-glass/epoxy and E-glass/polyurethane composite after the immersion of 1 month under different load

6.3 Differential Scanning Calorimetry (DSC) Analysis

The differential scanning calorimetry (DSC) for the E-glass/epoxy and E-glass/polyurethane composite was conducted on samples immersed at different temperature and exposure time. The test was performed in an inert environment using nitrogen gas. The experiment was run between 25°C and 250°C with a heating rate of 10.0°C/min. Three samples for each condition were considered to determine the glass transition temperature. Figure 54(a) represents the DSC curves for the E-glass/epoxy control sample and specimens immersed at 23°C and 65°C for 15 months. The glass transition temperatures (Tg) of the samples immersed at 23°C was close to the control sample (118.2°C). The glass transition temperature of the specimen immersed at 23°C without and with sustained load was 117.2°C and 116.8°C respectively. The Tg slightly reduced to 114.2°C and 113.5°C for the immersion without load and with sustained load respectively at 65°C.
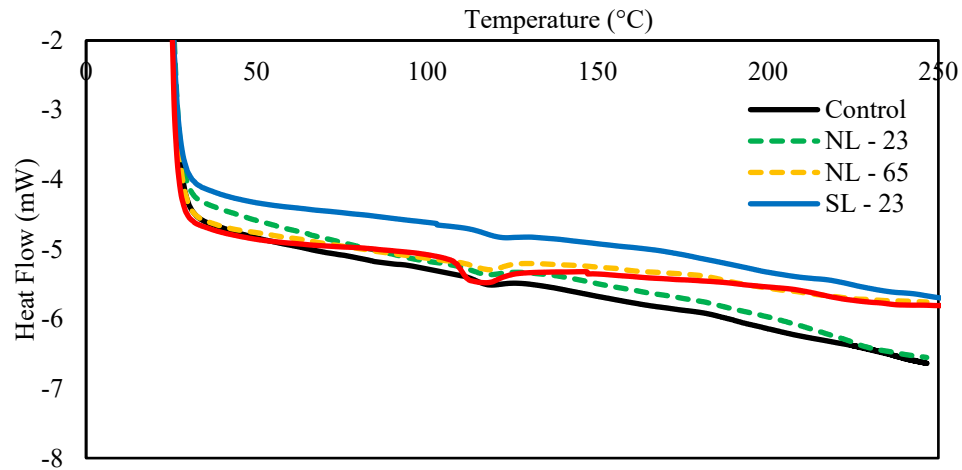
(a)
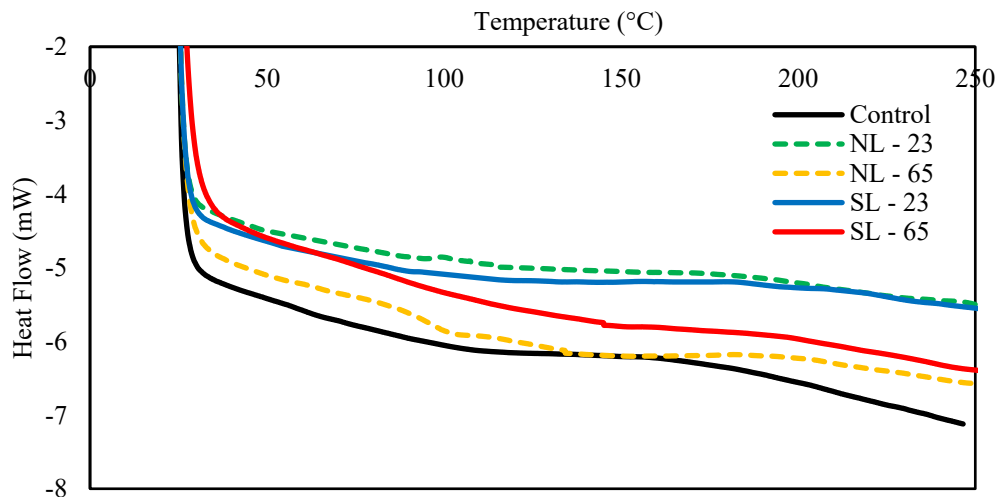
(b)

Figure 54: DSC curves of control sample and conditioned samples immersed without and with 15% sustained load for 15 months (a) E-glass/epoxy (b) E-glass/polyurethane

Similar behavior was observed for the E-glass/polyurethane composite as shown in Figure 54(b). The Tg of E-glass/polyurethane composite reduced from 87.6°C (control sample) to 86.1°C and 84.3°C for the immersion at 23°C and 65°C respectively without sustained load. The Tg for the samples immersion under sustained load reduced to 85.7°C and 83.4°C at the temperature of 23°C and 65°C

respectively. The shift in Tg could be due to the combined effect of high temperature and seawater aging. It is associated with the degree of cross-linking or the degree of polymerization after curing. The degradation in epoxy composite is owing to the existence of hydrophilic groups which form weak hydrogen bonds by reacting with water molecules during immersion at 65°C (Zafar et al., 2012). It demonstrates that the moisture uptake acts as a plasticizer and decreases Tg. The reduction in Tg represents thermal degradation and loss in mechanical properties which limits the service temperature of the polymer. The mechanisms of the long chain of the polymer may start to isolate at high temperature immersion and react with each other to alter the properties of the polymer (Kawagoe et al., 1999).

6.4. Fourier Transform Infrared Spectroscopy (FTIR) Analysis

The Fourier transform infrared spectroscopy (FTIR) was performed on Perkin Elmer Spectrum 100 FTIR spectrometer at room temperature in the transmission mode. FTIR spectra were logged in between 600 cm^{-1} and 4000 cm^{-1} at a resolution of 2 cm^{-1} with 10 scans. Before testing the samples, background spectra were taken in the empty chamber to eliminate the influence of moisture and CO_2 in air. Figure 55 presents a comparison of typical spectra for the control samples of E-glass/epoxy and E-glass/polyurethane, and samples immersed at 23°C and 65°C for 6 months and 12 months. The seawater exposure will lead to the presence of equivalent FTIR bands on the residue spectrum due to the leaching of functional groups from the resin of composite. The allocation of the representative absorbent bands is given in Table 19 for the samples and their allocated functional groups. The O–H stretching band is observed above 3000 cm^{-1} wavenumbers.
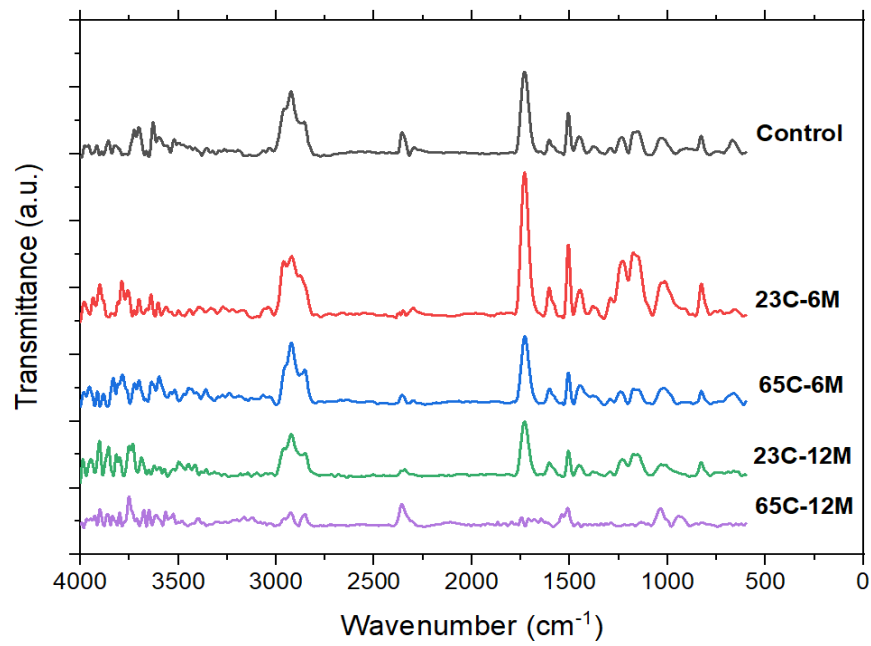
(a)
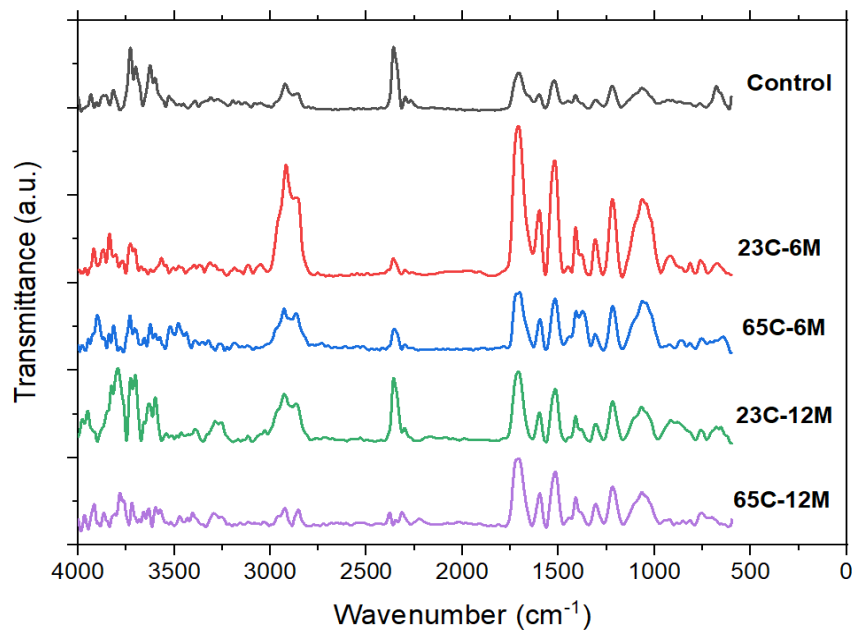
(b)

Figure 55: FTIR spectrum of control sample and conditioned samples (a) E-glass/epoxy (b) E-glass/polyurethane

The difference in intensity of O–H stretching vibration at 3400 cm^{-1} is due to

the seawater immersion of the specimen (Ngono et al., 1999; Noobut and Koenig,

1999). The next band is located between 2930 cm^{-1} and 2900 cm^{-1} and attributed to the stretching band of C–H group of epoxies (Ngono et al., 1999; Noobut & Koenig, 1999). The stretching of C–O non-conjugate ester detected at 1732 cm^{-1} (Yang et al., 2015). The existence of bands at 1509 cm^{-1} and 1610 cm^{-1} are allotted for C=C stretching in aromatics and alkenes respectively (Ngono et al., 1999; Smith et al., 1984; Socrates, 2004). Symmetric and asymmetric stretching vibration of C–O–Φ observed at 1040 cm^{-1} and 1245 cm^{-1} wavenumber respectively (Noobut & Koenig, 1999; Yang et al., 2015). The band at 1182 cm^{-1} is due to the vibration characteristics of C–O in an aromatic ring (Chike et al., 1993) whereas C–H bending in benzene ring detected at 827 cm^{-1} (Ngono et al., 1999).

Table 19: FTIR bands observed in E-glass/epoxy specimens

Bands (cm−1)	Assignment
3400	Stretching vibration O = H
~2930 and ~2900	C − H group stretching band
~1732	C–O non-conjugate ester stretching
~1610	stretching band of C = C (alkene)
~1509	C = C (aromatic nucleus)
~1245	Asymmetric C − O − Φ stretch
1182	C–O aromatic ring stretching
~1040	Symmetric C − O − Φ stretch
~827	Out of plane bending of C-H (benzene)

The immersion of specimen in seawater produces a band at ~840 cm−1 which indicates stretching vibration of the ether group as trapped moisture in specimen includes hydrogen bond with the C-O-C groups (Ngono et al., 1999). Another band

appeared at ~1125 cm^{-1} could be ascribed to the alteration in the vibrational C-OH band leading to the formation of hydrogen bond (C–O–H----OH$_2$) during hydration (Ngono et al., 1999). The presence of these bands confirm the leaching of E-glass/epoxy matrix into the seawater during immersion. In FTIR spectrum two peaks at 2296.3 cm^{-1} and 2353.2 cm^{-1} appeared for the control sample. It indicates the existence of unreacted−N=C=O groups in samples.
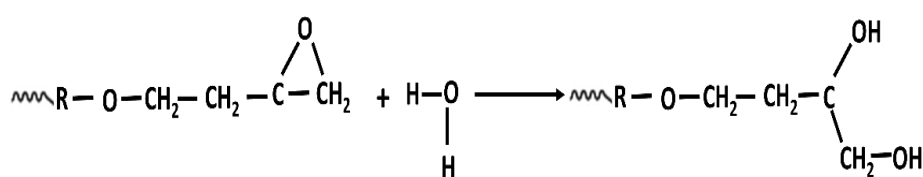
(a)
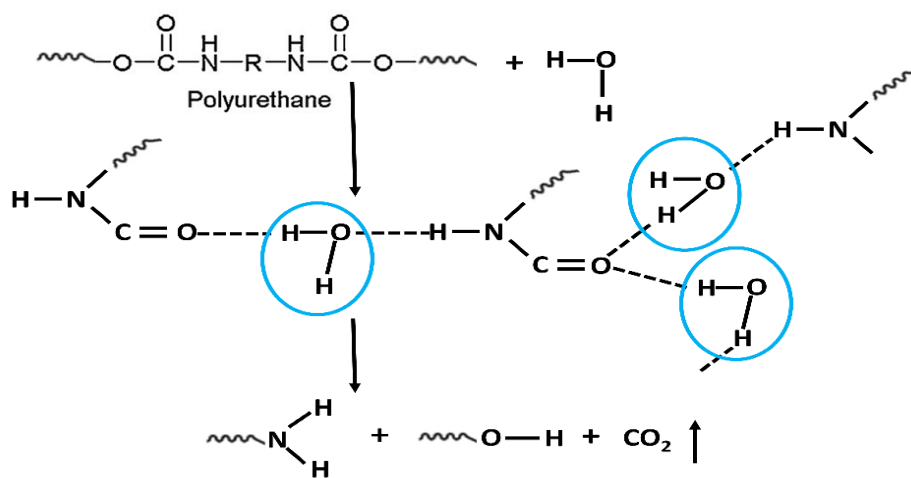
(b)

Figure 56: The schematic diagram for hydrolytic degradation mechanism of (a) epoxy and (b) polyurethane.

The exposure of E-glass/epoxy samples to moisture breaks the epoxy chain and forms an epoxy with OH- group. The degradation in epoxy composite is also due to

the existence of hydrophilic groups which form weak hydrogen bonds by reacting with water molecules during immersion at 65°C as shown in Figure 56(a). Hence, these breaks of epoxy chain led to reduction in the tensile strength of the composite. In other hand, polyurethane is composed of organic units joined by urethane links, shown in Figure 56(b). For the control sample, C=O acts as a proton acceptor while NH acted as a proton donor. This   C=O accepts a proton from the NH-group of urethanes to form a hydrogen bond. Hence, it favors a more flexible polymer structure with a variable degree of branching. Consequently, when it is treated with water i.e., H-O-H easily diffuses into urethane linkage -CONH, the hydrolytic degradation process occurs and leads to release a carbon-di-oxide along with NH_2 and O-H chain compounds (Mondal & Martin, 2012). Hence, for immersion temperature, the sustained release of CO_2 is responsible for the increase of mass loss results in a reduction in the tensile strength of the composite (Mourad et al., 2009; Zhou & Lucas, 1999b, 1999a).

6.5 Failure Analysis

The fractured surfaces of tested samples were analyzed using a Scanning Electron Microscope (SEM). Figure 57(a) represents the effect of seawater under sustained load at 23°C on the surface of the E-glass/epoxy composite. The bonding between fiber and matrix is slightly affected without the presence of any crack. However, minor matrix cracks and fiber/matrix debonding were detected on the surface of the sample immersed at 45°C as shown in Figure 57(b). The fiber/matrix debonding increased with the increase of immersion temperature. At the temperature

of 65°C, shown in Figure 57(c), significant delamination and fractured fibers observed on the surface of the composite.

Figure 58(a) represents the effect of seawater under sustained load at 23°C on the surface of the E-glass/polyurethane composite. The bonding between fiber and matrix is slightly affected due to the combined effect of sustained load and seawater immersion. At 45°C, fiber cracking and matrix ploughing were observed on the surface of the sample as shown in Figure 58(b). The fiber/matrix debonding significantly increased with the increase of immersion temperature as shown in Figure 58(c) for samples immersed at 65°C.
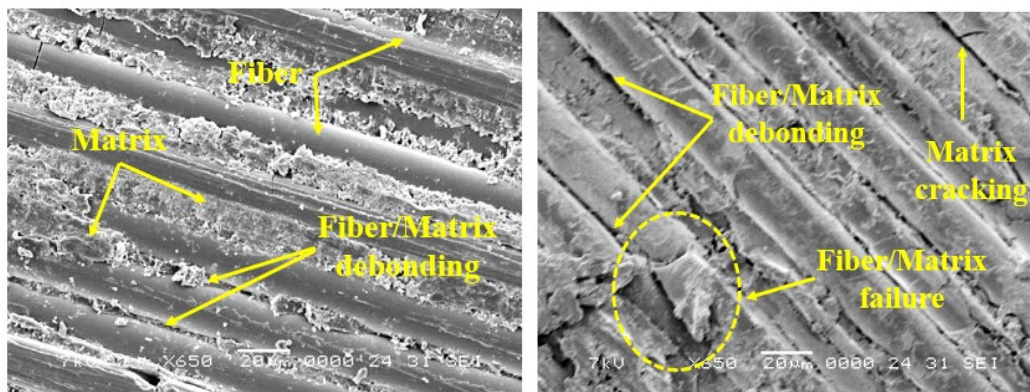
(a)   (b)
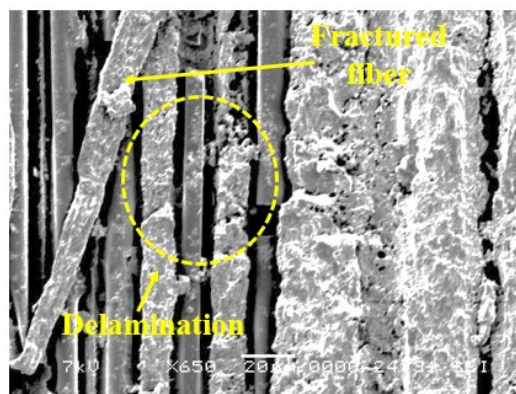
(c)

Figure 57: Surface micrograph of E-glass/epoxy composite immersed under sustained load for the duration of 15 months at (a) 23°C (b) 45°C (c) 65°C

(a)   (b)

(c)
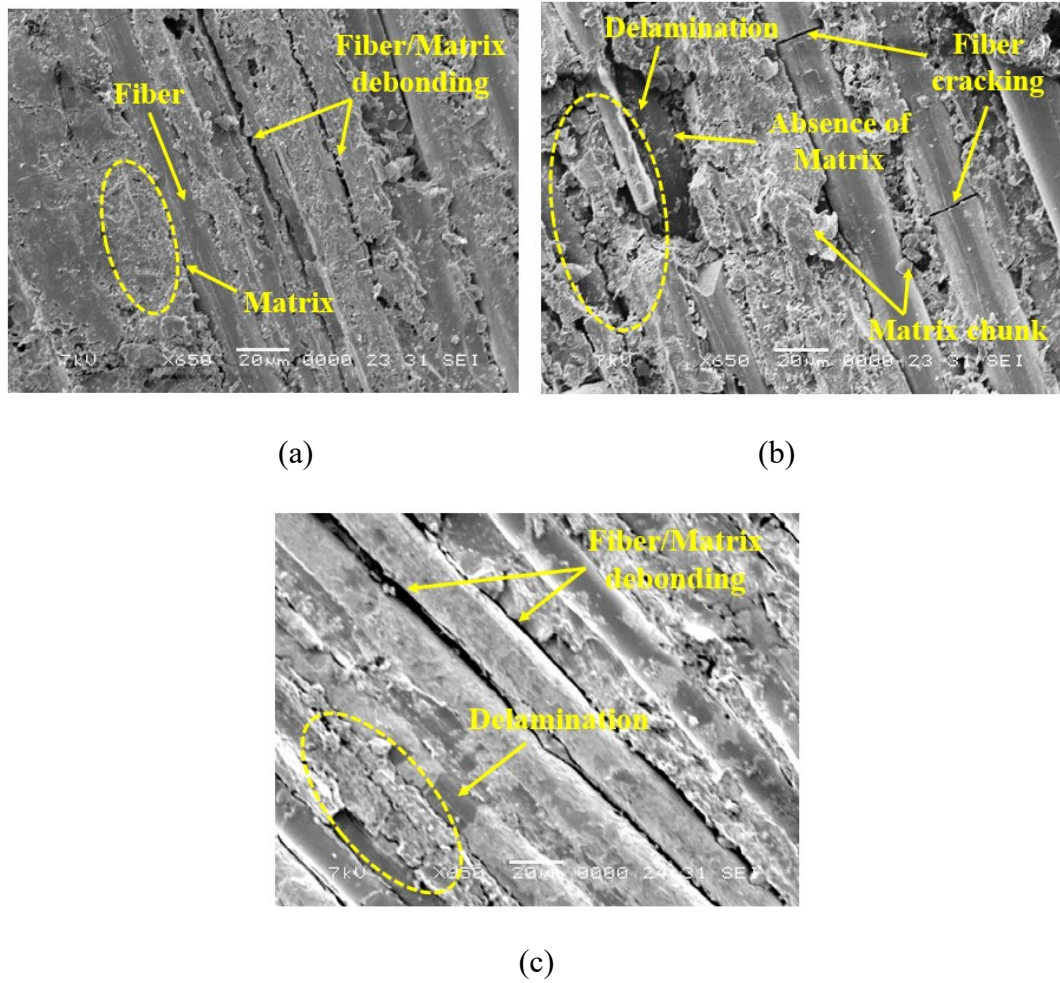
Figure 58: Surface micrograph of E-glass/polyurethane composite immersed under sustained load for the duration of 15 months at (a) 23°C (b) 45°C (c) 65°C

Figure 59 shows the failure surfaces of the E-glass/epoxy and E-glass/polyurethane composite. The rough surfaces of the matrix and fiber cross-sections of the E-glass/epoxy control sample in Figure 59(a) indicate ductile failure of the material. In addition, the image shows a perfect bond between fiber and matrix with minimum separation at the interface. The micrograph of the E-glass/polyurethane control specimen in Figure 59(b) shows corrugated surfaces of matrix and fiber cross-sections, indicating ductile failure with no debonding and fiber pull-out.
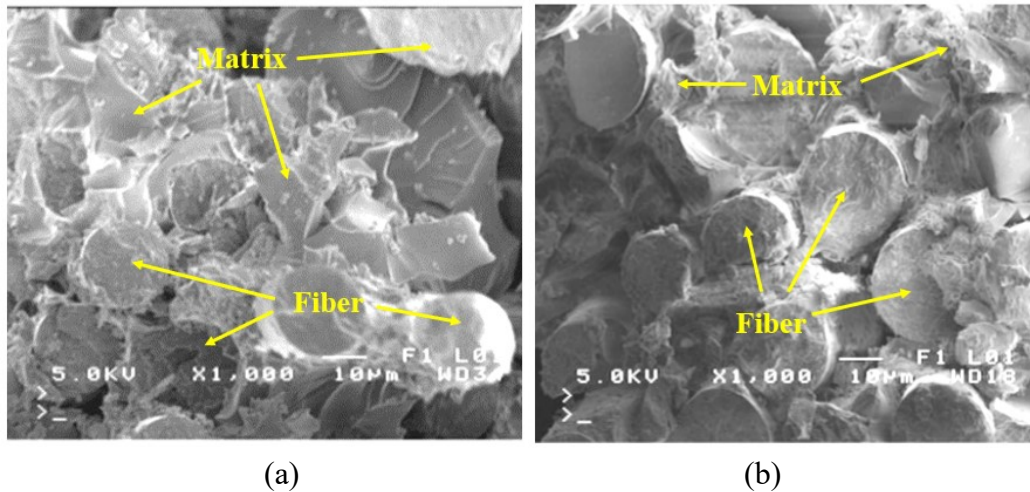
Figure 59: Control samples (a) E-glass/epoxy (b) E-glass/polyurethane

Figure 60 and Figure 61 represent the respective cross-section surface of E-glass/epoxy and E-glass/polyurethane composite immersed under sustained load for the duration of 15 months. With immersion in seawater under sustained load at different temperature, both materials started to fail in brittle manner shown by the smooth matrix surface in the SEM images and by the decrease in failure strains presented in Figures 35 and 44. It was observed previously that the E-glass/epoxy and E-glass/polyurethane material exhibited brittle failure after short durations of immersion in seawater (Mourad et al., 2010; Murthy et al., 2010).

SEM images for the E-glass/epoxy samples immersed under 15% sustained load at 23°C, 45°C, and 65°C mentioned in Figure 60 for the duration of 15 months. The smooth fractured surface of the fiber and matrix indicate the brittle failure of both fiber and matrix at all temperatures after 15 months. Figure 60(a) shows slight degradation in the fiber/matrix interface with some potholing evidence on the fractured surface. The composite indicated 6.2% decrease in tensile strength, 8.6% increase in modulus due to swelling of the matrix and failure strain reduced to 1.9% due to matrix plasticization. The micrograph in Figure 60(b) represents the failure surface of a

specimen immersed for 15 months at 45°C. The matrix flow, river line marks and fractured fiber indicate the degradation in fiber-matrix interface which increased with immersion temperature. This implies matrix breakdown owing to the hydrolysis reaction which accelerated at high temperature immersion results a non-uniform load distribution between fibers (Mourad et al., 2010). The reaction between water and epoxy believed to cause a breakdown of the polymer's molecular weight, leading to the fragile nature of the matrix. Water can also function as an anti-plasticizer, preventing polymer segments from moving and making the matrix more brittle (Chakraverty et al., 2015). The fiber/matrix debonding and potholing results 11.3% drop in tensile strength. The fiber/matrix debonding accelerated at 65°C results several potholes observed on the fractured surface of the composite as shown in Figure 60(c). It has been reported by Chen et al. (2007) that the degradation of E-glass fibers involves mainly the etching of free hydroxyl ions (OH) and leaching of water molecules. The free hydroxyl ions (OH) break the Si-O-Si bond of glass fiber, especially for etching in alkaline solution (Charles, 1959; Chen et al., 2007). The damage at the fiber/matrix interface involves a complex mechanism as the fiber/matrix interface is a heterogeneous area between the fiber and matrix (Robert & Benmokrane, 2013). Fiber-matrix interface damage for FRP composites is usually caused by debonding between fiber and resin which occurs mainly in two stages. The first part is the breakage of chemical bonding due to chemical corrosion between fiber and resin, and the second part is the poor interlocking between fibers and resin due to resin swelling through water absorption (Wang et al., 2016).

(a)　　　　　　　　　　　　　　　(b)

(c)
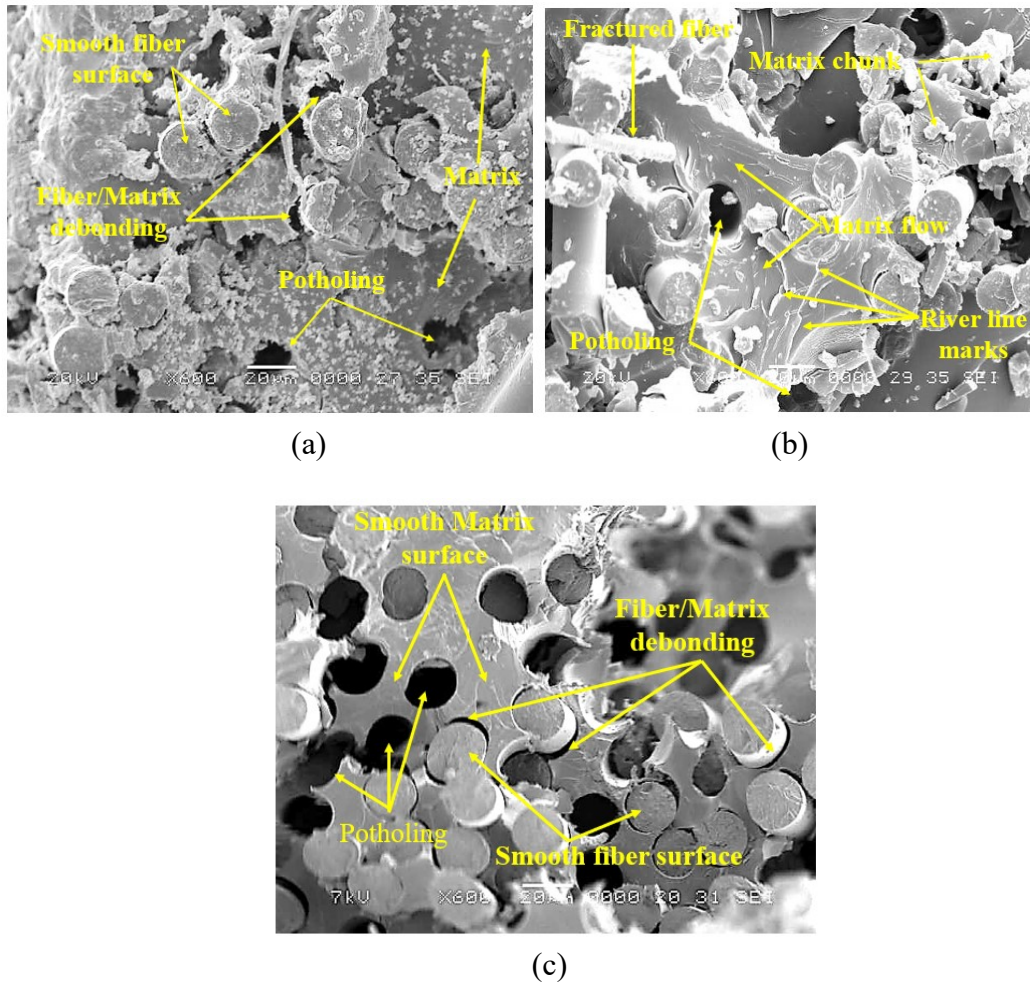
Figure 60: Failure surfaces of E-glass/epoxy composite immersed under sustained load for the duration of 15 months at (a) 23°C (b) 45°C (c) 65°C

Figures 61(a), (b) and (c) show the SEM micrograph of e-glass/polyurethane composite immersed at 23°C, 45°C. and 65°C respectively for the duration of 15 months. Figure 61(a) indicates strong bond between the fiber and matrix of the composite after immersion at 23°C. However, some fibers pullout can be seen on the fractured surface. The intensity of fiber pullout increased for the samples immersed at 45°C as shown in Figure 61(b). The image clearly shows the degradation of fiber/matrix interface with some potholing evidence. Few fibers have clean surfaces along the length and minor gap at the interface of fiber and matrix. Significant

debonding in the fiber/matrix interface was observed in the composite material immersed at 65°C as shown in Figure 61(c).

(a)   (b)

(c)
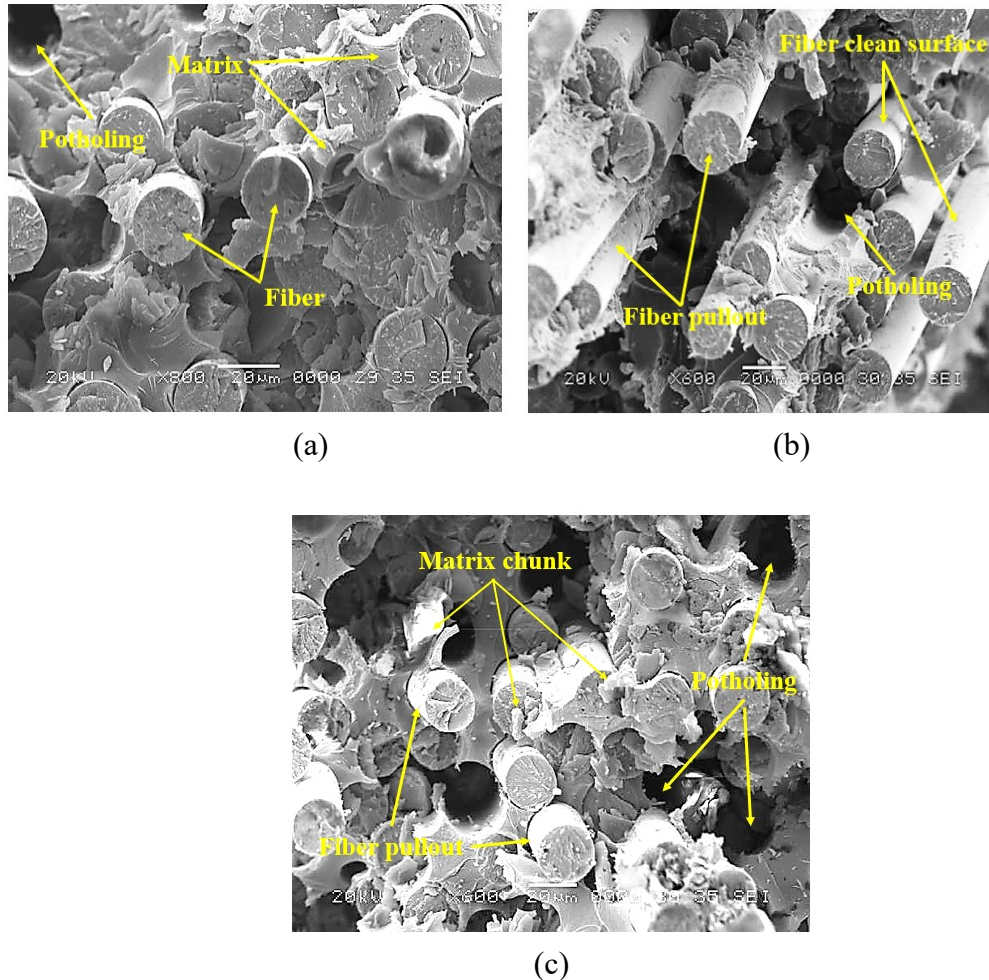
Figure 61: Failure surfaces of E-glass/polyurethane composite immersed under sustained load for the duration of 15 months at (a) 23°C (b) 45°C (c) 65°C

SEM micrograph shows shattered matrix on the failure surface of the composite which indicated brittle failure of the composite. Further degradation of the interface between fibers/matrix is the product of large and prevalent gaps between fibers and matrices. The reaction between water and polyurethane believed to cause a breakdown of the polymer's molecular weight, leading to the fragile nature of the matrix. Water can also function as an anti-plasticizer, preventing polymer segments from moving and making the matrix more brittle (Chakraverty et al., 2015). Damage

to glass fibers isn't evident, but its smooth cross-sectional surface of the pulled-out fibers reveals brittle failure of the fiber. This could be due to the loss in ductility of the fiber, lack of support from the brittle matrix, or unhindered crack propagation into the fiber (Mourad et al., 2010).

6.6 Prediction Models

6.6.1 Prediction of the Long-Term Effect of Seawater Immersion on Composites

In the development of prediction model 12 months of data was used as the remaining data was used for prediction and determination of relevant error. The first step in predicting the long-term effect of seawater immersion on the two composites was to plot the retention strength values against time, from which the values of the degradation rate K could be obtained by using regression analysis, and to check if the strength follows the Arrhenius equation. The tensile strength vs exposure plots for samples immersed without load and with sustained load were converted into Figures 62 for E-glass/epoxy composite and Figures 63 for E-glass/polyurethane composite by using Equation (13) below to calculate the strength retention in percent, SR (%), and then plotting the SR (%) against the exposure time.

$$SR(\%) = \frac{\text{Residual Tensile Strength}}{\text{Original Tensile Strength}} * 100 \qquad (13)$$
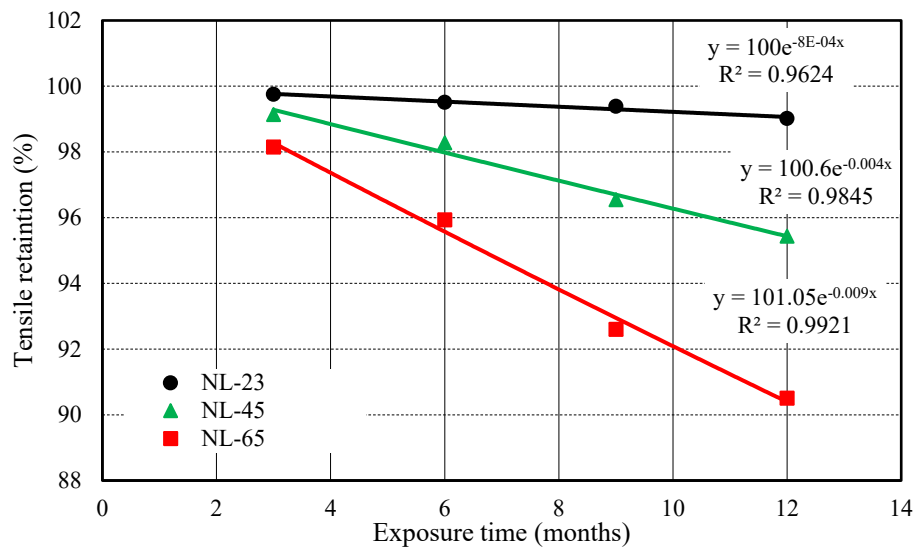
(a)
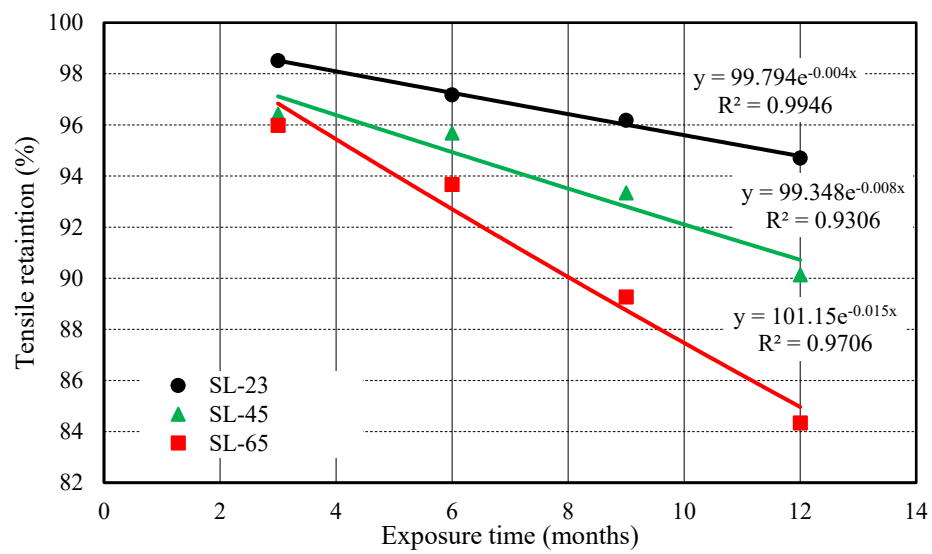
(b)

Figure 62: The relation between tensile strength retention and exposure time of E-glass/Epoxy composite at different temperatures (a) without load (b) sustained load
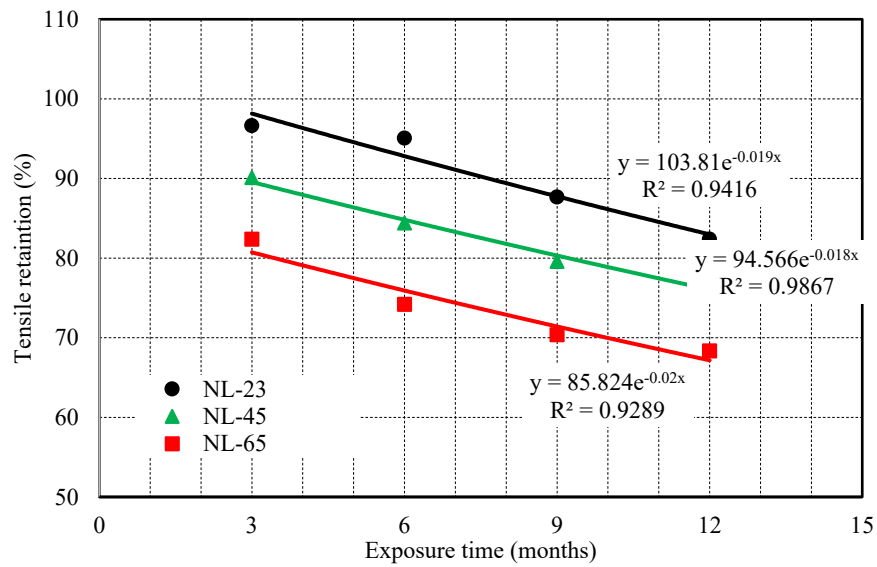
(a)
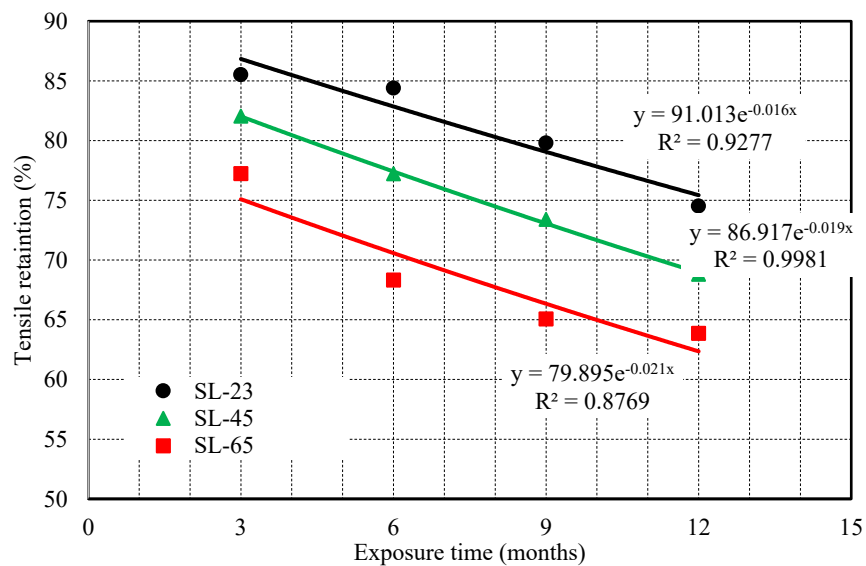
(b)

Figure 63: The relation between tensile strength retention and exposure time of E-glass/polyurethane composite at different temperatures (a) without load (b) sustained load

The plots in Figures 62 and 63 have correlation coefficients that are above 0.8, which indicate that they follow the Arrhenius model. These plots are based on the first model given in Equation (4).

Similarly, the tensile retention (%) was plotted against the exposure time, as shown in Figure 64 and 65, to test if the second model (Equation (5)) could also be used to predict the durability of the composite materials.
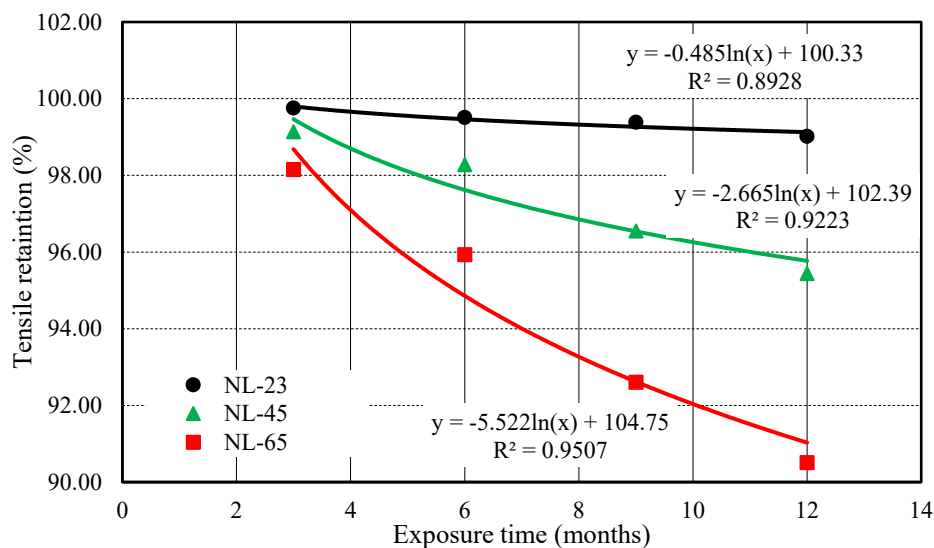
(a)
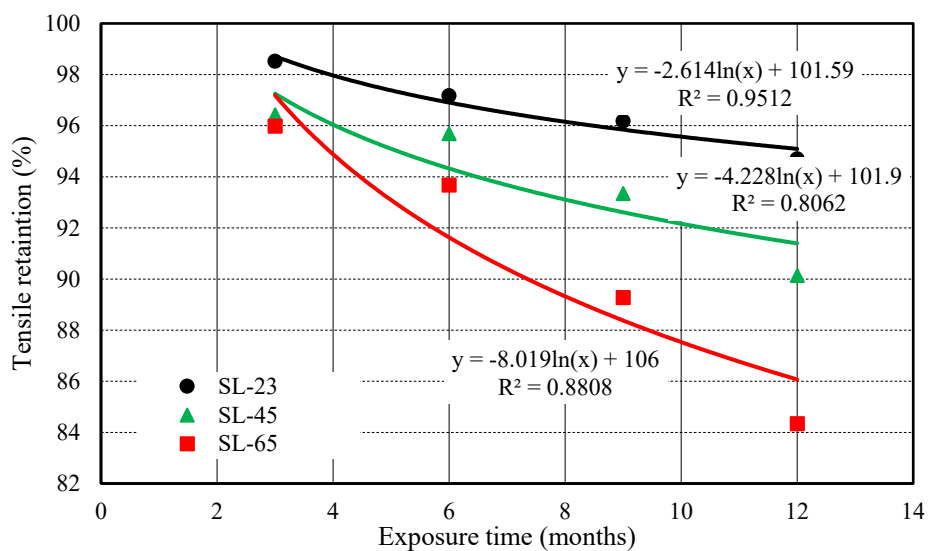
(b)

Figure 64: The relation between tensile strength retention and exposure time of E-glass/Epoxy composite at different temperatures (a) without load (b) sustained load
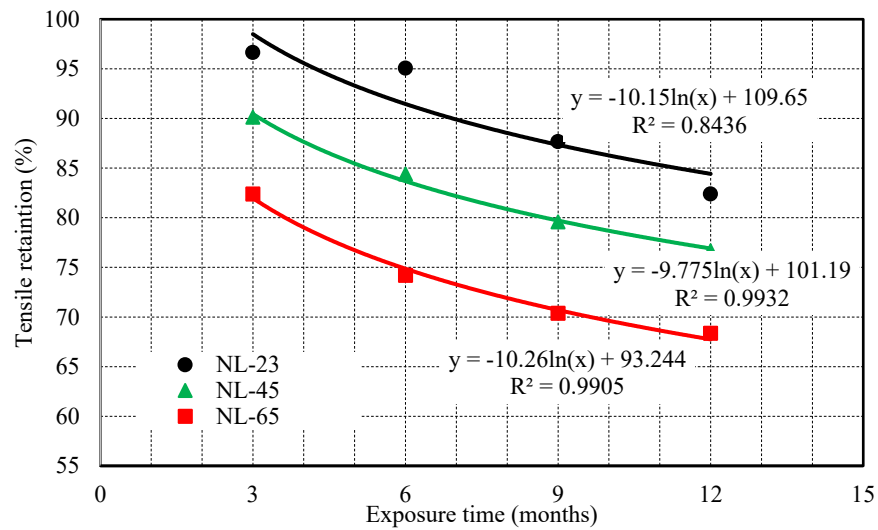
(a)
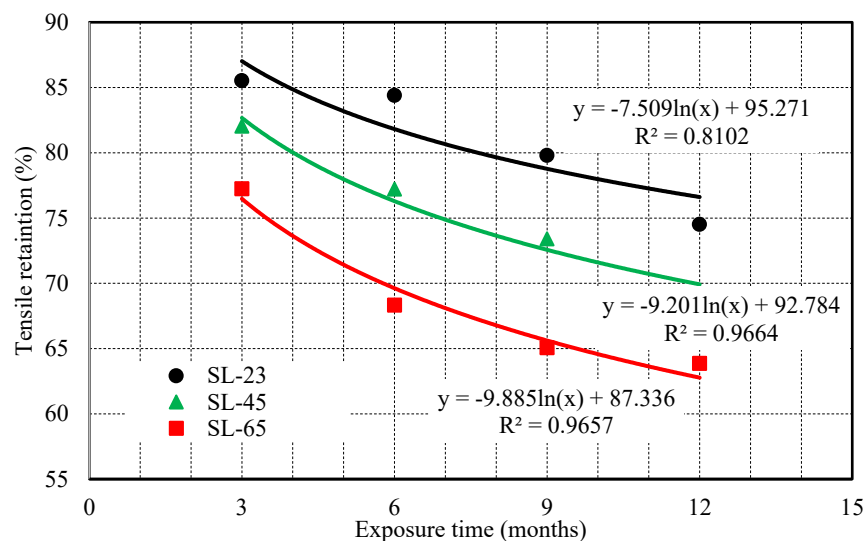
(b)

Figure 65: The relation between tensile strength retention and exposure time of E-glass/polyurethane composite at different temperatures (a) without load (b) sustained load

The predictions from the two models were compared with the experimental data and noted in Table 20. Both the models show good agreements between the experimental and predicted results. The present work shows that the tensile strength of E-glass/epoxy composite reduced by 11.1% and 18.2% for samples immersed without

and with sustained load respectively after 15 months of immersion at 65°C. The reduction in tensile strength of E-glass/polyurethane was 34.1% and 38.2% for samples immersed without and with sustained load respectively for the same conditions. The first model predicted that E-glass/epoxy would lose 11.7% and 19.2% of its tensile strength after 15 months at 65°C with an error of 5.5% and 5.4% while the E-glass/polyurethane would lose 36.4% and 41.7% of its tensile strength after the same duration with an error of 6.7% and 9.3% for without and with sustained load respectively. According to the second model, the E-glass/epoxy would lose 10.2% and 15.7% after 15 months with an error of 8% and 13.9%, while the tensile strength of E-glass/Polyurethane will be reduced by 34.5% and 39.4% with an error of 1.2% and 3.3% respectively under same immersion conditions.

Table 20: Comparison of experimental results with predicted results based on first and second model

Composites with immersion conditions	TS	Experimental results		1st Model prediction		2nd Model prediction		Error	
		TS_E	AR%	TS_P	PR %	TS_P	PR %	1st Model	2nd Model
EP-NL-23	811	802	1.1	801.3	1.2	803.0	1.0	7.5	11.4
EP-NL-45	811	766	5.5	768.4	5.3	771.9	4.8	5.2	13.0
EP-NL-65	811	721	11.1	716.0	11.7	728.2	10.2	5.5	8.1
EP-SL-23	811	761	6.2	762.2	6.0	766.5	5.5	2.4	11.0
EP-SL-45	811	719	11.3	714.6	11.9	733.6	9.5	4.8	15.8
EP-SL-65	811	663	18.2	655.0	19.2	683.5	15.7	5.4	13.9
PU-NL-23	891	726	18.5	727.6	18.3	732.1	17.8	1.0	3.7
PU-NL-45	891	662	25.7	643.2	27.8	665.7	25.3	8.2	1.6
PU-NL-65	891	587	34.1	566.5	36.4	583.2	34.5	6.7	1.2
PU-SL-23	891	649	27.2	637.9	28.4	667.7	25.1	4.6	7.7
PU-SL-45	891	603	32.3	582.4	34.6	604.7	32.1	7.2	0.6
PU-SL-65	891	551	38.2	519.5	41.7	539.7	39.4	9.3	3.3

Where;

TS - Tensile strength (MPa) of control samples

TS_E - Experimental tensile strength (MPa) of samples immersed in seawater for the period of 15 months

TS_P - Predicted tensile strength (MPa) of samples immersed in seawater for the period of 15 months

AR% - Actual reduction in tensile strength (%)

PR % - Predicted reduction in tensile strength (%)

Finally, the prediction based on the Arrhenius equations compares well with the experimental data in most cases, as shown in Table 20. In conclusion, in order to predict long-term durability, the data must be collected at least at three different temperatures and at three different exposure times. The more data collected, the more accurate are the predictions. Moreover, long-term exposure provides better results than short-term exposure (Davalos et al., 2012).

6.6.2 Time Shift Factor (TSF) Approach

The Arrhenius equation was utilized for the prediction of durability. We have a fundamental assumption that the single dominant degradation mechanism does not change regardless of the immersion time and temperature even under various sustained load, but the degradation rate increases with the immersion temperatures.

The fiber-matrix interfacial debonding occurred during the degradation of E-glass/epoxy and E-glass/polyurethane composite. To determine the degradation the exponential degradation model (Wu et al., 2015) was used, which is defined as

$$Y = 100\exp\left(-t/\tau\right) \tag{13}$$

where Y is the tensile strength retention (%), t is the immersion time (months), and τ is a constant.

On the basis of Equation (13), the fitted curves are shown in Figures 62 and 63 and corresponding τ values and correlation coefficients (R^2) are listed in Table 21. Secondly, with the regression coefficient τ listed in Table 21 the time (t) needed for the apparent horizontal shear strength retention to reach 50, 60, 70, and 80% at 23, 45, and 65°C were calculated from Equation (13).

Table 21: Coefficients of the regression equations in Eq. (8) for both composites.

Type	Temp	No-load (NL)		Sustained load (SL)	
		Tau	R^2	Tau	R^2
E-glass/epoxy	23	1250	0.9808	250.2076724	0.9965
	45	249.4014366	0.9811	125.3271037	0.9657
	65	110.6463962	0.9889	71.10150451	0.9811
E-glass/polyurethane	23	61.57028864	0.9427	47.19951139	0.9086
	45	46.48179308	0.9672	36.47193813	0.9034
	65	34.29228273	0.8864	30.38711975	0.8326

The time required to reach a certain value was calculated according to Equation (4), and the natural logarithm of time ($\ln(1/k) = \ln t$), to reach different tensile strength retention values was plotted against the inverse of the temperature (1/T), in kelvin. The line fitting was done by regression analysis, as shown in Figures 66 and 67 and Table 21.
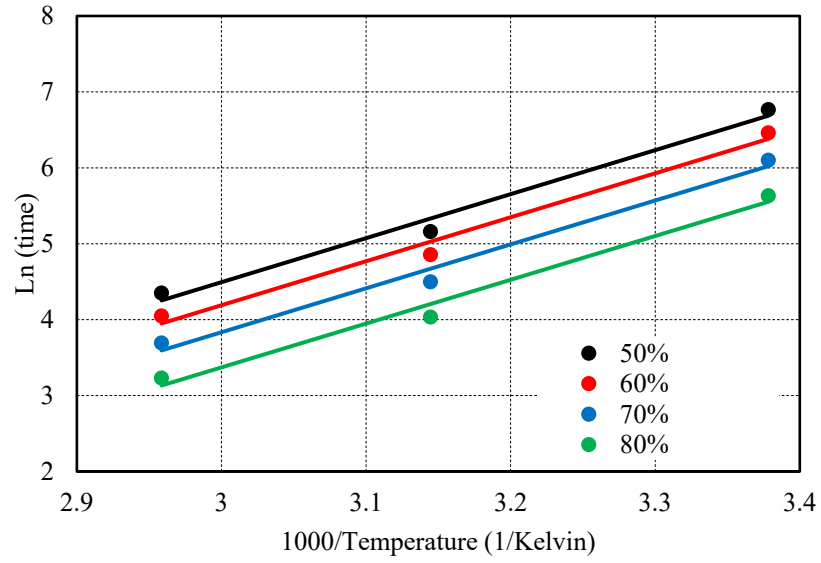
(a)
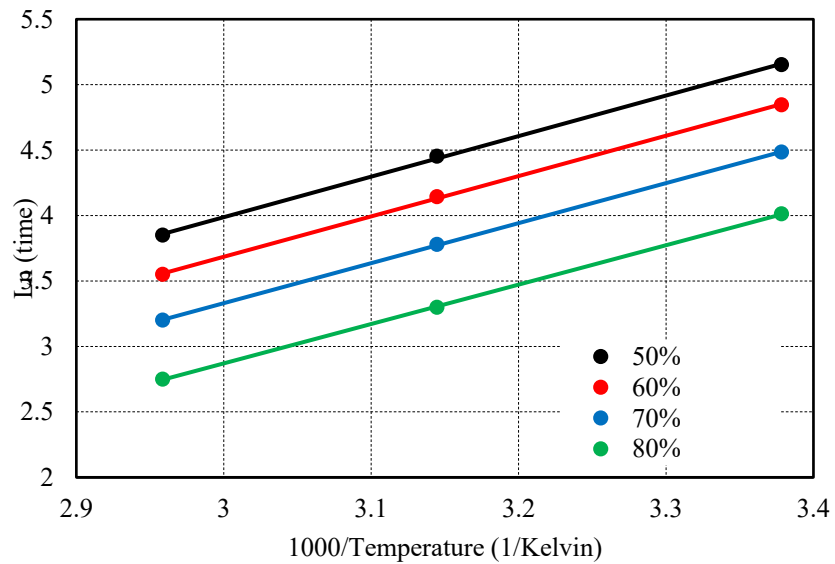
(b)

Figure 66: Arrhenius plots for E-glass/epoxy at different tensile strength retention (50% to 80%) (a) without load (b) sustained load
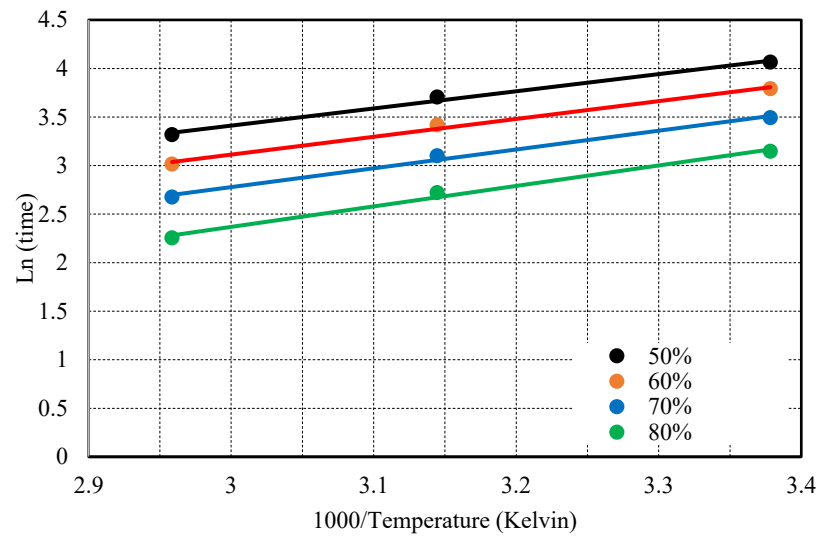
(a)
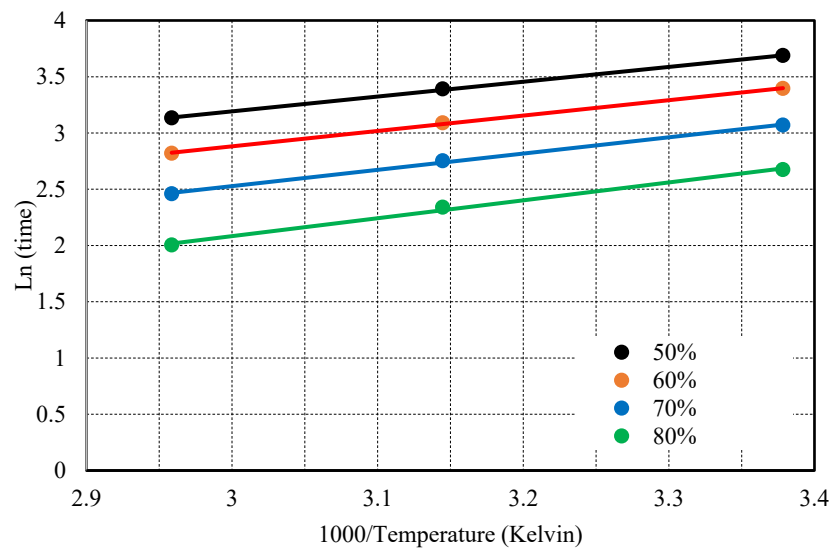
(b)

Figure 67: Arrhenius plots for E-glass/polyurethane at different tensile strength retention (50% to 80%) (a) without load (b) sustained load

Table 22: Coefficients of regression equation in Eq. (7) for Arrhenius plots.

Type	NL		SL	
	Ea/R	R²	Ea/R	R²
Epoxy	5785	0.99	3057	0.98
Polyurethane	1937	0.99	1447	0.99

Table 22 shows the activation energy of E-glass/epoxy to be larger than that of E-glass/polyurethane. These values are consistent and logical since E-glass/polyurethane degraded more than E-glass/epoxy due to the small activation energy for atoms to react, hence for the material to degrade more than the E-glass/epoxy.

Thirdly, based on Equation (1), the time-shift factor (TSF) for the apparent horizontal shear strength to reach the same value at temperatures T1 and T0 can be obtained from the previous Arrhenius plots. The time-shift is defined as the ratio of times (t_0 and t_1) required to reach a specific mechanical property at two different temperatures (T_0 and T_1). According to Equation (14) below, the time required to reach a specific mechanical property is the inverse proportion of the reaction rate K. The TSF can be expressed as:

$$\text{TSF} = \frac{t_0}{t_1} = \frac{K_1}{K_0} = \frac{Ae^{-\frac{E_a}{T_1 R}}}{Ae^{-\frac{E_a}{T_0 R}}} = e^{\frac{E_a}{R}\left(\frac{1}{T_0} - \frac{1}{T_1}\right)} \tag{14}$$

The TSF with reference temperatures T_0 equal to 20.3°C, 14.0°C, and 5.7°C, representing the annual temperature at northern latitudes 30°, 40°, and 50°, respectively, are listed in Table 23. In the northern latitude 50° area, for example, the tensile strength retention data in Figures 62 and 63 were transformed into those of Figures 68 and 69 by multiplying the exposure times at 65°C, 45°C, and 23°C with the corresponding TSF values. The master curve versus aging time at the annual

temperature of the northern area at latitude 50° could be obtained by fitting Equation 14 to the data in Figures 68 and 69. Following these steps, the master curves for northern areas at latitudes 30° and 40° were obtained, also as shown in Figures 68 and 69.

Table 23: Time-shift factors of both E-glass/epoxy and E-glass/polyurethane composite immersed without load and with sustained load in seawater for various latitudes.

Condition	Composite	Temperature (°C)	Northern latitude - 30°	Northern latitude - 40°	Northern latitude - 50°
			20.3°C	14°C	5.7°C
Without load	E-glass/epoxy	23	1.2	1.8	3.4
		45	4.6	7.1	13
		65	13.6	21	38.2
	E-glass/polyurethane	23	1.1	1.2	1.5
		45	1.7	1.9	2.4
		65	2.4	2.8	3.4
Sustained load	E-glass/epoxy	23	1.1	1.4	1.9
		45	2.2	2.8	3.9
		65	4	5	6.9
	E-glass/polyurethane	23	1	1.2	1.4
		45	1.5	1.6	1.9
		65	1.9	2.1	2.5
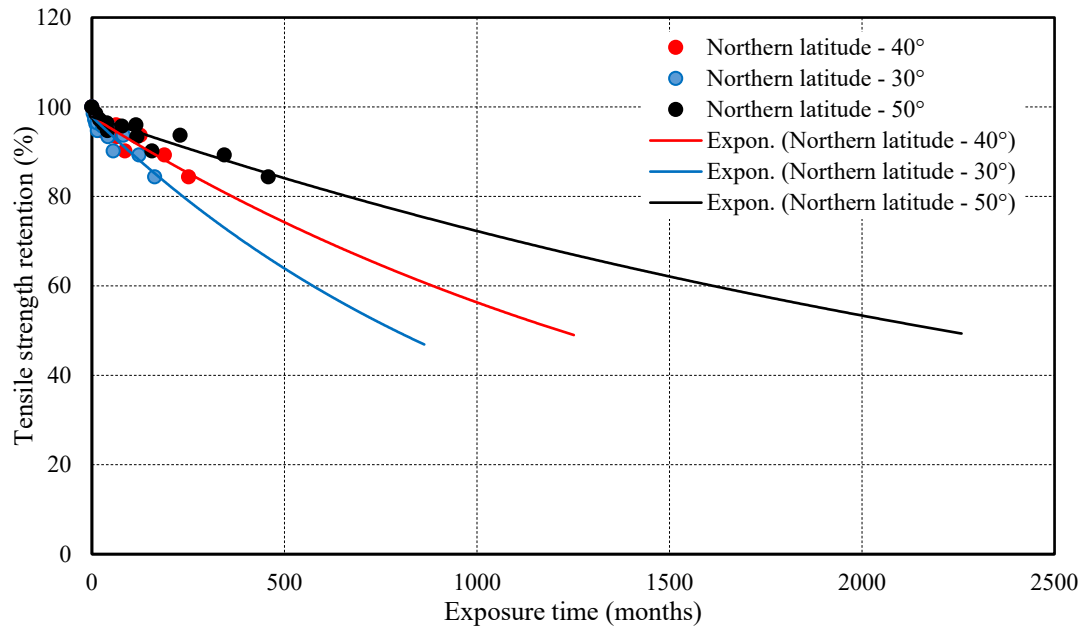
(a)
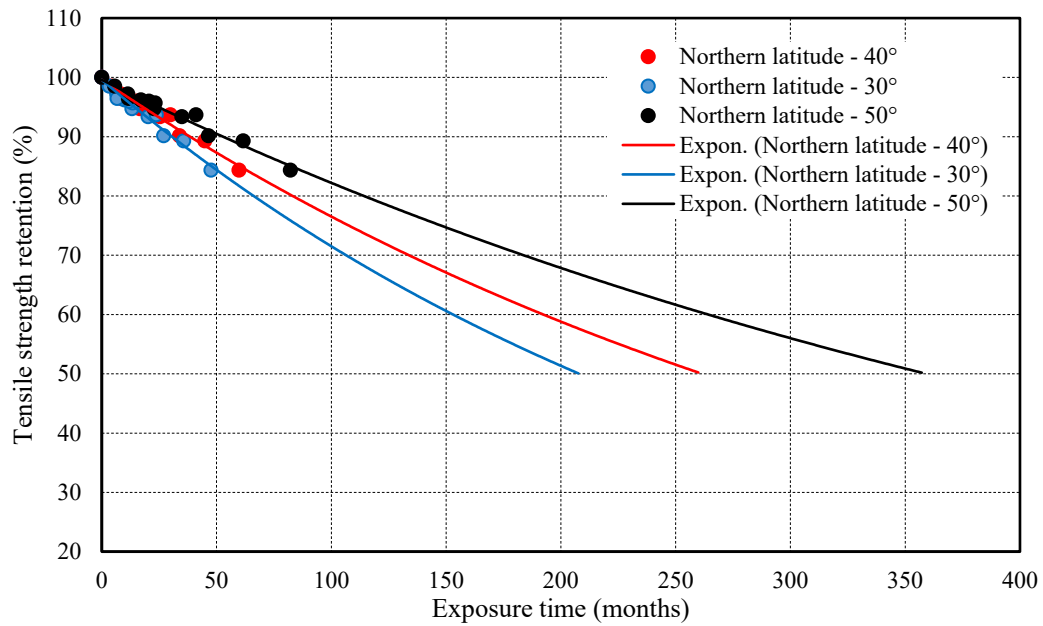
(b)

Figure 68: Life prediction of the tensile strength for E-glass/epoxy composite immersed (a) without load (b) with sustained load

(a)

(b)

Figure 69: Life prediction of the tensile strength for E-glass/polyurethane composite immersed (a) without load (b) with sustained load

Table 24 and Figures 68 and 69 indicate the prediction of tensile strength retention for E-glass/epoxy and E-glass/polyurethane composite for various northern latitude. The results show that the tensile strength retention of E-glass/Epoxy will reduce to 50% after immersion for 2252 months (approx. 188 years) without load and 358 months (approx. 30 years) under 15% sustained load for Northern latitude - 50°. The tensile strength retention of E-glass/polyurethane for the same latitude will reduce to 50% after immersion for 178 months (approx. 15 years) without load and 124 months (approx. 10 years) under 15% sustained. Similarly, the predicted results for Northern latitude - 30° and Northern latitude - 40° are shown in Table 24.

Table 24: Long-term predication results for the tensile strength retention to reach 50%, for E-glass/epoxy and E-glass/polyurethane in three Northern latitudes.

Composite	Temperature (°C)	Northern latitude - 30°	Northern latitude - 40°	Northern latitude - 50°
		20.3	14	5.7
E-glass/epoxy	Without load	780.0	1208.0	2252.0
	Sustained load	208.0	260.0	358.0
E-glass/polyurethane	Without load	126.0	145.0	178.0
	Sustained load	104.0	115.0	124.0

After considering the effect on the different Northern latitudes, the prediction procedure implemented on the physical structures. For this part, four serviced structures in Canada were chosen to predict the long-term durability. The TSF values of these structures are shown in Table 25. All the fitted results for the master curves of E-glass/epoxy and E-glass/polyurethane composite are shown in Figures 70 and 71.

Table 25: Time-shift factors of both E-glass/epoxy and E-glass/polyurethane composite immersed without load and with sustained load in seawater for various structures.

Condition	Composite	Temperature (°C)	HHW	CB	CT	WCB
			7.6°C	4.6°C	3.9°C	9.9°C
Without load	E-glass/epoxy	23	2.9	3.7	3.9	2.5
		45	11.3	14.1	14.9	9.6
		65	33.2	41.5	43.7	28.1
	E-glass/polyurethane	23	1.4	1.5	1.6	1.4
		45	2.3	2.4	2.5	2.1
		65	3.2	3.5	3.5	3.1
Sustained load	E-glass/epoxy	23	1.8	2	2	1.6
		45	3.6	4.1	4.2	3.3
		65	6.4	7.2	7.4	5.8
	E-glass/polyurethane	23	1.3	1.4	1.4	1.3
		45	1.8	1.9	2	1.8
		65	2.4	2.5	2.6	2.3

Where;

HHW - Hall's harbor wharf

CB - Chatham Bridge

CT - Crowchild Trail

WCB - Waterloo Creek Bridge
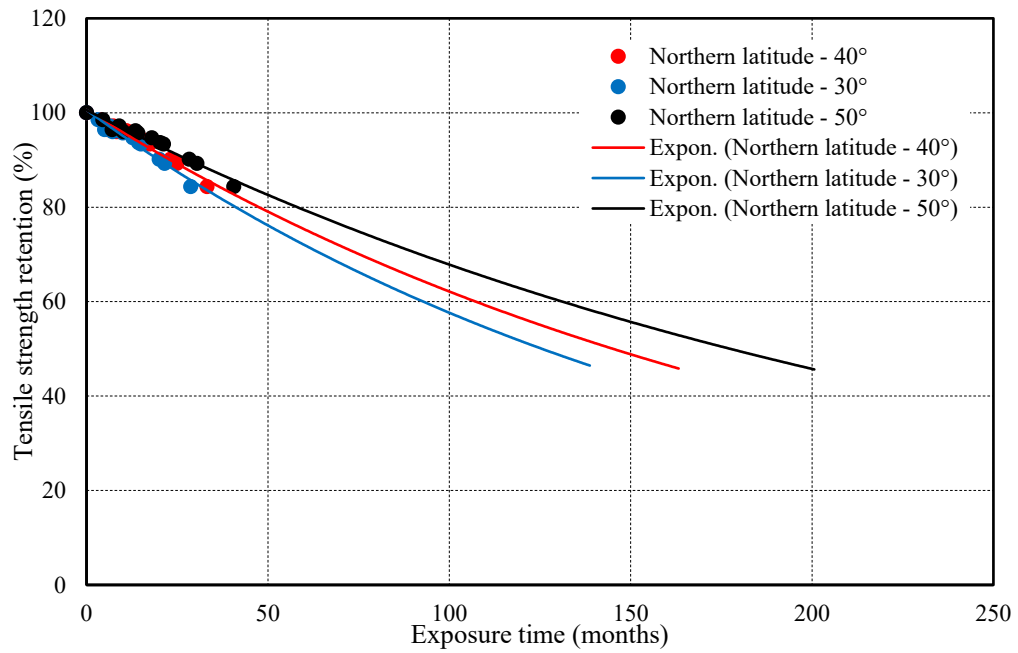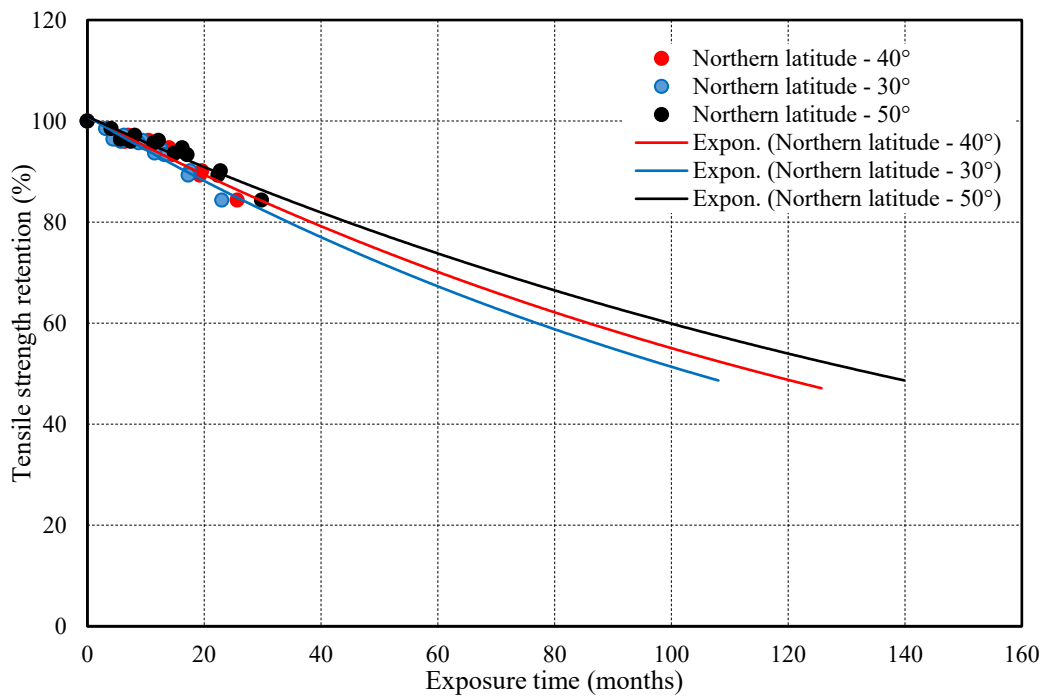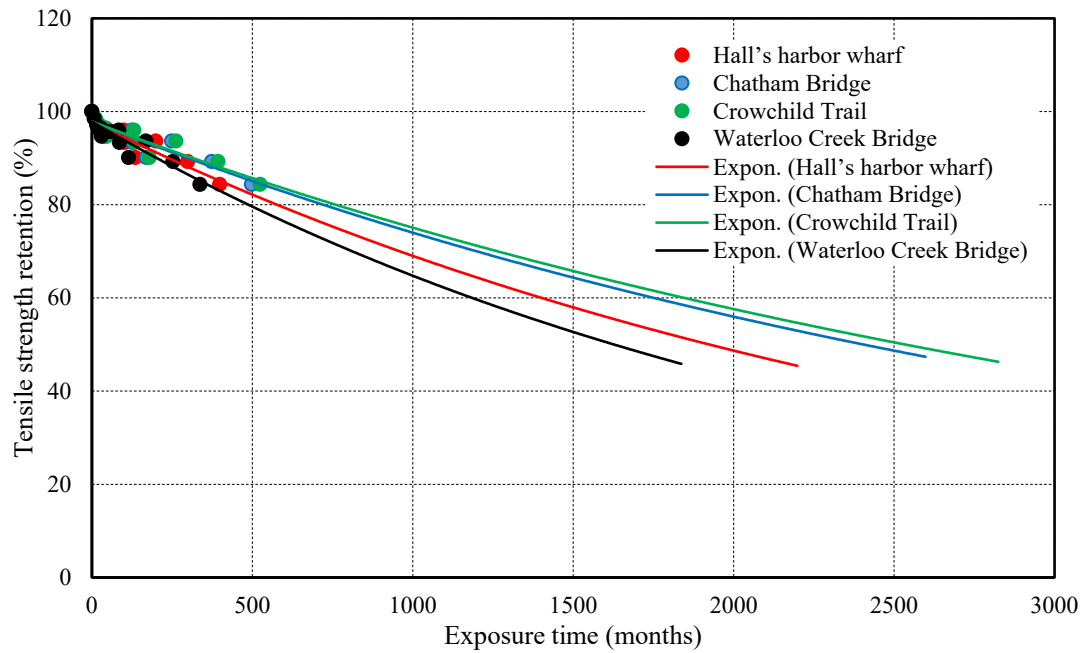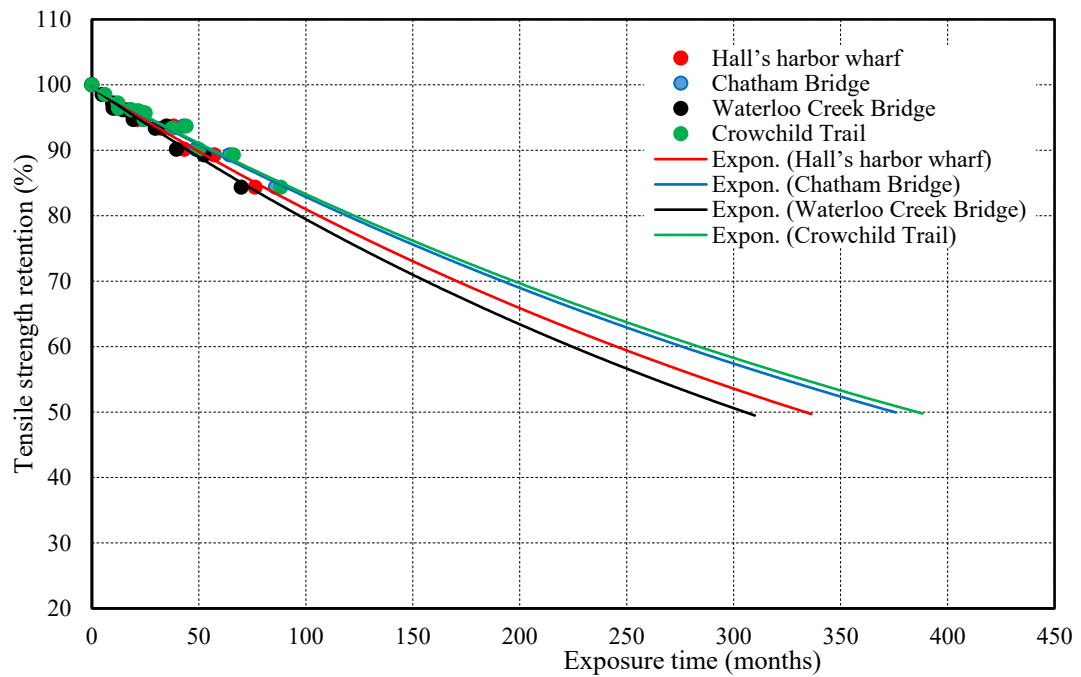
Figure 70: Life prediction of the tensile strength for E-glass/epoxy composite immersed (a) without load (b) with sustained load
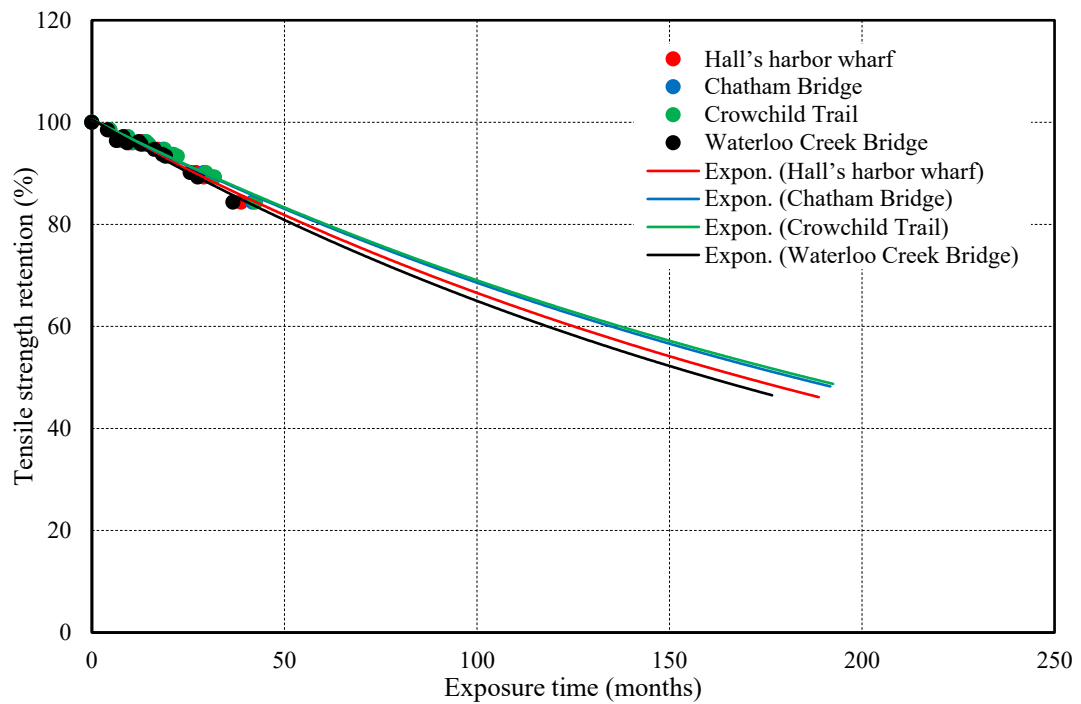
(a)
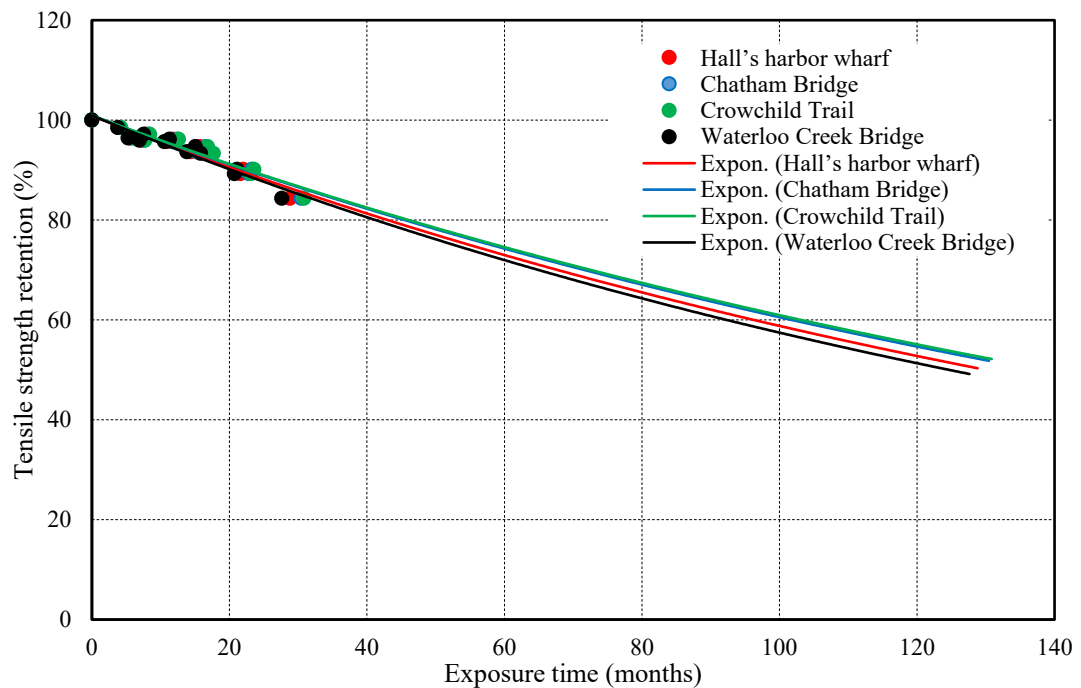
(b)

Figure 71: Life prediction of the tensile strength for E-glass/polyurethane composite immersed (a) without load (b) with sustained load

Table 26: Long-term predication results of tensile strength retention to reach 50%, for E-glass/epoxy and E-glass/polyurethane for four structures.

Composite	Temperature (°C)	HHW	CB	CT	WCB
		7.6	4.6	3.9	9.9
E-glass/epoxy	Without load	1905	2390	2530	1608
	Sustained load	336	376	388	305
E-glass/polyurethane	Without load	168	181	185	159
	Sustained load	129	138	140	126

Table 26 and Figures 70 and 71 indicate the prediction of tensile strength retention for E-glass/epoxy and E-glass/polyurethane composite for various structures. The results show that the tensile strength retention of E-glass/epoxy will reduce to 50% after immersion for 2390 months (approx. 199 years) without load and 376 months (approx. 31 years) under 15% sustained load for Chatham Bridge. Similarly, the tensile strength retention of E-glass/polyurethane for the same bridge will reduce to 50% after immersion for 181 months (approx. 15 years) without load and 138 months (approx. 12 years) under 15% sustained. Similarly, the predicted results for other structures are shown in Table 26. Based on the observations, it was determined that E-glass/epoxy performed better than E-glass/polyurethane composite under different environmental conditions and can be used preferably in application such as marine, aerospace, and pipeline industries.

Chapter 7: Conclusion

In this research, the impact of different environmental conditions on the durability of E-glass/epoxy and E-glass/polyurethane composites was investigated without load and under sustained load. The effect of exposure time was analyzed by immersing of the sample at exposure temperatures of 23°C, 45°C, and 65°C for the different period of time varied from 3 months to 15 months for both conditions i.e., without load and sustained load (15% of tensile strength). Furthermore, the effect of exposure time and sustained load was analyzed. Higher temperature also be used as the accelerating agent for durability in marine environment where loaded specimens immersed in seawater with temperatures ranging from 45°C to 95°C. Accelerated tests were conducted for one month and changes in properties with time and temperature calculated. Another analysis was successfully conducted to determine the effect of the sustained load varied from 10% to 25% of tensile strength on the durability of both. Results indicated a significant effect of exposure time, exposure temperature and sustained load on the durability of both composites.

The major findings of the experimental testing of the project are as follows:

Effect of exposure time

- Absorption of water increased gradually with immersion time for both composites under all condition of exposure. The water absorption was observed more in samples immersed without load compared to the samples immersed with sustained load. The highest increase in weight was 5.7% and 5.1% for E-glass/epoxy and E-glass/polyurethane composites respectively for the immersion period of 15 months without load at 65°C. This increase was 2.5% and 1.9% for E-glass/epoxy and E-glass/polyurethane composites respectively

for the immersion period of 15 months under 15% of sustained load at 65°C. These results also indicate that higher temperatures accelerated the absorption process.

- The tensile strength of the E-glass/epoxy reduced gradually with immersion time. It reduced by 11% from 811 MPa to 721 MPa and by 18.2% from 811 MPa to 663 MPa for samples immersed without load and with 15% sustained load respectively. The respective reduction for 23°C and 45°C was 1.1% and 5.5% for samples without load and 6.2% and 11.3% for samples immersion under 15% sustained load after 15 months of exposure.

- The tensile strengths of the E-glass/polyurethane composite after immersion in seawater at 23°C, 45°C, and 65°C without load was 18.5%, 25.7% and 34.1% respectively However this respective reduction was 27.2%, 32.3%, and 35.2% under sustained load for the exposure of 15 months.

- The elastic modulus of E-glass/epoxy composite immersed without load varied in the range of ±2 during the immersion period of 15 months. The tensile modulus of samples increased significantly from 37.1 GPa to 41.3 GPa, 38.9 GPa and 42.5 GPa for specimen immersed under 15% sustained load for 15 months at 23°C 45°C, and 65°C respectively.

- The elastic modulus of E-glass/polyurethane composite varied within a limited range of ±1.5 GPa from the original control value of 41.8 GPa for immersion without load. The lowest measured average was nearly 40.8 GPa, and the highest measured average was nearly 43.2 GPa during the 15 months of immersion. The variation in tensile modulus was comparatively higher for samples immersed under sustained load. The modulus increased from 41.8 GPa to 48.2 GPa, 46.2 GPa, and 44 GPa for the samples immersed in seawater at

23°C, 45°C and 65°C. This increase in percentage was 15.3, 11, and 5.5 respectively.

- The failure strain of E-glass/epoxy composite was slightly affected for the samples immersed without load during the period of 15 months. For sustained load immersion, the failure strain reduced from 2.2% to1.9% for immersion at 23°C and 45°C. It was more noticeable under 15% sustained load at 65°C when the tensile strain reduced to 1.65% after 15 months of immersion.

- The failure strain of E-glass/polyurethane composite was decreased for both types of immersion i.e., without load and with sustained load. The failure strain was reduced from 2.1% to 1.8%, 1.6% and 1.3% for the immersion without load at 23°C, 45°C, and 65°C respectively. However, this reduction was 1.35%, 1.3%, and 1.25% for immersion at 23°C, 45°C, and 65°C respectively under sustained load.

Effect of temperature

- The strength of the E-glass/polyurethane dropped gradually with an increase in temperature; However, for E-glass/epoxy it reduced gradually till immersion at 65°C but a sharp decrease detected with further increase in the temperature. The tensile strength of E-glass/epoxy composite reduced by 1.1%, 1.9%, and 2.4% with immersion at 23°C, 55°C, and 65°C but it jumped to 18%, 29.7%, and 41.2% with immersion at 75°C, 85°C, 95°C respectively in 1 month of exposure. For E-glass/polyurethane this reduction was 11.7% and 27.2% at 23°C and 95°C respectively.

- The tensile modulus of E-glass/epoxy and E-glass/polyurethane composite was determined after the immersion of one month at different temperature. The

modulus of both the composite increased compared to the control sample. The maximum increase for E-glass/epoxy composite was approx 5GPa Whereas this increase was 12 GPa for E-glass/polyurethane composite.

- The failure strain of both composites significantly affected by an increase in the immersion temperature. The tensile strain of E-glass/epoxy and E-glass/polyurethane reduced to 1.28% and 1.35% respectively for the immersion at 95°C.

Effect of Sustained load

- The tensile strength of E-glass/polyurethane composite reduced steeply with an increase of sustained load whereas it reduced gradually for E-glass/epoxy composite. The tensile strength of E-glass/epoxy composite reduced by 1.6%, 2.5%, 3.2%, and 4.9% with sustained of 10%, 15%, 20% and 25% respectively for immersion at 65°C in the period of 1 month. For E-glass/polyurethane this reduction was 18.7%, 23.3%, 42.6% and 44.6% with sustained of 10%, 15%, 20% and 25% respectively.

- The modulus of both the composite increased compared to the control sample. The maximum modulus for E-glass/epoxy and E-glass/polyurethane composite was 46.4 GPa and 56.6 GPa for the immersion with 20% and 25% sustained load respectively.

- The failure strain of E-glass/epoxy and E-glass/polyurethane composite significantly affected with an increase in the sustained load. The tensile strain of E-glass/epoxy and E-glass/polyurethane reduced to 1.95% and 1.1% respectively for the immersion with 25% sustained load.

Failure analysis and thermal analysis

- Failure analysis indicates that seawater immersion of E-glass/epoxy composite at 23°C, slightly affected the fiber/matrix interface results only 6.2% decrease in the tensile strength in the period of 15 months. The intermediate effect of seawater immersion observed at 45°C for E-glass/epoxy composite and E-glass/polyurethane composite conditioned for the period of 15 months. However, significant fiber/matrix debonding, fiber pullout and pot holes observed for the immersion at 65°C under 15% sustained load for both composites.

- The immersion at 23°C had not any significant effect on the glass transition temperature (Tg) of the E-glass/epoxy composite without load and with sustained load but reduced from 118.2°C to 114.2°C and 113.5°C for the immersion without load and with sustained load respectively at 65°C. Similarly, the Tg of E-glass/polyurethane reduced from 87.6°C to 84.3°C and 83.4°C for the immersion without load and with sustained load respectively at 65°C.

Prediction models

- Two prediction models developed using the experimental data of 12 months for both composites. Furthermore, these models used to predict the tensile strength retention for 15 months of immersion. The results of both models were in good agreement with the experimental data.

- The TSF approach h successfully implemented to determine the tensile strength retention of both composite for northern latitude 30°, northern latitude 40°, and northern latitude 50°. The study further extended to estimate the durability of four

service structures in Canada includes Hall's harbor wharf, Chatham Bridge, Crowchild Trail, and Waterloo Creek Bridge.

- The activation energy of each composite was determined under different environment. The activation energy was higher for E-glass/epoxy composite as compared to E-glass/polyurethane composite. These values are consistent and logical, since E-glass/Polyurethane degraded more than E-glass/Epoxy due to the small activation energy for atoms to react, hence for the material to degrade more than the E-glass/Epoxy.

Recommendations:

- In the presents work effect of seawater immersion investigated on the E-glass/epoxy and E-glass/polyurethane composite. The work can be extended with different fluid i.e., crude oil, acid solution, alkaline solution on the same composite or different composite.

- The effect of sustained load was investigated for only one moths due to lack of time. The work can be extended to long-term immersion for different percentage of sustained load on different composite and environments.

- The work can be extended to design and manufacture another system for determining the durability of composite under sustained twisting load, also combined effect of torsion and tension can be evaluated by modifying the existing system.

- The study can be extended to determine the long-term effect of sustained load for the samples maintained at sub-zero temperature.

References

Abdel-Magid, B., Ziaee, S., Gass, K. & Schneider, M. (2005). The combined effects of load, moisture and temperature on the properties of E-glass/epoxy composites. *Composite Structures*, *71*(3–4), 320–326.

Akbar, S. & Zhang, T. (2008). Moisture diffusion in carbon/epoxy composite and the effect of cyclic hygrothermal fluctuations: Characterization by Dynamic Mechanical Analysis (DMA) and Interlaminar Shear Strength (ILSS). *Journal of Adhesion*, *84*(7), 585–600. https://doi.org/10.1080/00218460802255434

Al-Kuwaiti, M. H. H. & Mourad, A. H. I. (2015). Effect of different environmental conditions on the mechanical behavior of plain weave woven laminated composites. *Procedia Engineering*, *130*, 638–643.

Al-Tamimi, A. K. (2013). Sustainability of Carbon Fiber Reinforced Concrete Beams Sunder Sea Water Splash Zone. *International Journal of Engineering and Technology*, *3*(3), 322-326.

Almudaihesh, F., Holford, K., Pullin, R. & Eaton, M. (2020). The influence of water absorption on unidirectional and 2D woven CFRP composites and their mechanical performance. *Composites Part B: Engineering*, *182*(November 2019), 107626. https://doi.org/10.1016/j.compositesb.2019.107626

Bank, L. C., Gentry, T. R. & Barkatt, A. (1995). Accelerated test methods to determine the long-term behavior of FRP composite structures: environmental effects. *Journal of Reinforced Plastics and Composites*, *14*(6), 559–587.

Bank, L. C., Gentry, T. R., Thompson, B. P. & Russell, J. S. (2003). A model specification for FRP composites for civil engineering structures. *Construction and Building Materials*, *17*(6–7), 405–437.

Bhise, V. S. (2002). *Strength degradation of GFRP bars*. Virginia Polytechnic and State University, USA.

Buck, S. E., Lischer, D. W. & Nemat-Nasser, S. (1997). The combined effects of load, temperature and moisture on the durability of E-glass/vinyl ester composite materials. *Evolving Technologies for the Competitive Edge.*, *42*, 444–454.

Chakraverty, A. P., Mohanty, U. K., Mishra, S. C. & Satapathy, A. (2015). Sea water ageing of GFRP composites and the dissolved salts. *IOP Conference Series: Materials Science and Engineering*, *75*(1), 12029. doi:10.1088/1757-899X/75/1/012029

Charles, R. J. (1959). The strength of silicate glasses and some crystalline oxides. *Proceedings of the International Conference on Atomic Mechanisms of Fracture*, 225–250.

Chen, Y., Davalos, J. F. & Ray, I. (2006). Durability prediction for GFRP reinforcing bars using short-term data of accelerated aging tests. *Journal of Composites for Construction*, *10*(4), 279–286.

Chen, Y., Davalos, J. F., Ray, I. & Kim, H.-Y. (2007). Accelerated aging tests for evaluations of durability performance of FRP reinforcing bars for concrete structures. *Composite Structures*, *78*(1), 101–111.

Chike, K. E., Myrick, M. L., Lyon, R. E. & Angel, S. M. (1993). Raman and near-infrared studies of an epoxy resin. *Applied Spectroscopy*, *47*(10), 1631–1635.

D3039 ASTM. (2008). Standard test method for tensile properties of polymer matrix composite materials. *ASTM International*.

Davalos, J. F., Chen, Y. & Ray, I. (2012). Long-term durability prediction models for GFRP bars in concrete environment. *Journal of Composite Materials*, *46*(16), 1899–1914.

De Paiva, J. M. F., Mayer, S. & Rezende, M. C. (2005). Evaluation of mechanical properties of four different carbon/epoxy composites used in aeronautical field. *Materials Research*, *8*(1), 91–97. https://doi.org/10.1590/s1516-14392005000100016

Dejke, V. (2001). *Durability of FRP reinforcement in concrete: literature review and experiments*. Chalmers University of Technology, Sweden.

Dogan, A. & Atas, C. (2016). Variation of the mechanical properties of E-glass/epoxy composites subjected to hygrothermal aging. *Journal of Composite Materials*, *50*(5), 637–646.

Ellyin, F. & Maser, R. (2004). Environmental effects on the mechanical properties of glass-fiber epoxy composite tubular specimens. *Composites Science and Technology*, *64*(12), 1863–1874.

Erden, S. & Ho, K. (2017). Fiber reinforced composites. *Fiber Technology for Fiber-Reinforced Composites*, 51–79. https://doi.org/10.1016/B978-0-08-101871-2.00003-5

Fiberglass Market. (2020). https://www.marketsandmarkets.com/Market-Reports/fiberglass-market-6124844.html (Accessed on 03 June 2021).

Garcia-Espinel, J. D., Castro-Fresno, D., Gayo, P. P. & Ballester-Muñoz, F. (2015). Effects of sea water environment on glass fiber reinforced plastic materials used for marine civil engineering constructions. *Materials & Design (1980-2015)*, *66*, 46–50.

Gates, T. S. & Feldman, M. (1996). Effects of physical aging at elevated temperatures on the viscoelastic creep of IM7/K3B. In *Composite Materials: Testing and Design: Twelfth Volume*. ASTM International.

Gates, T. S., Veazie, D. R. & Brinson, L. C. (1997). Creep and physical aging in a polymeric composite: comparison of tension and compression. *Journal of Composite Materials*, *31*(24), 2478–2505.

Gellert, E. P. & Turley, D. M. (1999). Seawater immersion ageing of glass-fibre reinforced polymer laminates for marine applications. *Composites Part A: Applied Science and Manufacturing*, *30*(11), 1259–1265.

Helbling, C. & Karbhari, V. (2004). Investigation of the tensile strength behavior of E-glass/vinyl-ester composite under synergistic hygrothermal exposure and sustained strain. *Proceedings of SAMPE 2004 Conference,* California, USA.

Helbling, C. S. & Karbhari, V. M. (2008). Investigation of the sorption and tensile response of pultruded E-glass/vinylester composites subjected to hygrothermal exposure and sustained strain. *Journal of Reinforced Plastics and Composites*, *27*(6), 613–638.

Hong, B., Xian, G. & Li, H. (2017). Comparative study of the durability behaviors of epoxy-and polyurethane-based CFRP plates subjected to the combined effects of sustained bending and water/seawater immersion. *Polymers*, *9*(11), 603. doi:10.3390/polym9110603

Hossain, M. K., Imran, K. A., Hosur, M. V. & Jeelani, S. (2011). Degradation of mechanical properties of conventional and nanophased carbonepoxy composites in seawater. *Journal of Engineering Materials and Technology, Transactions of the ASME*, *133*(4). https://doi.org/10.1115/1.4004691

Hughes, J. D. H. (1991). The carbon fibre/epoxy interface—a review. *Composites Science and Technology*, *41*(1), 13–45.

Kafodya, I., Xian, G. & Li, H. (2015). Durability study of pultruded CFRP plates immersed in water and seawater under sustained bending: Water uptake and effects on the mechanical properties. *Composites Part B: Engineering*, *70*, 138–148. https://doi.org/10.1016/j.compositesb.2014.10.034

Karbhari, V. M., Stachowski, C. & Wu, L. (2007). Durability of pultruded E-glass/vinylester under combined hygrothermal exposure and sustained bending. *Journal of Materials in Civil Engineering*, *19*(8), 665–673.

Kawagoe, M., Takeshima, M., Nomiya, M., Qiu, J., Morita, M., Mizuno, W. & Kitano, H. (1999). Microspectroscopic evaluations of the interfacial degradation by absorbed water in a model composite of an aramid fibre and unsaturated polyester. *Polymer*, *40*(6), 1373–1380.

Khan, L. A., Nesbitt, A. & Day, R. J. (2010). Hygrothermal degradation of 977-2A carbon/epoxy composite laminates cured in autoclave and Quickstep. *Composites Part A: Applied Science and Manufacturing*, *41*(8), 942–953. https://doi.org/10.1016/j.compositesa.2010.03.003

Kootsookos, A. & Mouritz, A. P. (2004a). Seawater durability of glass- and carbon-polymer composites. *Composites Science and Technology*, *64*(10–11), 1503–1511. https://doi.org/10.1016/j.compscitech.2003.10.019

Kootsookos, A. & Mouritz, A. P. (2004b). Seawater durability of glass-and carbon-polymer composites. *Composites Science and Technology*, *64*(10–11), 1503–1511.

Koshima, S., Yoneda, S., Kajii, N., Hosoi, A. & Kawada, H. (2019). Evaluation of strength degradation behavior and fatigue life prediction of plain-woven carbon-fiber-reinforced plastic laminates immersed in seawater. *Composites Part A: Applied Science and Manufacturing*, *127*(August), 105645. https://doi.org/10.1016/j.compositesa.2019.105645

Li, S., Hu, J. & Ren, H. (2017). The combined effects of environmental conditioning and sustained load on mechanical properties of wet lay-up fiber reinforced polymer. *Polymers*, *9*(7), 244. doi:10.3390/polym9070244

Li, Y., Li, R., Huang, L., Wang, K. & Huang, X. (2016). Effect of hygrothermal aging on the damage characteristics of carbon woven fabric/epoxy laminates subjected to simulated lightning strike. *Materials and Design*, *99*, 477–489. https://doi.org/10.1016/j.matdes.2016.03.030

Mangalgiri, P. D. (1999). Composite materials for aerospace applications. *Bulletin of Materials Science*, *22*(3), 657–664. https://doi.org/10.1007/BF02749982

Masmoudi, R., Nkurunziza, G., Benmokrane, B. & Cousin, P. (2003). Durability of glass FRP composite bars for concrete structure reinforcement under tensile sustained load in wet and alkaline environments. *Proceedings of the 31st Annual Conference*, 4–7.

Materials, A. S. for T. and. (2006). *Standard test method for tensile properties of polymer matrix composite materials*. ASTM international.

Merah, N., Nizamuddin, S., Khan, Z., Al-Sulaiman, F. & Mehdi, M. (2010). Effects of harsh weather and seawater on glass fiber reinforced epoxy composite. *Journal of Reinforced Plastics and Composites*, *29*(20), 3104–3110.

Mondal, S. & Martin, D. (2012). Hydrolytic degradation of segmented polyurethane copolymers for biomedical applications. *Polymer Degradation and Stability*, *97*(8), 1553–1561.

Mourad, A.-H., Akkad, R. O., Soliman, A. A. & Madkour, T. M. (2009). Characterisation of thermally treated and untreated polyethylene–polypropylene blends using DSC, TGA and IR techniques. *Plastics, Rubber and Composites*, *38*(7), 265–278.

Mourad, A.-H.I., Idrisi, A. H., Wrage, M. C. & Abdel-Magid, B. M. (2019). Long-term durability of thermoset composites in seawater environment. *Composites Part B: Engineering*, *168*, 243–253. doi.org/10.1016/j.compositesb.2018.12.076

Mourad, Abdel-Hamid I, Abdel-Magid, B. M., El-Maaddawy, T. & Grami, M. E. (2010). Effect of seawater and warm environment on glass/epoxy and glass/polyurethane composites. *Applied Composite Materials*, *17*(5), 557–573.

Mouritz, A. (2012). Polymers for aerospace structures. In *Introduction to Aerospace Materials* (pp. 268–302). https://doi.org/10.1533/9780857095152.268

Narasimha Murthy, H. N., Sreejith, M., Krishna, M., Sharma, S. C. & Sheshadri, T. S. (2010). Seawater durability of epoxy/vinyl ester reinforced with glass/carbon composites. *Journal of Reinforced Plastics and Composites*, *29*(10), 1491–1499.

Ngono, Y., Maréchal, Y. & Mermilliod, N. (1999). Epoxy− Amine Reticulates Observed by Infrared Spectrometry. I: Hydration Process and Interaction Configurations of Embedded H2O Molecules. *The Journal of Physical Chemistry B*, *103*(24), 4979–4985.

Noobut, W. & Koenig, J. L. (1999). Interfacial behavior of epoxy/E-glass fiber composites under wet-dry cycles by fourier transform infrared microspectroscopy. *Polymer Composites*, *20*(1), 38–47.

Patel, S. R. & Case, S. W. (2002). Durability of hygrothermally aged graphite/epoxy woven composite under combined hygrothermal conditions. *International Journal of Fatigue*, *24*(12), 1295–1301. https://doi.org/10.1016/S0142-1123(02)00044-0

Patel, Sneha Ramesh. (1999). *Durability of Advanced Woven Polymer Matrix Composites for Aerospace Applications,* Virginia Polytechnic Institute and State University, USA .

Phani, K. K. & Bose, N. R. (1987). Temperature dependence of hydrothermal ageing of CSM-laminate during water immersion. *Composites Science and Technology*, *29*(2), 79–87.

Rana, S. & Fangueiro, R. (2016). Advanced composites in aerospace engineering. In *Advanced Composite Materials for Aerospace Engineering* (Vol. 2023). Elsevier Ltd. https://doi.org/10.1016/b978-0-08-100037-3.00001-8

Ray, B. C. (2006). Temperature effect during humid ageing on interfaces of glass and carbon fibers reinforced epoxy composites. *Journal of Colloid and Interface Science*, *298*(1), 111–117.

Reis, P. N. B., Neto, M. A. & Amaro, A. M. (2018). Effect of the extreme conditions on the tensile impact strength of GFRP composites. *Composite Structures*, *188*(August 2017), 48–54. https://doi.org/10.1016/j.compstruct.2018.01.001

Renaud, C. M. & Greenwood, M. E. (2005). Effect of glass fibres and environments on long-term durability of GFRP composites. *Proceedings of 9 EFUC Meeting, Wroclaw,* Poland.

Robert, M. & Benmokrane, B. (2013). Combined effects of saline solution and moist concrete on long-term durability of GFRP reinforcing bars. *Construction and Building Materials*, *38*, 274–284.

Silva, M. A. G., da Fonseca, B. S. & Biscaia, H. (2014). On estimates of durability of FRP based on accelerated tests. *Composite Structures*, *116*, 377–387.

Siriruk, A., Penumadu, D. & Weitsman, Y. J. (2009). Effect of sea environment on interfacial delamination behavior of polymeric sandwich structures. *Composites Science and Technology*, *69*(6), 821–828.

Smith, R. E., Larsen, F. N. & Long, C. L. (1984). Epoxy resin cure. II. FTIR analysis. *Journal of Applied Polymer Science*, *29*(12), 3713–3726.

Socrates, G. (2004). *Infrared and Raman characteristic group frequencies: tables and charts*. John Wiley & Sons.

Starke, E. (1996). Accelerated Aging of Materials and Structures. In *Accelerated Aging of Materials and Structures*. National Academies Press. https://doi.org/10.17226/9251

Strait, L. H., Karasek, M. L. & Amateau, M. F. (1992). Effects of seawater immersion on the impact resistance of glass fiber reinforced epoxy composites. *Journal of Composite Materials*, *26*(14), 2118–2133.

Sun, P., Zhao, Y., Luo, Y. & Sun, L. (2011). Effect of temperature and cyclic hygrothermal aging on the interlaminar shear strength of carbon fiber/bismaleimide (BMI) composite. *Materials and Design*, *32*(8–9), 4341–4347. https://doi.org/10.1016/j.matdes.2011.04.007

Uomoto, T. & Katsuki, F. (1995). Prediction of Deterioration of FRP Rods Due to Alkali Attack, Non-Metallic (FRP) Reinforced for Concrete Structures: Proceedings of the Second International RILEM Symposium (FRPRCS-2). *By Luc Taerwe. New York: E & FN Spon*.

Vieille, B., Aucher, J. & Taleb, L. (2012). Comparative study on the behavior of woven-ply reinforced thermoplastic or thermosetting laminates under severe environmental conditions. *Materials and Design*, *35*, 707–719. https://doi.org/10.1016/j.matdes.2011.10.037

Wang, J., GangaRao, H., Liang, R., Zhou, D., Liu, W. & Fang, Y. (2015). Durability of glass fiber-reinforced polymer composites under the combined effects of moisture and sustained loads. *Journal of Reinforced Plastics and Composites*, *34*(21), 1739–1754.

Wang, Z., Huang, X., Xian, G. & Li, H. (2016). Effects of surface treatment of carbon fiber: Tensile property, surface characteristics, and bonding to epoxy. *Polymer Composites*, *37*(10), 2921–2932.

Wang, Z., Zhao, X.-L., Xian, G., Wu, G., Raman, R. K. S., Al-Saadi, S. & Haque, A. (2017). Long-term durability of basalt-and glass-fibre reinforced polymer (BFRP/GFRP) bars in seawater and sea sand concrete environment. *Construction and Building Materials*, *139*, 467–489.

Wu, G., Dong, Z.-Q., Wang, X., Zhu, Y. & Wu, Z.-S. (2015). Prediction of long-term performance and durability of BFRP bars under the combined effect of sustained load and corrosive solutions. *Journal of Composites for Construction*, *19*(3), 4014058. doi:10.1061/(ASCE)CC.1943-5614.0000517.

Yang, Y., Xian, G., Li, H. & Sui, L. (2015). Thermal aging of an anhydride-cured epoxy resin. *Polymer Degradation and Stability*, *118*, 111–119.

Zafar, A., Bertocco, F., Schjødt-Thomsen, J. & Rauhe, J. C. (2012). Investigation of the long term effects of moisture on carbon fibre and epoxy matrix composites. *Composites Science and Technology*, *72*(6), 656–666.

Zhang, X. & Deng, Z. (2019). Durability of GFRP bars in the simulated marine environment and concrete environment under sustained compressive stress. *Construction and Building Materials*, *223*, 299–309.

Zhou, J. & Lucas, J. P. (1999a). Hygrothermal effects of epoxy resin. Part I: the nature of water in epoxy. *Polymer*, *40*(20), 5505–5512.

Zhou, J. & Lucas, J. P. (1999b). Hygrothermal effects of epoxy resin. Part II: variations of glass transition temperature. *Polymer*, *40*(20), 5513–5522.

List of Publications

Idrisi, A. H., & Mourad, A. H. I. (2021). Fiber reinforced polymer composites sustainability under prolonged exposure to hot seawater: Experimental and prediction study. Materials Letters, 130689. doi:10.1016/j.matlet.2021.130689

Idrisi, A. H., Mourad, A. H. I., Abdel-Magid, B. M., & Shivamurty, B. (2021). Investigation on the Durability of E-Glass/Epoxy Composite Exposed to Seawater at Elevated Temperature. Polymers, 13(13), 2182. doi:10.3390/polym13132182

Idrisi, A. H., Mourad, A. H. I., & Sherif, M. M. (2021). Impact of Prolonged Exposure of Eleven Years to Hot Seawater on the Degradation of a Thermoset Composite. Polymers, 13(13), 2154. doi:10.3390/polym13132154

Mourad, A. H. I., Idrisi, A. H., Wrage, M. C., & Abdel-Magid, B. M. (2019). Long-term durability of thermoset composites in seawater environment. Composites Part B: Engineering, 168, 243-253. doi:10.1016/j.compositesb.2018.12.076

Idrisi, A. H., & Mourad, A. H. I. (2019, October). Impact of the harsh environment on GFRE and GFRPol composite. In OCEANS 2019 MTS/IEEE SEATTLE (pp. 1-5). IEEE, Seattle, USA.

Idrisi, A. H., Ismail Mourad, A. H., Abdel-Magid, B., Mozumder, M., & Afifi, Y. (2019, July). Impact of the harsh environment on E-glass epoxy composite. In Pressure Vessels and Piping Conference (Vol. 58974, p. V06AT06A019). American Society of Mechanical Engineers, Texas, USA.